Aus dem Zoologisches Institut, Abteilung Zoophysiologie II
der Christian-Albrechts-Universität zu Kiel

Hypoxia induces processes related to inflammation and remodelling in the airways of the fruit fly *Drosophila melanogaster*

DISSERATION
zur Erlangung des Doktorgrades
der Mathematisch-Naturwissenschaftlichen Fakultät
der Christian-Albrechts-Universität zu Kiel

vorgelegt von

Ahmed Abdelsadik Mohammed Khalil
aus Aswan, Ägypten

Kiel, 2012

Dekan:	Prof. Dr. Lutz Kipp
1. Berichterstatter:	Prof. Dr. Thomas Roeder
2. Berichterstatter:	PD Dr. Holger Heine
Tag der mündlichen Prüfung:	27.03.2012
Zum Druck genehmigt:	27.03.2012

Table of Contents

Abbreviation, units and acronyms

Yw	yellow White
w	Wildtype
DTT	Dithiothreitol
IKK β	I kappaB-Kinase β
IMD	immune deficiency pathway
Kb	kilo base pairs
NF-κB	Nuklear Faktor-kappa B
PAMP	pathogen-associated molecular pattern
TARGET	temporal and regional gene expression targeting
TBE	Tris-Borat-EDTA-buffer
AMP	Antimicrobial Peptide
JNK	c-Jun N-terminal-kinase
dNTPs	deoxynucleotide triphosphate
DNA	deoxyribonucleic acid
ddH_2O	double distilled water
DEPC-H_2O	Diethylpyrocarbonate treated water
DMSO	Dimethyl sulfoxide
EtOH	Ethanol
EDTA	Ethylendiamintetraazetat acetic acid
e.g.	Example gratia
F1	First filial form
FSB	First strand buffer
FoxO	Forkhead box, sub-group O

GFP	Green fluorescent protein
Hr	Hour
i.e.	id est. (that means)
IM	Immune induced molecules
JAK/STAT	Janus kinase/ signal transducers and activators of transcription
Kbp	kilo base pairs
KDa	Kilo Dalton
L1-L3	Larvae1-3
LA-PCR	Long and accurate PCR
LPS	Lipopolysaccharide
Tm	Melting temperature
mRNA	messenger RNA
Metch	Metchnikowin
MAP	Mitogen-Activated Protein
NCBI	National center for Biotechnology Information
PAMP	Pathogen Associated Molecular Pattern
PRR	Pattern recognition receptor
P	P-Element
PGN	Peptidoglycan
PGRP	Peptidoglycan Recognition pattern
PBS	Phosphate Buffered Saline
PPK	Pickpocket
Pwo	*Pyrococcus woesii*
RNS	Reactive nitrogen species
ROS	Reactive Oxygen Species

qRTPCR	Real-time quantitative polymerase chain reaction
RT	Reverse transcriptase
RT-PCR	Reverse transcription polymerase chain reaction
RNA	Ribonucleic acid
RNase	Ribonuclease
ss-cDNA	Single stranded cDNA
NaAc	Sodium acetate
SSC	sodium chloride/sodium citrate
S.E.M	Standard error of the mean
Ts	Temperature sensitive
Xg	Times gravity
TLR	Toll-like receptor
TNFR	Tumor necrotic factor receptor
UAS	Upstream Activating system
V	Volume

List of figures

List of tables

1. Introduction

Multicellular organisms strictly depend on their immune system to cope with potential pathogens such as bacteria, viruses, parasites and fungi. Special interest gained the innate immune system that utilizes phagocytosis, antimicrobial peptide (AMPs) production and many other strategies, representing the first line of defence. Animals that lack the adaptive arm of the immune system completely rely on this ancient type of immunity. As the adaptive immune system evolved in vertebrates, all other animals, including invertebrates have to combat infections exclusively with their innate immune system. Amongst these animals are all insects as the currently most diverse and successful group on earth. One peculiar insect, the fruit fly *Drosophila melanogaster* is widely used as one of the most important model organisms in biomedical research. The identification of Toll-receptors as the first pathogen associated molecular pattern receptors [1] revitalized the interest in innate immunity, a discovery that was merited by the 2011 Nobel prize to Jules Hoffmann. Although innate immunity has been studied in the fly since then, one very important aspect of this ancient immune reaction, the epithelial immunity, has almost completely been overlooked. In this work, I will focus on one epithelial organ, the larval airway epithelium (tracheal system). It is considered to be the largest area exposed to the outer milieu and thus to a huge number of pathogens and environmental effectors which are able to induce various inflammatory responses. In addition, the *Drosophila* tracheal system is a good model to study epithelial diseases such as asthma and COPD (Chronic Obstructive Pulmonary Disease), because this system has a well-understood development and a plastic reaction to different environmental cues. One of these common stressors is hypoxia, which animals or tissues are faced with during normal life (e.g. by living at high altitude) or during some pathological situations (asthma, stroke and cancer).

1.1 The *Drosophila* immune system

Vertebrates have a highly specific type of immune response (adaptive immune response) that is based on the selection of somatically recombined B and T cells. All other animals and plants lack this type of immune response. They have fully functional defense strategies without any signs of an acquired immune response. Instead they rely on a relatively simple system of inborn immune defenses. Interestingly, even vertebrates depend totally on their innate immune system during the first few days before developing a specific immune response [2, 3]. The simplicity of the *Drosophila* immune system in combination with its homology to the vertebrate innate immune system, made it to a useful model to study the principles of innate immunity. Although several important discoveries were primarily made in other insects, the genetic and molecular techniques available for *Drosophila* have been instrumental in the rapid progress of the field during the past few years [4]. The immune response in *Drosophila* is manifested in at least three ways: first, a humoral response generates circulating antimicrobial peptides; second, cellular response results in phagocytosis and/or encapsulation of the intruder and the third is a phenoloxidase reaction that deposits black melanin around wounds and foreign objects. The inducible antimicrobial peptides are important effectors of the humoral but also of the epithelial response [5, 6]. At least, 34 antimicrobial peptides in eight major families are encoded in the *Drosophila* genome (Figure 1). They include broad-spectrum antibiotic peptides such as the cecropins, which kill Gram-negative bacteria, Gram-positive bacteria and fungi. They include broad-spectrum antibiotic peptides such as the cecropins, which kill Gram-negative bacteria, Gram-positive bacteria and even fungi [7].

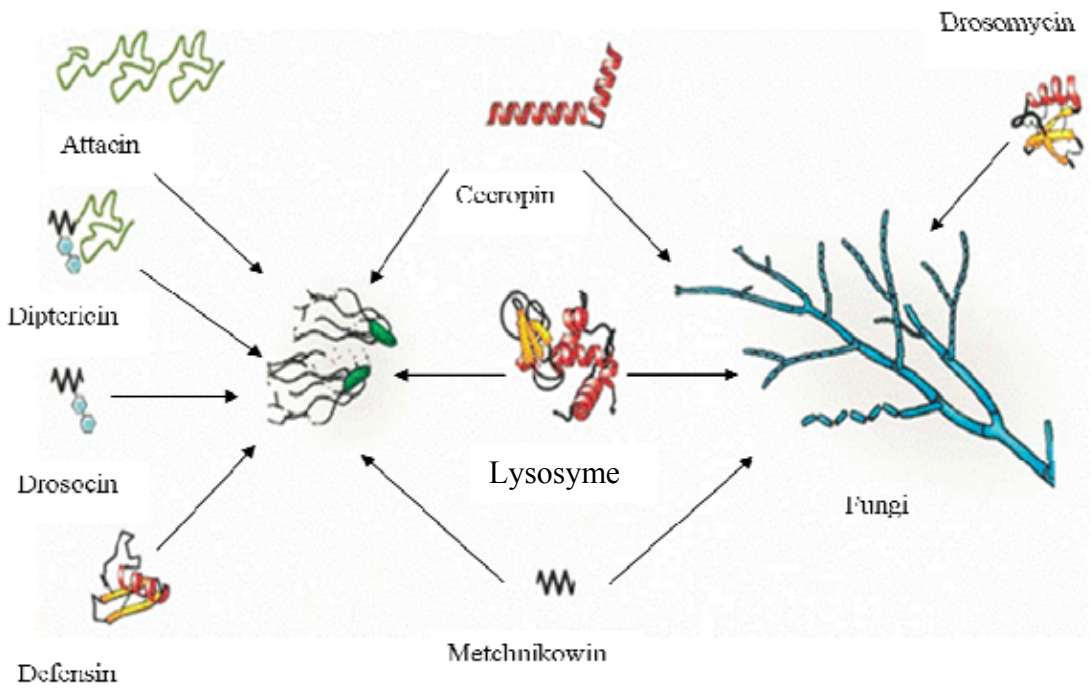

Figure 1: Families of antimicrobial peptides in *Drosophila*.
AMPs except the lysozymes, which are expressed constitutively, are induced in infected animals. Most of these families have several members, which are encoded typically by small clusters of related genes. The attacins and diptericins share similar glycine-rich domains, and drosocin may be related to the proline-rich amino-terminal domain in diptericin. Drosomycin belongs to a family of seven very similar peptides [4].

Other peptides are more specialized, such as the glycine-rich diptericins and attacins, which affect growing Gram-negative bacteria, and drosomycin, which kills fungi. The production of most of these peptides is triggered by the presence of microorganisms. Within a few hours of an infection, these peptides reach micromolar concentrations or higher in the insect hemolymph which thus becomes a very hostile environment for the pathogens.

The cellular response involves circulating blood cells, called hemocytes. At least, three classes of hemocytes can be distinguished morphologically: plasmatocytes, lamellocytes and crystal cells. Plasmatocytes, the main class of hemocytes, are phagocytically active and take up bacteria and other foreign particles. Lamellocytes are produced in a more specialized cellular reaction after host infection by larger parasites, which trigger the proliferation and differentiation of hemocytes

into this second class of cell. The large flat lamellocytes are involved in forming a cellular capsule around the parasite. Crystal cells, which are characterized by the presence of a crystalline inclusion, contain phenoloxidase and have an as yet unknown role in the pathway that activates this enzyme [4]. In fact, the immune defence in *Drosophila* relies mainly on three major signalling systems, the Toll, IMD and JAK/STAT pathways as described in the following sections.

1.1.1 Toll Signaling Pathway

The Toll-pathway of insects has to fulfill two different functions, the patterning of the early embryo ensuring the dorso-ventral patterning and to recognize invading microorganisms and launching an appropriate immune response. For the latter response, PAMPs of potential pathogens have to be recognized and this recognition translated into the expression of e.g. antimicrobial peptide genes. Recognition of bacterial products is not direct; it is mediated via a cascade present in the hemolymph. Two different types of signals can be recognized, 1) peptidoglycans and ß-glucans on one hand and 2) Danger associated molecules on the other hand [8]. Whereas the first type of reaction depends on binding of these PAMPs to e.g. soluble PGRPs and GNBPs, the latter one activates Persephone, a protease. All Toll-activating pathways converge onto spätzle, a soluble cytokine that is cleaved and therewith activated. Activated spätzle in turn can than bind to the Toll-receptor and trigger Toll-dependent events in the target organs [8]. This type of activation differs substantially from the one observed in mammalian Toll-like receptors (TLR). There, a set of more than ten different TLRs recognize different PAMPs, including LPS, peptidoglycans, lipoteichoic acid, flagellin or CpG [9]. Activation of these TLRs leads to induction of antimicrobial peptide genes, cytokines (e.g. IL6), chemokines and maturation of dendritic cells [10-12]. A direct link between innate and adaptive immunity is seen in the TLR-induced dendritic cell maturation that is required for activation of CD4+, and CD8+ T-cells [12]. Fur-

thermore, some members of TLRs are directly expressed on T- and B-cells activating cell differentiation, proliferation, affecting memory cells and antibodies production [13, 14].

Thus, both mammals and invertebrates use the TLRs/Toll pathway to recognize and typify invading pathogens, in similar signaling pathways as described in Figure 2 adapted from [2].

In *Drosophila*, signalling from the membrane receptor encoded by the *Toll* gene activates two NF-κB factors, Dif and Dorsal. From these two, Dif is more important for immune responses, whereas Dorsal functions mainly in the embryo, where the *Toll* signaling pathway determines the dorsal–ventral polarity [15]. At the resting stage, Dif and Dorsal form inactive complexes with Cactus, a *Drosophila* member of the IκB family of NF-κB inhibitors. Toll signaling results in the phosphorylation of Cactus, followed by the ubiquitination and proteasome-dependent degradation of this inhibitor. Dif (and Dorsal) then translocate to the nucleus where they participate in the transcriptional activation of target genes.

Numerous gene products mediate the signaling between Toll and Dif and most of them are related to factors in the human IL-1 and Toll-like receptor (TLR) pathways. Pelle and Tube were identified in early embryonic mutant screens [15], whereas *MyD88* and Traf2 were identified recently by their similarity to human factors [16, 17]. No mammalian homolog of Tube has been identified, but the other genes all have counterparts in human IL-1 receptor signaling: the kinase *Pelle* corresponds to human IRAK, *Drosophila* Traf2 to human TRAF6, and MyD88 to the human homolog with the same name [4].

The final phosphorylation of Cactus is carried out by a kinase that remains unknown. The *Drosophila* IκB kinase (IKK) homolog was first described as a Cactus kinase [18] but is not required for the Toll pathway [19]. Instead, it has a vital role in the activation of another NF-κB factor Relish [20].

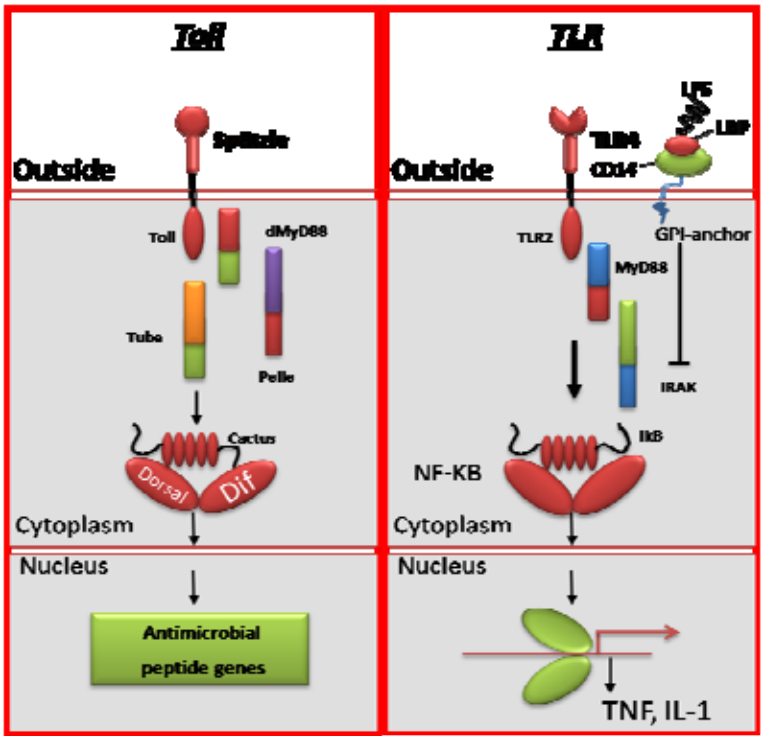

Figure 2: Toll/ TLR (Toll-like receptor) signaling pathway.
In invertebrates, the Toll pathway is activated by binding to spätzle and downstream activation via dMyD88 dependent or non-dMyD88 dependent, leading to activation of cactus and subsequent Dif/Dorsal nuclear translocation and finally upregulation of antimicrobial peptide gene expression. In vertebrates TLRs function as pattern-recognition receptors of the innate immune system. Their recognition of microbial products leads to the activation of the nuclear factor κB (NF-κB) signaling pathway by binding lipopolysaccharide or CD14 (in case of TLR4). Once TLR4 is activated, it recruits the adapter protein MyD88, which is associated with the serine–threonine protein kinase interleukin-1 receptor-associated kinase (IRAK). IRAK/TRAF-6 activates the IκB kinase 1 (IKK1) and IκB kinase 2 (IKK2). These kinases phosphorylate IκB on serine residues, thus targeting IκB for degradation and releasing NF-κB, which moves into the nucleus and induces the transcriptional activation of a wide variety of inflammatory- and immune-response genes [2].

The major humoral response of *Drosophila* to infection is the stimulation of genes encoding antibacterial peptides in the fat body, the functional equivalent of the mammalian liver [21]. The first evidence suggesting that *dorsal* or a related gene might be important in the humoral immune response was the discovery of κB binding motifs in the upstream regulatory regions of the genes encoding the antibacterial agents cecropin, diptericin, and attacin [22-25]. The identification that activation of the Toll-signaling pathway induces an anti-fungal response and that animals defective in the Toll-receptor are more susceptible to fungal infections was the starting point for the

rebirth of innate immunity as a major discipline in immunity [1]. This discovery was awarded with the nodel prize in medicine to Jules Hoffmann and Bruce Beutler.

1.1.2 The IMD Signaling Pathway

Immune deficiency pathway (IMD) is the second signalling pathway that leads to activation of NF-κB factors in the fruit fly. In this case the corresponding factors are known as Relish. Within seconds after an infection, Relish is cleaved into two parts. The amino (N)-terminal REL-68 fragment, which contains the DNA-binding Rel homology domain, translocates to the nucleus where it binds to κB-like enhancer elements in the promoters of antimicrobial peptide genes. The other fragment, REL-49, is IκB-like and remains in the cytoplasm, surprisingly without inhibiting the activity of REL-68 [26].

Two human Rel factors, p105 and p100, have a compound structure that is comparable to Relish, with carboxy (C)-terminal IκB-like domains that are detached by processing. The rapid signal-dependent cleavage of Relish is, however, very different from the currently established picture of p105 and p100 processing, in which the proteasome degrades the IκB-like half of the molecules in a constitutive manner. By contrast, Relish processing is proteasome-independent and requires the product of the *Dredd* gene, a member of the caspase family of proteases [26].

The IMD pathway drives the expression of *diptericin* and most other antimicrobial peptide genes. The signalling pathway shows a high degree of homology between vertebrates and invertebrates. The IMD pathway of insects shows congruencies with the tumour necrosis factor receptor (TNFR1) cascade [27]. Despite these similarities between the insect and vertebrate innate immune system, recognition of pathogen associated molecular pattern (PAMPs) varies significantly between them. The characteristic feature of the humoral response in *Drosophila* is the synthesis and secretion of seven (plus isoformes) types of antimicrobial peptides (AMPs). AMPs are

mostly small cationic molecules with high activity against different infections with microorganisms [28-31]. The production of antimicrobial peptides is also an important aspect of host defence in vertebrates. Similar to insects, mammals express multiple peptide antibiotics, such as the antibacterial defensins, cathelicidins and the antifungal histatin [32]. Genetic analyses have further supported the hypotheses that both, the TNF- (mammalian) and IMD- (insects) pathways are homologous [33-36] as illustrated in Figure 3.

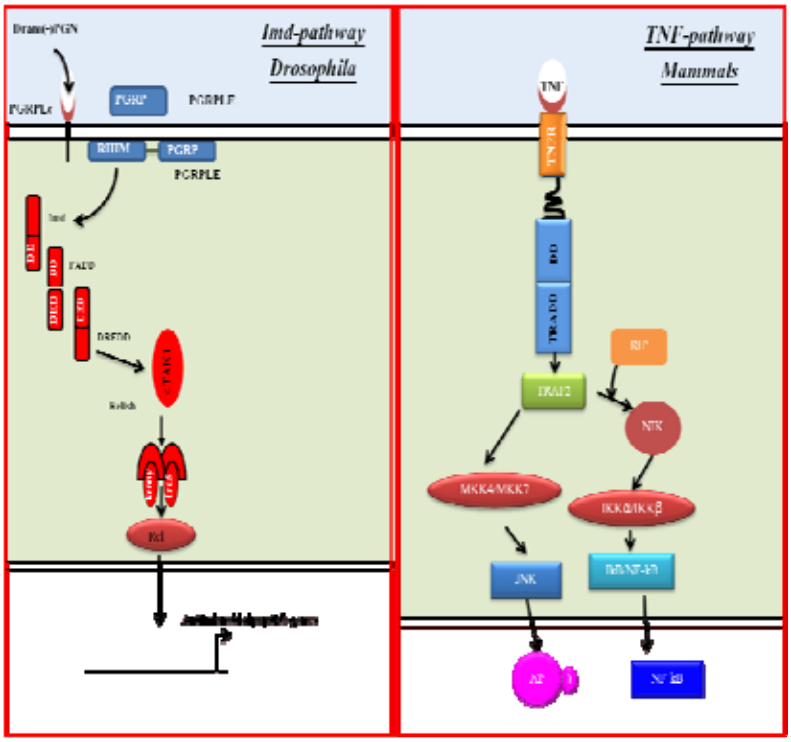

Figure 3: Schematic representation of IMD/TNF Signal pathway activation.
The IMD pathway is probably triggered by an interaction between the transmembrane receptor PGRP-LC and peptidoglycan from Gram-negative bacteria. Following PGRP-LC activation, the death-domain (DD) adaptor protein, IMD, is recruited and binds to Fadd, which interacts with the caspase DREDD (Death-related ced-3/Nedd2-like protein). DREDD has been shown to associate with Relish. Phosphorylation Relish is in turn responsible for activating AMP genes and thus regulating immunity modified from [36].

1.1.3 JAK/STAT pathway

1.1.3.1 The JAK/STAT-signaling pathway in mammals

The JAK/STAT signal-transduction cascade was initially defined in mammals and elucidated to impact numerous cytokines and growth factor signals [37]. JAKases activated following ligand binding and receptor dimerization phosphorylate tyrosine residues in their associated receptors, allowing normally cytosolic STAT molecules to anchor onto the receptor complex via their SRC homology2 (SH2) domains. The mobilized STAT molecules are themselves activated by JAK-mediated phosphorylation of an invariant tyrosine residue in their C-terminal region and then either homo- or heterodimerize prior to nuclear translocation. Upon translocation into nuclei, activated STAT dimers bind to consensus DNA target sites (consensus TTCNNNGAA). In mammals, four JAK and seven STAT genes have been identified and additionally more than 30 cytokines and growth factors have been shown to be part of this signaling pathway [37, 38] .

1.1.3.2 Structure of the JAK/STAT and the JNK pathway in flies

Through its role in embryonic segmentation, the JAK/STAT pathway was identified in flies [39]. The pathway is mainly composed of four components; the ligand unpaired (Upd), the receptor domeless (Dome), the JAK kinase (Hopscotch/Hop), and the STAT transcription factor (STAT92E/Marelle). Whereas three different *upd* genes are present in the fly's genome (*upd1-upd3*), all other components have one representative gene [38] as shown in Figure 4.

In the airway epithelia, the JAK/STAT-pathways is fully functional in response to pathogens. All components of the pathway are present in this tissue, allowing for an organ autonomic response of this signaling pathway [40, 41].

Various studies have been shown that stimulation of the *Drosophila* immune response activates both NF-κB and JNK signaling pathways. Bacterial infection activates also the JNK pathway,

by induction of the *Drosophila* homolog of the mammalian MAPK kinase, TAK1 (transforming growth factor β-activated kinase 1), which functions as a *Drosophila* IκB kinase-activating kinase and as the JNK kinase-activating kinase. However, JNK signaling is not required for antimicrobial peptide gene expression but is required for the activation of other immune inducible genes, including *Punch, sulfated,* and *malvolio*. Apparently, JNK signaling may play a vital role in the cellular immune response and the response to stress presumably also including hypoxia [42].

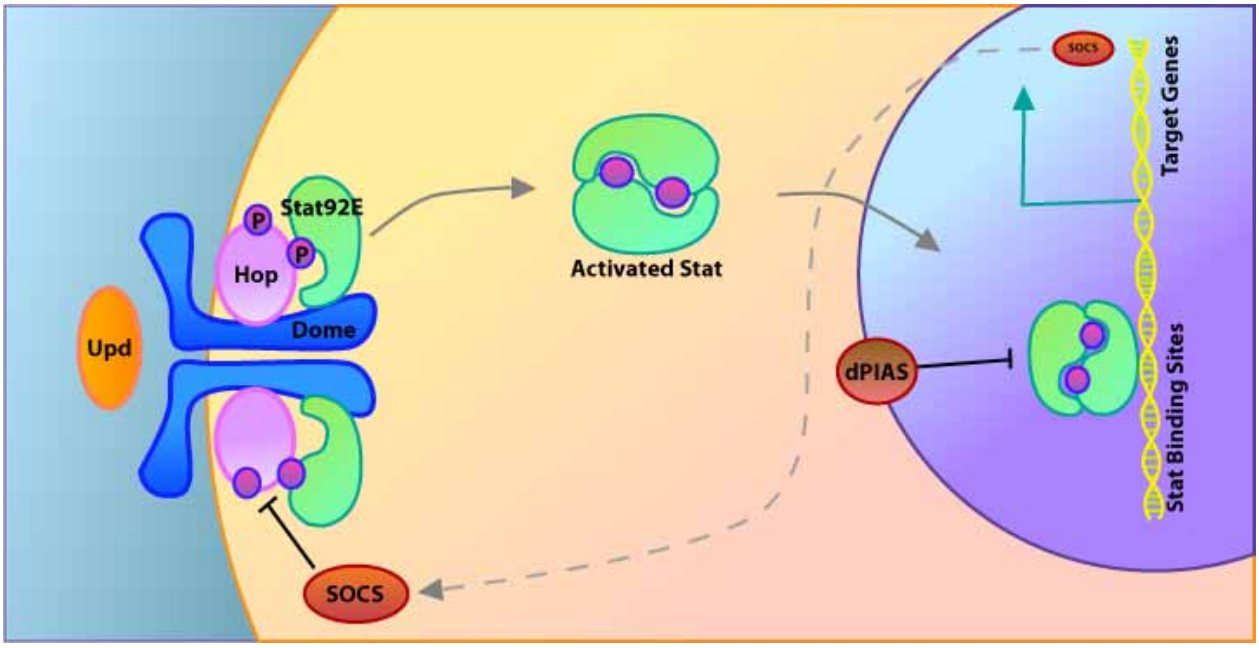

Figure 4: Overview of the JAK/STAT dependent *Drosophila* immune responses.
Upon septic injury or other stressor such as ROS, Upds (e.g. Upd3) occur in the hemolymph and subsequently activates JAK/STAT signaling in fat body. These signaling events control the activation of genes coding for e.g. the thioester-containing proteins (TEP) and the TOT peptides. The TEP proteins presumably promote phagocytosis, whereas the function of the TOT peptides is unknown. Upon wasp parasitization, plasmatocytes spread on the surface of the eggs and are thought to send a yet uncharacterized signals to the lymph glands. This signaling event triggers massive JAK/STAT-dependent differentiation of lamellocytes in the lymph glands. Upon lymph gland dispersal, lamellocytes are released into the hemolymph and encapsulate the wasp eggs. Adapted from [38].

1.2 Interconnection between IMD and JNK pathway

For innate immune responses to infections, regardless if in vertebrates or invertebrates, the JNK family of MAP kinases plays a central role in its signal transduction. Activation of JNK conduces the regulation of main cellular processes, such as differentiation, apoptosis and directed cell movements [43-46]. Recently, a whole-genome RNAi screen utilizing *Drosophila S2* cells

focused on modifiers of the IMD-pathway, revealed that core elements of the JNK pathway have this capacity [43].

Moreover, Relish-mediated JNK inhibition involves proteasomal degradation of TAK1, the MAPKKK responsible for JNK activation in response to LPS. These data conclude that specific targets of Relish that are induced during immune responses promote ubiquitination of TAK1 thus blocking the JNK cascade [47]. The fact that cycloheximide and actinomycin D also down-regulate JNK activity suggests that genes targeted by Relish rather than Relish itself promote this interaction, which is depicted in Figure 5.

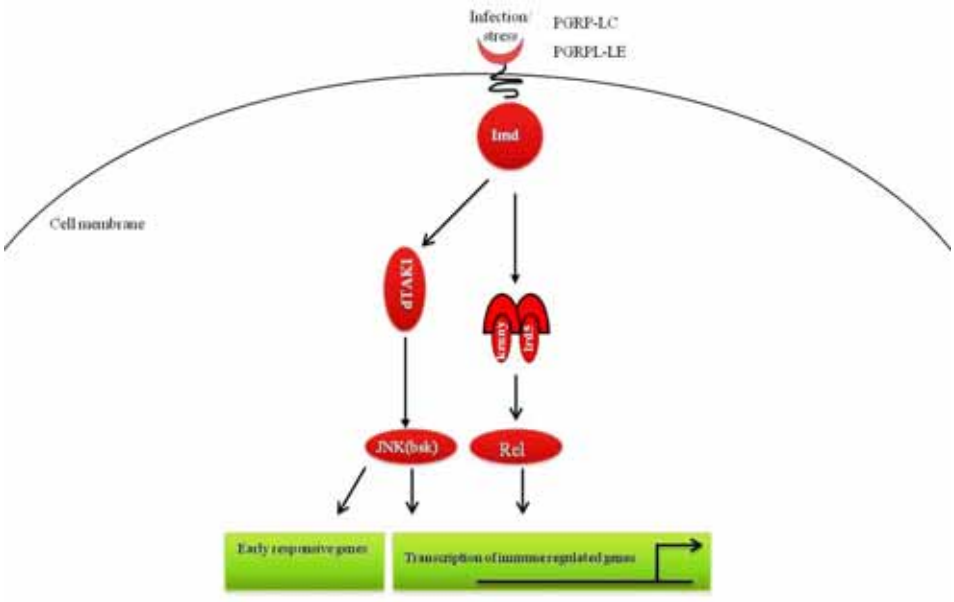

Figure 5: Activation of the *Drosophila* IMD/JNK branches in signal transduction.
Gram-negative peptidoglycan might bind directly to PGRP-LC and -LE, to signal to Imd. Imd regulates at least three downstream events. First is TAK1, which then stimulates IKK-dependent cleavage and activation of Relish. Second is the FADD–Dredd pathway that also activates Relish; this branch has a negative regulatory loop that involves the caspase inhibitor Dnr-1. Third is the activation through TAK1 of the JNK pathway, which regulates early response genes, wound healing and melanization. The JNK pathway is also negatively regulated by Relish. The protein level of Relish, and thus the responsiveness of the Imd pathway, might also be regulated by an ubiquitin–proteasome complex, modified from [48, 49].

Antagonism between JNK and NF-κB signaling is evolutionary conserved. Inactivation of either IKKβ or NF-κB RelA (p65) in mice cells lead to JNK activation in response to TNFα [50]. Various studies have identified distinctive molecules as mediators for the NF-κB mediated inhibition of

JNK signaling in the TNFα pathway, including XIAP [51], GADD45β [52], and reactive oxygen species [53]. In *Drosophila*, bacterial infection always results in a brief increase of phospho-dJNK levels that parallels IMD/dJNK pathway activation, while no increase in dredd^{B118} mutant flies could be observed [45].

1.3 Epithelial immunity

Epithelia act as the first line of defense to inhibit bacterial invasion. Epithelial cells are spread over different tissues such as the epidermis, the digestive tract (gut), the respiratory system (trachea), and the reproductive systems. These tissues are in direct contact with microbes, and they function as standard routes of microbial infection [32, 54]. Those strains (transgenes) that carry AMP promoter-GFP fusions reveal that AMP genes are expressed in surface epithelia locally in a cell- or tissue-specific manner. This expression may be constitutive (e.g., *drosomycin* in the female spermatheca; [32] or inducible (e.g., *diptericin* or *drosomycin* in trachea and gut). The production of the inducible AMPs is at least partially under the control of the Imd pathway as reviewed recently [34] .

The major effector system in the intestinal epithelium is depends on the local production of reactive oxygen species (ROS). For this, the dual oxidase (Duox) of the host produces hydrogen peroxide to kill invading pathogens and an immune-regulated catalase seems to abolish the damage to the host tissue [55-57]. Disturbing the redox homeostasis in the intestine by knocking out the *duox* gene led to a highly increased susceptibility to oral bacterial infections. These results imply that immune-regulated catalase and *Duox* activities are important for regulating reactive oxygen species levels and therewith protecting the fly against gut infections [55, 56].

Another aspect associated with epithelial immunity becomes apparent following wounding of these structure. Breaking the barrier epithelial activates the cellular immunity to form clots that trap microbes and also limit the loss of hemolymph [58]. Various proteins have been identified to be entitled making the clot fibers (e.g., *hemolectin* and *fondue*, a multidomain protein expressed in plasmatocytes). Both proteins are required for melanization but do not disrupt the animals' viability; proposing that these proteins are necessary for wound healing [58-60]. Melanization independent clotting can occur, as pro-phenol oxidase-compromised mutants form normal clots [58]. The process of hemolymph coagulation is presumably similar to the production of extracellular fibrous traps expressed by mammalian neutrophils after cytokine activation, which kills bacteria independently of phagocytosis [61, 62].

In *Drosophila*, like in mammals, the barrier epithelia are in continuous contact with large numbers of microorganisms. These surfaces must be governed with competent immunity for microbial recognition and defense. For that, the gut and trachea, the two major routes of infection, are lined with a chitinous matrix [34]. In addition, local production of AMPs and ROS provides two complementary inducible defense mechanisms in the gut as shown in Figure 6.

The response is triggered upon natural infection by Gram-negative bacteria and is mediated by the IMD pathway [32, 54]. For example, *drosomycin* and *diptericin* are induced in both trachea and gut via the IMD pathway in response to local infection by bacteria such as *Erwinia carotovora* [41, 63]. The response initially is mediated through the recognition of Gram-negative PGN by PGRP-LC [64].

The second arm of immunity in *Drosophila*, Toll, is not implicated to be relevant in the local immune response [5, 34, 41]. In mammals, pathogen removal depends on production of ROS. In fact, balancing between ROS production and elimination seems to be imperative [5, 65].

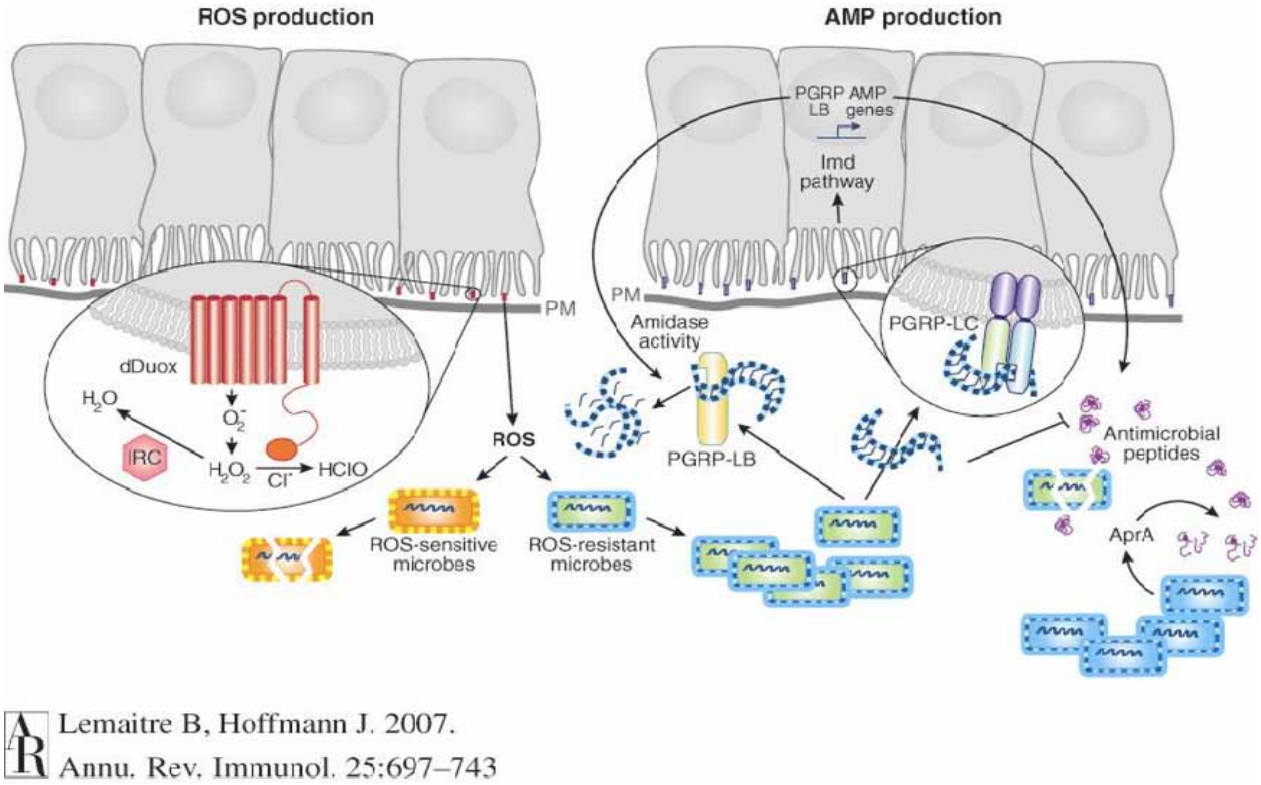

Figure 6: Gut immune response is composed of two independent pathways.
Local production of ROS (*left*) and AMPs (*right*) provides two inducible defense mechanisms in the gut. ROS are produced by the Duox protein and are detoxified by the IRC catalase. Enzymatic assays demonstrated that the PHD domain of *Drosophila* DUOX can transform H_2O_2 into the highly microbicidal HOCl. AMPs (e.g., Diptericin or Attacin) are produced by epithelial cells under the control of the IMD pathway upon recognition of PGN released by Gram-negative bacteria. Amidase PGRPs degrade PGN in non-immunostimulatory fragments, thereby reducing the gut immune reactivity. Bacteria such as *Pseudomonas entomophila* secrete an abundant protease (AprA) that degrades AMPs and PM, peritrophic matrix [34].

The Duox proteins belong to a conserved family that contain, an N-terminal extracellular peroxidase domain (PHD); alongside the NADPH domain; this structure gives it the ability to produce ROS in a regulated manner [66]. *Duox* RNAi flies have not the ability to produce ROS upon bacterial infection, indicating that this enzyme is the main machinery of epithelial ROS production [56].

The airway epithelium of the fly reacts different to bacterial infection if copmpared with the intestine. In the latter one, ROS production appears to be the most relevant type of reaction whereas the conventional IMD-mediated response dominates in the airways [41, 65].

This difference might be attributed to the presence of the endogenous microbiota in the intestine that has to be secured and not erased by a strong IMD-dependent immune reaction. In the airway this restriction of the response is not necessary.

1.4 Reaction to hypoxia

Tissues suffer depletion in oxygen delivery at high altitude or during certain pathological conditions, such as cancer, myocardial infarction and stroke. Various strategies have been branched out to maintain survival of the organism in such low oxygen conditions; nevertheless, tissue tolerance to hypoxia is distinctive between the different species. The molecular mechanisms underlying survival in those intensive hypoxic conditions are not fully understood at the moment [67].

Oxygen plays a multitude of essential roles in eukaryotic cellular physiology (e.g., metabolism and energy production). Since its critical role in cell survival, eukaryots have evolved different mechanisms to cope with low oxygen levels (hypoxia). One of the most important ways of adaptation to hypoxia is the differential regulation of specific gene sets [68]. By varying the amounts of transcripts for various genes, cells are able to alter quantities of assorted proteins, and by doing so, change their physiology in ways that allow them to better cope with hypoxia. This hypoxia-induced transcriptional modulation is accomplished through the action of hypoxia-responsive transcription factors, proteins that are directly involved in regulating the quantities of transcripts that are produced from specific sets of genes. The best-characterized transcription factor in response to hypoxia is the Hypoxia Inducible Factor-1 (HIF-1) [69, 70]. HIF-1 is a heterodimeric transcription factor composed of dual subunits known as HIF-1 α and HIF-1β. HIF-1 β is a protein that is dominantly present in many cells, and dimerizes with several other transcription factors other than HIF-1α in order to regulate transcription of diverse cellular responses ranging from reaction to environmental toxins, up to neural development [71]. HIF-1β

is essential for the function of HIF-1 as a hypoxia responsive transcription factor, but plays a minor role in the regulation of its activation. Otherwise, HIF-1α is a protein that is the major sensor for cellular oxygen levels. This regulation is the main core in the regulation of HIF-1 activity [70]. Under normal levels of oxygen (normoxia), HIF-1α is hydroxylated at a proline residue by an enzyme known as HIF-1 Proline Hydroxylase (HPH). When HIF-1α is hydroxylated, it is recognized by the *Von Hippel Lindau* tumor suppressor protein (*VHL*), which facilitates the ubiquitination and rapid proteasomal degradation of the HIF-1α. Upon hypoxia, HIF-1α is not degraded, translocates to the nucleus and dimerizes with HIF-1β. The dimeric HIF-1 transcription factor activates the expression of its target genes, by binding to DNA sequence motifs characterized by the core sequence 5'- TRCGTG-3'. These elements are present, often in clusters, near genes that are regulated by HIF-1 under hypoxia. Large number of genes has been identified as HIF-1 targets in mammalian and other model systems. HIF-1 is responsible for the transcriptional upregulation of genes such as erythropoietin (EPO), and Vascular endothelial growth factors (VEGF) which increase oxygen delivery to hypoxic areas by stimulating production of red blood cell, and the recruitment of blood vessels respectively in mammals as shown in Figure7 [72]. In the fruit fly *Drosophila melanogaster*, HIF-1 regulates HPH, providing a feedback mechanism by which HIF-1 activity is attenuated during hypoxia [73]. Other studies showed that in *Drosophila*, HIF-1 directly regulates the transcription of the Heat shock factor (HSF), a transcription factor that activates the expression of heat shock protein genes [68]. The full complement of HIF-1 regulated genes in *Drosophila* has not been cataloged yet. However, another factor that has been shown to regulate gene expression during hypoxia is the Forkhead transcription factor FoxO. Basically, FoxO activity is repressed by insulin signaling, its activation results in stimulation sets of genes' serving to cope with stress conditions (e.g., starvation). Interestingly, increase in FoxO activity is leads to an increased longevity in *Drosophila melano-*

gaster and *Caenorhabditis elegans*. Several genes involved in reactive oxygen species detoxification have been described as FoxO targets, as well as other genes involved in protecting cell from other stressors [74]. Recently, FoxO factors have been shown to activate gene expression in response to hypoxia in human cells [75].

Another transcription factor that has been shown to activate gene expression in response to hypoxia is the nuclear factor kappa-B (NF-κB). As a central transcriptional regulator of the inflammatory response in mammals, NF-κB has been characterized [76]. NF-κB can be activated through a wide range of stimuli, including bacterial antigens, pro-inflammatory cytokines, oxidative stress, and ultraviolet radiation. As mentioned before, in *Drosophila*, there are three NF-κB proteins, Dorsal (Dl), Relish (Rel), and Dorsal-related immunity factor (Dif) [77]. Various studies have shown that NF-κB is activated by hypoxia, the mechanism by which this occurs is unclear [78, 79]. Hypoxia can induce the production of Nitric Oxide (NO) and of other reactive oxygen species (ROS) [80, 81]. Although we are not sure regarding the underlying mechanism, we and others have observed multiple targets of Rel, as well as Rel itself being transcriptionally regulated by hypoxia in *Drosophila* [82].

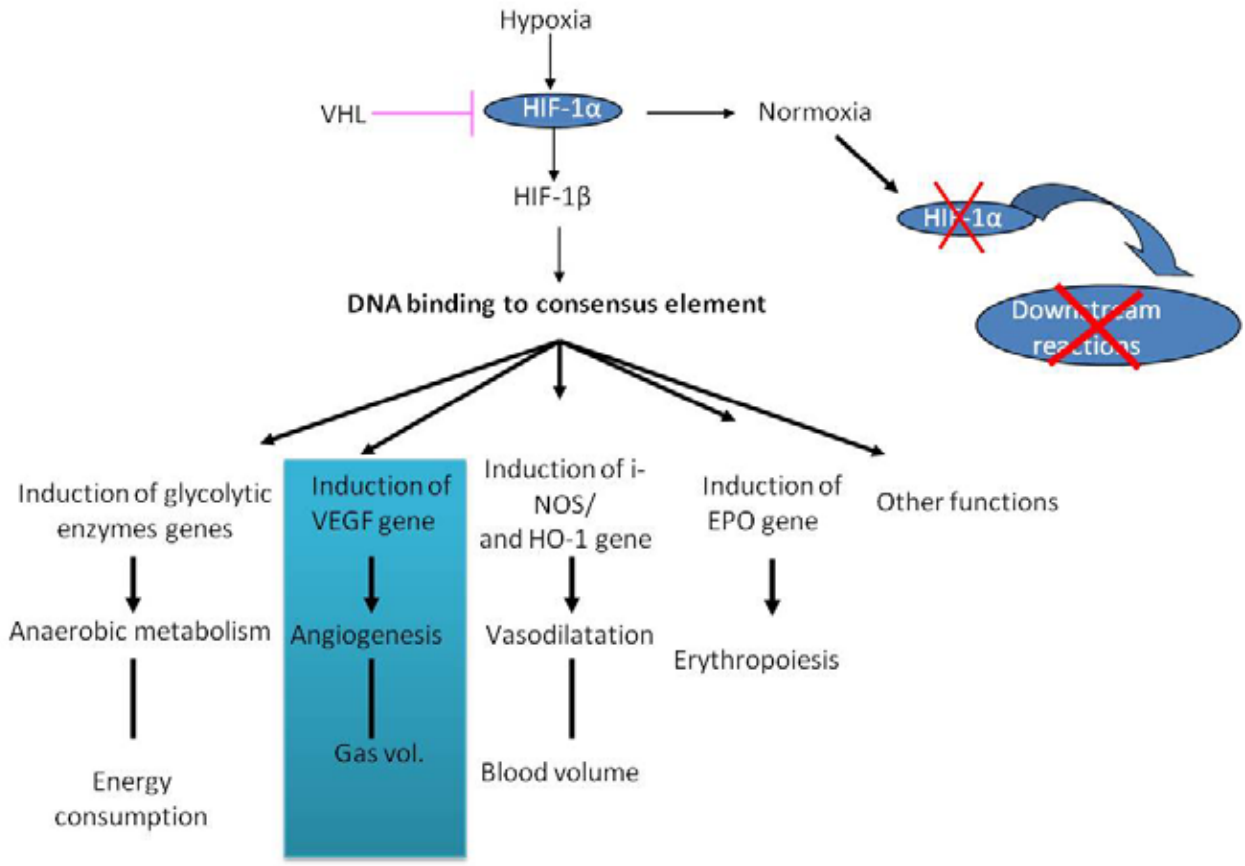

Figure 7: Tissue responses to Hypoxia/ischemia.
The alpha subunits of *HIF* are hydroxylated at conserved proline residues by *HIF* prolyl-hydroxylases, allowing their recognition and ubiquitination by the VHL ubiquitin ligase, which labels them for rapid degradation by the proteasome [83]. This occurs only in normoxic conditions. In hypoxic conditions, *HIF* prolyl-hydroxylase is inhibited results in stabilizing HIF-1α (pseudohypoxia). HIF-1, when stabilized by hypoxic conditions, upregulates several genes to promote survival in low-oxygen conditions. These include glycolysis enzymes, vascular endothelial growth factor (VEGF), which promotes angiogenesis and activate other responsive genes. Modified from [84]

1.5 The airway epithelium

1.5.1 Anatomy of the human lung

Lungs are the organs of respiration in humans. Humans have two lungs, with the left being divided into two lobes and the right into three lobes. Together, the lungs contain approximately 2400 km of airways and 300 to 500 million alveoli, having a total surface area of about 70 m^2 in adults — roughly the same area as one side of a tennis court [85]. Furthermore, if all of the capillaries that surround the alveoli were unwound and laid end to end, they would extend for

about 992 km. Each lung weighs 1.1 kg; therefore making the entire organ about 2.2 kg. Oxygen enters the respiratory system through the mouth and the nose to the trachea, which splits into two smaller tubes called the bronchi. Each bronchus then divides again forming the bronchial tubes. The bronchial tubes lead directly into the lungs where they divide into many smaller tubes, which connect to tiny sacs called alveoli. The average adult's lungs contain about 600 million of these spongy, air-filled sacs that are surrounded by capillaries. Each lung consists of approximately 300 million alveoli which closely form each other recumbent the surface required for the gas exchange of 80-100 m² [86]. The inhaled oxygen passes into the alveoli and then diffuses through the capillaries into the arterial blood. Meanwhile, the waste-rich blood from the veins releases its carbon dioxide into the alveoli. The carbon dioxide follows the same path out of the lungs during exhaling.

The diaphragm is a sheet of muscles that lies across the bottom of the chest cavity. As the diaphragm contracts and relaxes, breathing takes place (Figure 8).

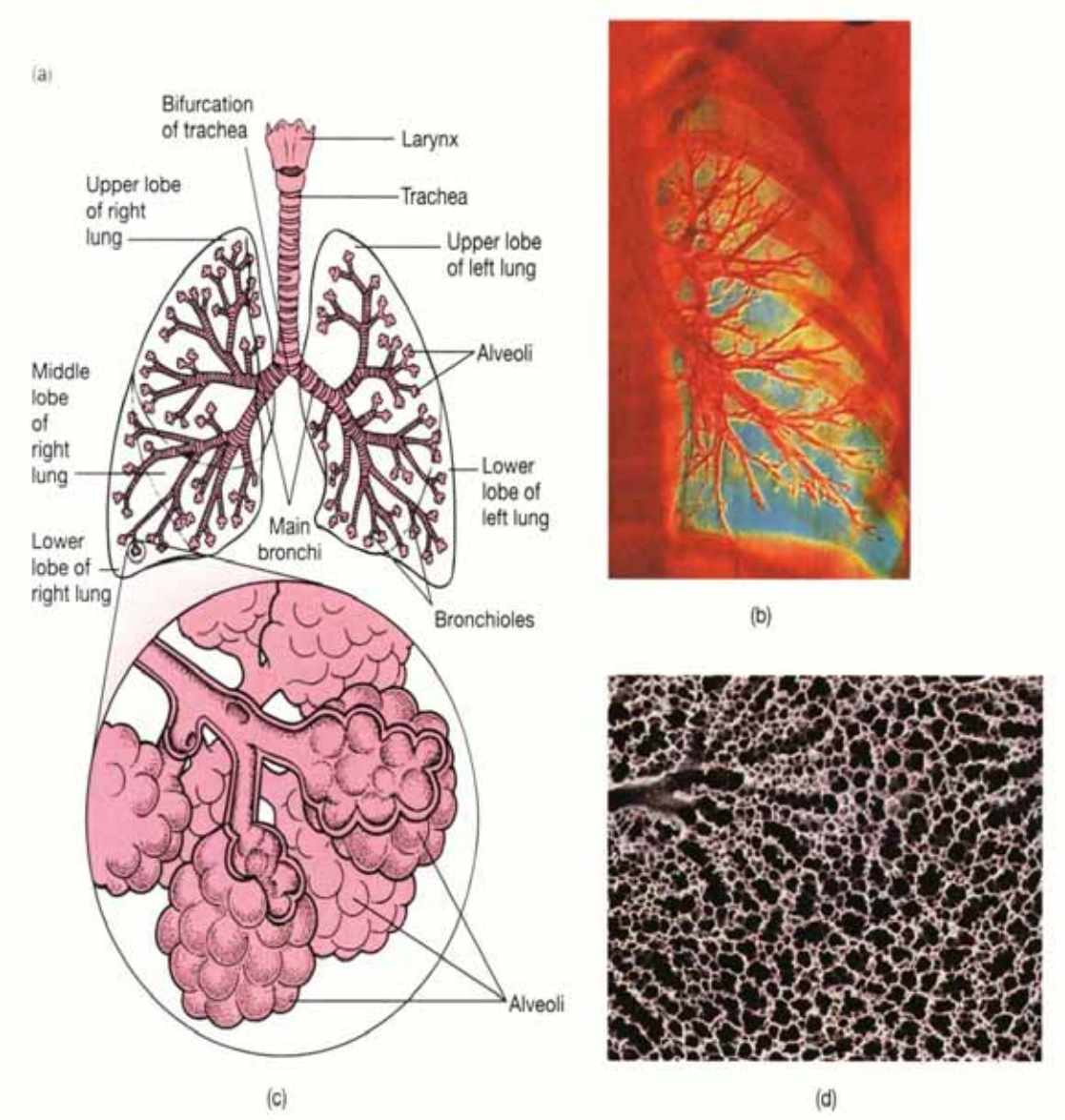

Figure 8: Structure of the human lung.
A) Schematic representation of the human lung, with its two lobed lung and lower airways that are dichotomously branched. B) Representation of a contrast right lung with his bronchial tree. C) Alveolar ducts of the human lung, which open in the Alveolar sacs (alveoli). D) Semi-thin section of a human lung alveolar sac. Modified from [86]

1.6 Structure of the fruit fly's larval tracheal system

The larval tracheal system of *Drosophila* is a widespread, bilaterally symmetric tube system that permeates the entire body of the larva. It consists in late larval stage of about 10,000 interconnected tubes and two pairs of respiratory openings (*spiracles*) on the front or rear end of the

larva. Small structures embedded in skin folds (*stigma*), these stigmas with short movable and lockable structures are dorsally located in the larval tracheal system as shown in figure 9.

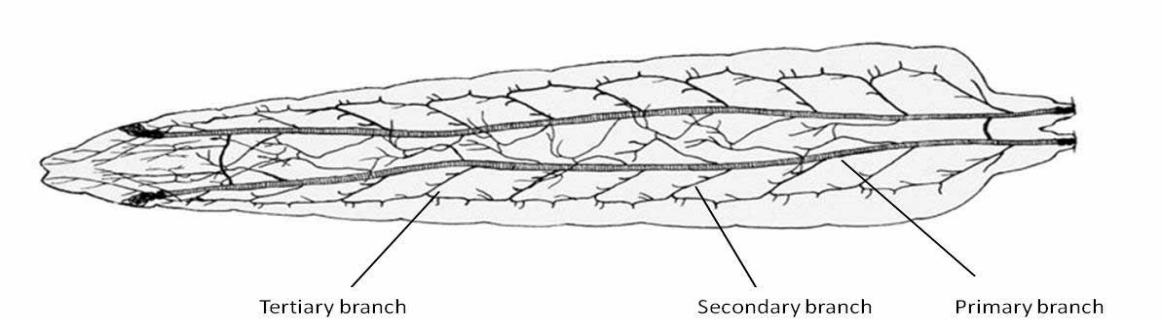

Figure 9: Tracheal system of larval stage of *Drosophila melanogaster* [87].

The both primary branches run parallel in a stereotype way through the entire body of the larva, they split in nearly every segment to the inner and outer secondary branches. While the inner secondary branches are very short and only extend dorsally, the outer secondary branches pulled deeply throughout of the whole body of the larva on both sides of the body. These secondary branches are branched into hundreds of fine tertiary branches (*tracheoles*), which with their terminals in direct contact with the organs. While the ramifications of the primary and secondary branches in the larval tracheal system are formed during embryonic development in a stereotype way, the making of the tertiary branches in the larva are variable and dependent on the oxygen content of the surrounding tissue. Thus, especially in low-oxygen areas of the body cavity dense networks of tertiary branches can be observed [87, 88]. The main task of the larval tracheal system is the efficient supply of the body with oxygen. The oxygen is passively transported through the two respiratory openings included in the body of the larva. Usually, the larvae keep the posterior part in direct contact with the oxygen milieu while the anterior part is used for feeding from the first larvae to late third stage (L3) of their lives. The oxygen passes through the primary and secondary branches to the tertiary, where the direct diffusion to the tissue taken place. Since the whole of the tracheal epithelium is layered, it can be assumed that even in the

field of primary and secondary branches, the oxygen exchange to body tissues can take place. Branches of the larvae tracheal system are lined with a thin cuticle made of chitin. It stabilizes the trachea with cuticular bars (*Taenidia*) and prevents its collapse. In the tertiary branches, this cuticular structure is reduced to a minimum level which allow maximum oxygen supplementation to the organs [89, 90].

1.7 Physiology and the plasticity of the airway system

Various stimuli can affect physiology and development of animals, such as nutrient availability, and oxygen tension. Different adaptations occur to maintain organismal survival in these distinct milieu conditions, implies upregulation or repression of supportive genes maintaining the cellular homeostasis. Reactions that can be seen in response to hypoxia may include enhancment of oxygen transport from respiratory surfaces to tissues or reduction of the metabolic process. In many lower species, enhanced tolerance to hypoxia results from a marked and controlled reduction of metabolism [91, 92]. Mammals adapt to the low oxygenation through a wide range of reactions like, increase of heart and respiratory frequency, synthesis of more red blood cells, vasodilatation, and angiogenesis. The latter process (angiogenesis) is a developmental process that is common to many physiological and pathological conditions such as formation of the placenta, endometrial growth, wound healing, ischemic heart disease, stroke, and cancer [93, 94]. This includes the budding of new fine capillaries from the basically existing blood vessels. This happens when hypoxia seeking cells secrete angiogenic growth factors, mainly the Vascular Endothelial Growth Factor (VEGF), which binds its receptors on the endothelial cells of blood vessels [70]. VEGF transcription in hypoxic cells is mainly depended on the nuclear translocation of Hypoxia-Inducible Factors (HIFs) [93, 95].

In Drosophila melanogaster, HIF is also a bHLH-PAS heterodimer in which Similar (Sima) is the oxygen-regulated α subunit [96, 97], whereas the constitutive β subunit is named Tango [98, 99]. The circulatory system of insects is rudimentary, and nearly without function [100]. In fact, tissue oxygenation is achieved directly through the tracheal system, a network of ramified, interconnected, and progressively narrowing air-containing epithelial tubes [101, 102]. By mid-embryogenesis stages, the *Drosophila* tracheal system develops from ectodermal primordia, in a process that largely depends on guided cell migration [103]. Branchless (Bnl) is an FGF homologue expressed in the outer-tracheal cell subset is recognized by the FGF receptor breathless (Btl) which is located on the tracheal cell surface [104, 105]. Upon Bnl/Btl binding, a new cluster of branches is formed. The third instar larvae have a complete tracheal system with only few cells able to respond to low-oxygen tension -the terminal cells. They can differentiate and make new small outer projections called terminal branches [106] in a process analogous to mammalian angiogenesis [107]. In addition, Bnl protein accumulation in hypoxia and ectopic activation results in tracheal chemoattraction and new branches formation. Therefore, the angiogenic-like response of the *Drosophila* tracheal system is activated by hypoxia-inducible expression of Bnl in nontracheal cells, which promotes the formation of new terminal ramifications [70, 108].

1.8 Aim of the study

Hypoxia is associated with a great variety of diseases including inflammatory diseases of the airways such as asthma or COPD. Although much is known regarding the mechanisms underlying these diseases, the contribution of hypoxia to the pathological phenotype is not well understood. This is true all the more regarding the role of the airway epithelium itself. Therefore, the major aim of this study is to characterize yet unknown effects of hypoxia on the airway epithelium and to unravel the underlying molecular mechanisms. For this, I used the fruit fly

Drosophila melanogaster as a model. A special focus was on those aspects of hypoxia that are related to disease phenotypes including inflammation and remodeling of the airways. Finally, this work should increase our understanding regarding the physiological adaptation of the airway epithelium to hypoxia and their role during pathogenesis.

2. Materials and Methods

2.1 Materials used in this study

2.1.1 Hypoxia chambers

Experimental chambers (26 cm x 16 cm x 16 cm) were specially designed and supplied with 5% O_2 balanced with N_2 as depicted in figure 10. Humidity was maintained by passing the gas through water prior to entry into the chambers. The flow speed was monitored with a 565 Glass Tube Flow meter (Concoa, Virginia Beach, VA, USA), and the O_2 level within the chamber was periodically tested with a Diamond General 733 Clark Style electrode (Diamond General Development Corp., Ann Arbor, MI, USA).

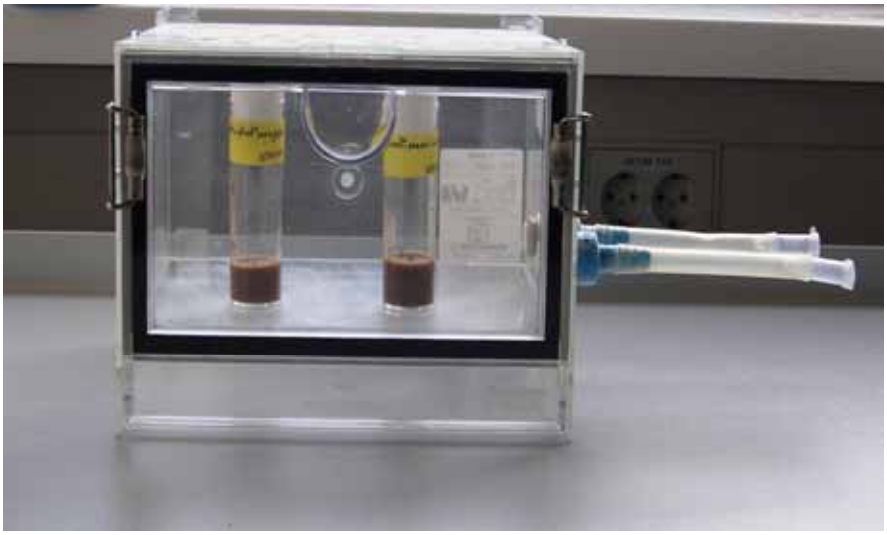

Figure 10: Photograph of hypoxia Chambre.
Home-designed hypoxia chamber made of polyethylene and titied with two screws, and supplied with input/ouput sources. The system qligned with 565 Glass Tube Flow meter to control the gas flow, standard treatment condition was used during the whole experiments.

2.1.2 Standard fly food

Ninety gram of agar was added to eight liters of aqua bi-distilled, and boiled until agar is dissolved. Then, 165 g brewer's yeast, 615 g cornmeal and 1 l syrup were added to 3.3 liters of aqua

bi-distilled, and added to the soluble agar. It is boiled for 15 minutes and stirred sporadically. After cooling down to 55 °C, 200 ml of a 10% nipagin solution were added.

2.1.3 Fly Strains and Genetic Crosses

Stocks were raised on standard cornmeal-agar medium at 25°C in a 12h/12h light dark cycle. w^{1118} served as the wild-type control; controls in transgenic experiments are usually based on lines under study crossed with w^{1118} [109]. The transgenic strains *drosomycin::gfp* (drs), *p*pppk-Gal4, btl-gal4, UAS-*dFoxO-gfp*, *foxo*^{21}, *foxo*^{24}, *relish*^{E38}, UAS-sima-RNAi, UAS-PGRP-LC_x, UAS-GFP, UAS-Pi3K92E(DN) , UAS-P^{53}(DN), Atg5-RNAi and LDH-Gal4/UAS-nGFP were used and have been described elsewhere [32, 110-115].

2.1.4 Oligonucleotides used for RT and qRT-OCR

Primer	Sequence
OdT-T7I	GAGAGAGGATCCAAGTACTTATACGACTCACTATAGGGAD AT(25)V
CF-SP6rG1	AGCGGCCGCAGATTTAGGTGACACTATAG ArGrGrG
OdT T7II	GAGAGAGGATCCAAGTACTAATACGACTCACTATAG
CF-Sp6-PCR	CAG CGG CCG CAG ATT TAG GTG ACA CTA TAG
attacin_FOR	CACAATGTGGTGGGTCAGG
attacin_REV	GGCACCATGACCAGCATT
cecropin_FOR	AAGATCTTCGTTTTCGTCGC
cecropin_REV	GTTGCGCAATTCCCAGTC
defensin_FOR	TTTTGCTCTGCTTGCTTGC
defensin_REV	ACATGATCCTCTGGAATTGGA
diptericin_FOR	CGCAATCGCTTCTACTTTGG
diptericin_REV	TCCCTGAAGATTGAGTGGGTA
drosocin_FOR	CCATCGAGGATCACCTGACT
drosocin_REV	CTTTAGGCGGGCAGAATG
drosomycin_FOR	GAGGAGGGACGCTCCAGT
drosomycin_REV	TTAGCATCCTTCGCACCAG
metchnikowin_FOR	TCTTGGAGCGATTTTTCTGG
metchnikowin_REV	TCTGCCAGCACTGATGTAGC
Rpl13_For	CGTGGTTTCACCCTGGAG
Rpl13_Rev	TGGTCTTGGCGAAGTTGG

2.1.5 Devices buffers, antibodies and materials

Prouct name	Manufacturer
Water bath Thermostat	Eppendorf AG (Hamburg)
Agarose Electrophoresis Chamber	Biometra GmbH (Göttingen)
My Cycler PCR	Bio-Rad Laboratories GmbH (München)
Vortex Genie 2	Scientific Industries, Inc (New York, USA)

NanoDrop® (ND-1000)	Peqlab (Erlangen)
Glas homogenizer (konisch 1 ml)	VWR International GmbH (Darmstadt)
StepOne user QRT-PCR	Applied Biosystems
Olympus SZX12 stereomicroscope	Oberkochen
Plastic material	Sarstedt AG & Co (Nümbrecht)
Glycogen 5mg/ml	Merck (Darmstadt)
Sodium acetate	Merck (Darmstadt)
6X Loading Dye	MBI Fermentas GmbH (St.Leon-Rot)
$MnCl_2$	Sigma-Aldrich GmbH (Taufkirchen)
dNTPs set	Promega (Mannheim)
Superscript III™ Reverse Transcriptase	Invitrogen Life Technologies (Karlsruhe)
RNase inhibitor (40U/µl)	Applied Biosystems (Darmstadt)
Taq DNA Polymerase (5 U/µl)	Invitrogen Life Technologies (Krlsruhe)
SAWADY PWO DNA polymerase	Peqlab Biotechnologie GmbH (Erlangen)
GeneRulerTM 1 kb DNA ladder	MBI Fermentas GmbH (St.Leon-Rot)
JETQUICK PCR Purification Spin Kit	Genomed (Löhne)
10x Advantage PCR Buffer	BD Biosciences Clontech (Heidelberg)
SciHypChamber	Scienon (Berlin)
GenePix™4000B scanner	Molecular Devices GmbH (München)
NanoDrop® (ND-1000)	Peqlab (Erlangen)
LiferSlip(22x60)	Implen GmbH (München)
PBS, 0.15 M pH7.4	0.14 M sodium chloride (NaCl); 2.7 mM (KCl;8.1 mM (Na_2HPO_4); 1.5 mM KH_2PO_4; adjust the pH to 7.4 HCl
0.3M $NaHCO_3$ pH9	Dissolve 2.52 g of $NaHCO_3$ in 80ml of water; adjust to pH9 with 0.3 M Na_2CO_3; bring up to 100ml with water
10x TBE Buffer	108 mg Tris base; 9.3 mg Na_4EDTA; 55 mg Boric acid; fill up to 1 liter with ddH_2O
20X SSC pH 7	175 g NaCl; 88 g Na_3citrate $2xH_2O$ and adjust to pH 7 with 1M HCl, fill up to 1l with ddH_2O
Rat monoclonal α-GFP	Santa Cruz Biotechnology, Inc. cat: sc-101536
Rabbit polyclonal α-dfoxo	Cosmo Bio Co., LTD. (Tokyo, Japan)
Mouse monoclonal α -Relish	DSHB; anti-relish-C 21F3 (University of Iowa, USA)
Mouse monoclonal α-MMP1	DSHB; 3B8D12 (University of Iowa, USA)
Secondary Dylight-594	JacksonImmunoResearch (Dianova, Hamburg)
Secondary Dylight-488	JacksonImmunoResearch; (Dianova, Hamburg)

2.2 Methods

2.2.1 Hypoxia treatment

Third instar larvae were collected from each genotype and placed in separate vials containing standard *Drosophila* medium for each hypoxia experiment. Six replicate population were collected for each genotype. After a 24-hour recovery period following counting, three of the vials for the wild type strain and each mutant were placed in a sealed chamber at room temperature

that was then flushed with a mixture of 5% O_2 and 95% N_2 (hypoxia). The three other vials for each respective genotype were placed in an identical chamber containing normal atmospheric oxygen concentrations (normoxia). The flies were incubated in the hypoxia and normoxia chambers for four hours, following which they were rapidly removed and takeout the trachea for downstream preparations.

2.2.2 Fly construction

The yw67c23;pkk4-gal4;+/+[113], w*; P[UAS-PGRP-LC.x]2; P[Dipt2.2-lacZ]3, PGRP-LC1 ca1/TM6B, Tb1(Bloomington stock center), w[*]; P-foxo^{21}/foxo^{21} homozygot and y[1] w[*]; foxo w24/ TM6B, Tb, Hue (gift from Marc Tatar) were crossed to double balancer w-; Sp/CyO P[elav-lacZ, ry+]; TM2/TM6 B P[ubx-lacZ, w+](gift from Tobias Storck). First generation of each line was crossed *vis-a-vis* and sorted according to the balancer inserted; the detailed procedure listed in the supplementary data (Fig.38). The homozygous line was sorted and used for downstream experimental procedures.

2.2.3 The binary GAL4/UAS-Expression system

The Gal4/UAS-expression system in *Drosophila* allows the study of ectopic expression of genes in different spatial and temporal expression patterns [116]. The binary system comes originally from the yeast *Saccharomyces cerevisiae* and passes of the transcription factor Gal4 and the accompanying Gal4-binding sites UAS (upstream activating sequence). It is activated in the yeast by presence of galactose and activates the transcription of genes, which are necessary for the galactose metabolism. In the fly the binary Gal4/UAS-expression system the GAL4 gene is placed under the control of a native gene promoter, or driver gene, while the UAS controls expression of a target gene. GAL4 is then only expressed in cells where the driver gene is usually active. In turn, Gal4 should only activate gene transcription where a UAS has been introduced.

For example, by fusing a gene encoding a visible marker such as GFP (Green Fluorescent Protein) the expression pattern of the driver genes can be determined as depicted in figure 8. GAL4 and the UAS are very useful for studying gene expression in *Drosophila* as they are not normally present and their expression does not interfere with other processes in the cell. For example, Gal4/UAS-regulated transgenes in *Drosophila* have been used to alter glial expression to produce arrhythmic behavior in a known rhythmic circadian output called pigment dispersing factor [117]. However, some research has indicated that over-expression of GAL4 in *Drosophila* can have side-effects, probably relating to immune and stress responses to what is essentially an alien protein [118].

The GAL4-UAS system has also been employed to study gene expression in organisms besides *Drosophila*, such as the African clawed frog *Xenopus* [119] and zebrafish [120]. The GAL4/UAS system is also utilized in Two-Hybrid Screening, a method of identifying interactions between two proteins or a protein with DNA.

A big disadvantage of the Gal4/UAS-expression system lies in its lack of temporal inducibility. Because numerous GAL4 drivers are expressed already during the very early phases of embryonic development and during different developmental stages, a specific activation of the expression system is nearly impossible to a certain developmental stage of the fly. Thanks to the development of the expression system TARGET that is dependent on temperature shifts (temporal and on the regional level gene expression targeting) exists the possibility to handle this lacking temporal variability of the Gal4/UAS system [121]. The expression system TARGET comes like the Gal4/UAS system from the yeast and is based on the availability of a temperature-sensitive Gal80 protein. If one integrates ubiquitously expressed Gal80 (driven by the tubulin promotor) into a Gal4/UAS background, one sets up in the F1 generation a TARGET system,

which is depending on the surrounding temperature. At the repressive temperature (19°C), Gal80 completely represses Gal4. Shifting the temperature to 29-30 °C inhibits Gal80, thus removing the repressive effect from Gal4 and expression starts in the Gal4 dependent manner [122].

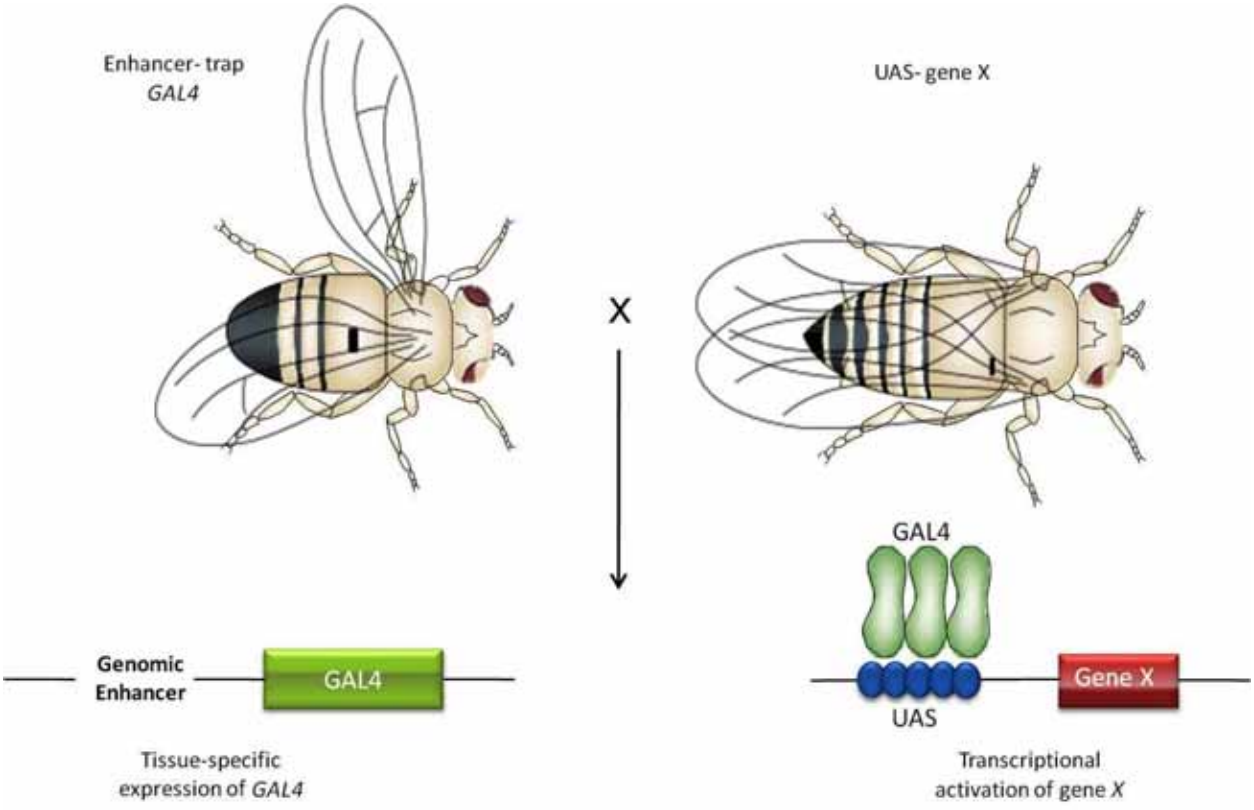

Figure 11: The binary Gal4/UAS-Expressions system of *D. melanogaster*.
Through two separate transposase insertions transgenic fly strains expressing either Gal4-cell and / or developmentally (Driver strain) or a gene of interest under UAS control are made. The resultant F1 generation is expressing the gene of interest in the pattern of Gal4 expression. Adapted from [123].

2.2.4 Infection Experiments

For infection experiments, early 3rd instar larva was confronted with the gram-negative bacterium *Erwinia carotovora* according to protocols used in [5]. Briefly, overnight cultures of the bacterium were centrifuged, concentrated (OD600 = 100) and mixed with banana at a ratio of 1:1. Larvae was allowed to feed for 6 h on these bacteria, subsequently, they were allowed to

feed for another 6 h on normal medium, and the trachea were prepared out of the animals and used for further experiments.

2.2.5 Immunohistochemistry and Microscopy

Third instar larvae (early 3rd instar larvae or young adults, 6-8 days after an imaginal moult) were dissected inside-out in PBS with 4% paraformaldehyde and fixed for 20 minutes. The trachea were washed for six times 10 minutes with 0.1% Triton X-100, 10% NGS in PBS and then incubated with the primary antibody overnight. After washing for 6 times for 10 minutes with 0.1% Triton X-100 in PBS the secondary antibody was applied for 2 h. All antibodies were diluted in the respective washing buffer. In all tissue samples, nuclei were stained with diamidinophenylindole (DAPI) and mounted with 80% glycerol in PBS. Anti-dFoxO antibodies was diluted 1:1000 (Cosmo Bio Co., LTD), anti-MMP1 1:50 (DSHB) and anti-Relish 1:100 from (DSHB) were used in this experiment. Microscopic analysis was performed either with an Olympus SZX12 stereomicroscope equipped with an epifluorescence support or with a Zeiss Axio Imager Z.1 microscope.

2.2.6 Total RNA isolation

The total RNA extracted from the trachea of the 3rd larvae instars was performed using *RNAmagic solution* as follows: Take 20 pairs of dissected 3rd instars larvae trachea in 100µL of *RNA magic*; homogenize flies using a homogenizer for 30sec, then incubate the homogenized material at RT for ≤ 5min. Fill up to 1 ml with RNA magic, add 200µL of chloroform and vortex vigorously for 15-30 sec and centrifuge at 12,000 x g for 20 min at 4^{o}C. Isolate the upper, aqueous layer and precipitate with 1 volume isopropanol, centrifuge at maximum speed for 20 min at 4^{o}C.

Finally, wash the RNA pellet with 1000 µL ice cold 75% ethanol, dry and resuspend in 52 µl of nuclease free water

2.2.7 Preparation of complementary DNA (cDNA)

cDNA is a DNA copy, synthesized from mRNA. The enzyme used is reverse transcriptase an RNA-dependent DNA polymerase isolated from a retrovirus (AMV or MMLV). As with other polymerases a short double-stranded sequence is needed at the 3' end of the mRNA, which acts as a start point for the polymerase. This is provided by the poly (A) tail found at the 3' end of most eukaryotic mRNAs to which a short complementary synthetic oligonucleotide (oligo dT primer) is hybridized (polyT-polyA hybrid). Together with all 4 deoxynucleotide triphosphates, magnesium ions and at neutral pH, the reverse transcriptase synthesizes a complementary DNA on the mRNA template. The protocol is put into practice as follow, 3µl of total RNA was added in a 200 µl sterile tube on ice, mixed gently with 1 µl Oligo(dT7 I) ,1µl SP6rG1 primers (0.5 µg/µl) 0.25µl $MnCl_2$ (40mM), 1 µl of DTT and spun down for 5 seconds in a microfuge. The mixture was incubated at 70 °C for 5 min and the tube placed on ice. Then following components were added: 2 µl of 5 x reaction buffers, 0.5 µl of Ribolock^{TM} Ribonuclease inhibitor (20 U/µl) and 1 µl of 10 mM dNTPs mix. I mixed gently and incubated at 37°C for 5 minutes. In the last step I added 1 µl of Primescript RTase 200u/µl from TaKaRa (200 U/µl) and incubated the mixture at 42 °C for 60 min. The reaction was stopped by heating at 70 °C for 10 min. The newly prepared cDNA could be used directly in PCR reaction or frozen by –80°C freezer.

2.2.8 Preparation of PCR

The PCR reaction was performed by adding 5 µl 10X advanced buffer, 2µl of dNTPs, 1 µl of OdT7II and SP6PCR or sense/antisense specific primer in case of global amplification or specif-

ic gene amplification, respectively. 40µl of water and 0.5 µl of Taq/Pwo mixture (19:1) were added. Mix all previous components and finally add 2µl of sscDNA into a final volume of 50µl.

I mixed the sample by pipetting up and down, loaded it in a thermocycler at 94°C, followed by the next program using: Initial denaturation at start: 94°C for 2 min; denaturation at 94°C for 1 min; annealing at 72°C for 30 seconds; elongation at 59°C for 2 min with 5 seconds time increasing every cycle. The steps 1 to 3 were repeated 28 times and at end the sample was heated at 72°C for 5 minutes to allow complete elongation of all DNA products and then chilled at 4 °C.

2.2.9 Agarose gel electrophoresis of DNA

Agarose gel electrophoresis is a method used in biochemistry and molecular biology to separate DNA or RNA molecules by size. This is achieved by moving negatively charged nucleic acid molecules through an agarose matrix with an electric field (electrophoresis). Shorter molecules move faster and migrate further than longer ones. To pour a gel, agarose powder was mixed with electrophoresis buffer (TBE) to the desired concentration (e.g. 1 % agarose solution), then heated in a microwave oven until it is completely melted (10 min, 400 W). After cooling the solution to about 60 °C, ethidium bromide was added to the gel. Then it was poured into a casting tray containing 2 combs, one at the middle of the gel and the other at one side, about 5 mm from the end of the gel and allowed to solidify at room temperature or in a refrigerator. After the gel had solidified, these combs were removed, using care not to rip the bottom of the wells. The gel, still in its plastic tray, was inserted horizontally into the electrophoresis chamber and just covered with buffer. Samples containing DNA mixed with loading buffer were then pipetted into the sample wells (30 µl), the lid and power leads were placed on the apparatus and a current was applied (100 V, 400 mA). DNA migrates towards the positive electrode. When adequate migra-

tion had occurred (usually after 30-35 min), DNA fragments were visualized by using the gel documentation camera (Molecular Imager Gel Documentation, Bio-Rad, München).

2.2.10 Purification of PCR-Products

The PCR products were purified using a JETQUICK PCR Purification Spin Kit 250^{TM} according to the manufacturer's protocol with small modifications; Step 1). Sample Prepared by adding 400 µl of solution H1 to 100 µl PCR assay and mix thoroughly. Step 2) Load the mixture from step 1 into the prepared spin column. Centrifuge at >12,000 x g for 1 min. Discard the flow through. Step 3) Column washing; re-insert the spin column into the empty receiver tube and add 500 µl of reconstituted solution H2. Centrifuge at >12,000 x g for 1 min. Discard flow through and place the JETQUICK column back into the same receiver tube. Centrifuge again at maximum speed for 1 min. Step 4) DNA Elution Place the JETQUICK spin column into a new 1.5 ml microfuge tube and add 80 µl TE buffer directly onto the center of the silica matrix of the JETQUICK spin column. Centrifuge at >12,000 x g for 2 min. Repeat the last step 3 times at 65°C.

2.2.11 Concentration of PCR products

To 240 µl of purified DNA I added 24 µl of 3 M Sodium acetate pH 5.5 and 600 µl of 100% EtOH. Then, I mixed thoroughly and centrifuged for 20 minutes at maximum speed, washed two times with 75% ice cold EtOH. Subsequently, the pellets were dried and resuspended in 12 µl of TE buffer.

2.2.12 Labeling of total RNA for microarray hybridization

High quality RNA may also be obtained from whole larvae or adult flies, but as with any tissue sample a secondary cleanup may be required. At present we are labeling 600µg of RNA per

sample. The amount of RNA to be labeled can be reduced, but correspondingly the hybridization signal will also decrease.

2.2.13 Synthesis of Non-radioactively Labelled RNA Probes (cRNA)

The reaction based on the method of in vitro cRNA-synthesis [124]. In our laboratories we use Ambion MEGAscript®Kit (Cat #AM1330, AM1333, AM1334, and AM1338). According to the manufacturer's protocol with small modifications in the volume of materials, for one sample, the following components were combined on ice and in the following order. Then the reaction was incubated at 37°C for 4hrs I used to take 2 µl dATP; 2 µl dTCP; 2 µl dGTP; 1 µl dUTP; 1.5 µl aa-UTP; 4.5 µL H_2O; 2 µl 10X reaction buffer; 3 µl template and 2µl enzyme mix to make 20 µl per sample.

2.2.14 Recovery of amplified RNA

The Phenol: chloroform extraction and isopropanol precipitation is the most rigorous method for purifying transcripts. It will remove all enzyme and most of the free nucleotides from MEGA script®Kit reactions. Since the RNA is precipitated, this method can also be used for buffer exchange. To each sample add 1 ml of RNAmagic and 200 µl of chloroform, and mix thoroughly by vortexing. Precipitate the RNA by adding 1 volume of isopropanol and mixing well, then chill the mixture for at least 15 min at –20°C. Centrifuge at 4°C for 15 min at maximum speed, wash with 75% ice cold ethanol, carefully remove the supernatant and resuspend the dried pellet in required volume of nuclease free water.

2.2.15 Quantification of reaction products using the NanoDrop device

The NanoDrop® ND-1000 Spectrophotometer (NanoDrop Technologies) was used to determine: 260/280 ratio, to assess total RNA and aRNA purity; 320/550 and 320/650 ratios, to evaluate Cy3 and Cy5-labelled aRNAs, respectively.

2.2.16 Labeling of aminoallyl amplified RNA (aaRNA)

Remove the Cy-Dyes from the fridge and put in the room temperature until it reaches ambient temperatures, add 36 µl of fresh DMSO. For 3.33 µl of amplified aa-modified cRNA, added 6.67 µl of 0.3 M $NaHCO_3$ pH 9 and 10 µl 1mM Cy3-dCTP *or* Cy5-dCTP. Mix very well by gently pipetting up and down and keep in the dark for 90 minutes.

2.2.16.1 Precipitation of aminoallyl Amplified RNA

Fill up to 1 ml with RNA magic and add 200 µL of chloroform, then vortex vigorously for 15-30 sec and spin at maximum speed for 20 min at 4°C. Transfer the clear, aqueous phase to a new tube, precipitate by adding an equal volume of ice cold isopropanol with gentle invert 7-10 times to mix and centrifuge at 21,000 x g for 15 min at 4°C. Wash with 1000 µl of 75% ice cold EtOH and elute the dried pellet in 11 µl ddH_2O.

2.2.16.2 Probe Hybridization to Microarray Chips

For hybridisation I used the microarray chips produced by Canadian *Drosophila* Micoarray Centre (*http://www.microarrays.ca/index.html*). Gene expression analysis was performed by using the *Drosophila* OLIGO 14k_version1 gene chip (Canadian *Drosophila* Microarray Center, University of Toronto, Canada). This chip contais 48 subarray, each contais 336 spot. Total of 16.128 spots are available on each chip. 14,444 are transcript-specific oligonucleotide and the other controls to lapse. All transcript-specific spots are presented as duplicates.

I prepare a new coverslip by immersing in ice-cold Ethanol, wash the hybridization chamber with ddH_2O and leave it to dry in the room teperature. The hybridization solution for all arrays used has the following recipe: Per 54 µl DIG Easy Hyb I added:

2.88 µl 10 mg/ml yeast tRNA

2.88 µl 10 mg/ml salmon sperm DNA

Adjust the probes to 200 pmol each, mix with the buffer and take 40 µl of the previous mixture into a 500 µl tube; incubate at 65 °C for 10 minutes to denature the probe. Set the coverslip on a raised surface over the microarray slide and pipette the denatured probe between them avoiding any bubbles introducing. Close the hybridization chamber, enclosed with Aluminum foil, and incubate in a 42 °C hybridization oven for 16-18 hours.

2.2.16.3 Washing of the microarray slides

Carefully remove the cover of the chamber and the cover slip. In a Falcon tube that is wrapped with aluminum foil, and filled with 1X SSC insert the slide, stir for 90 minutes. Wash 15 minutes 2 times with 1X SSC, 0.1 % Triton x-100 at 60°C, and with 0.1 X SSC, Triton x-100 at 37 °C for 10 minutes 2 times. Immerse the slide in a coplin jar filled with 0.1 XSSC for 30 seconds and in ddH_2O for 10 seconds. Dry the rest of water with a stream of nitrogen.

2.2.16.4 Image acquisition and analysis

The slides were scanned by using the GenePix^{TM}4000B scanner (Axon Instruments, Molecular Devices, München, Germany), the based scanner capable of multi-channel fluorescence scanning, was used to analyze and scan the slides at the two wavelengths to detect emission from both dyes. Random areas of the slide were examined to determine proper exposure for each channel. The images were analyzed photometrically by the GenePix Pro 6.0 from Axon Instruments/Molecular Devices Corp to identify the arrayed spots and to measure the relative

fluorescence intensities and ratios for each spot. The signal intensity was calculated as the mean pixel value minus the local regional background. Gene expression could then be observed as an increase or decrease in gene expression relative to the fly base information.

2.2.16.5 Bioinformatics tools and analysis

Gene expression analysis was performed by using the *Drosophila* OLIGO 14k_version1 gene chip (Canadian *Drosophila* Microarray Centre, University of Toronto, Canada). The slides were scanned by using the GenePix™ 4000B scanner (Molecular Devices, München, Germany). For spot finding and generating preliminary results, files of the scanned images were analyzed using GenePixPro version 6.0, whereas data normalization, quality assurance and control, filtering and clustering were carried out with *Acuity 4.0* (Applied Biosystems, Germany). Venn diagram analyses were performed with the online tool Venn diagram generator of the pangloss laboratory (*http://www.pangloss.com/seidel/Protocols/venn.cgi*)

2.2.17 Relative quantification of qRT-PCR data

In order to perform relative quantification, all C_t values must be transformed into relative quantification data, expressed as $2^{-\Delta\Delta Ct}$ [125]. Crossing threshold data can be imported into Excel from real-time PCR platforms and subsequent analyses can be performed in Excel. During $2^{-\Delta\Delta Ct}$ analysis, each sample (run in triplicate) was treated separately. The mean C_t of each sample and standard deviations were calculated. Standard deviations should be within 1 C_t, and if there were outliers (>2 standard deviations), these data points were removed from the analysis. The means of each sample were used for analysis. The first step of analysis ($^{\Delta}C_t$) was to normalise all the samples with respect to the least expressed sample, thus subtracting the highest C_t value from the C_t value of each sample. In this step, the least expressed sample had a $^{\Delta}C_t$ value of 0 and all the other samples had negative values. Hence all data was expressed relative to the expression of the

least expressed gene. The second step was to perform the function ($^{\Delta}C_{t\ sample} - {}^{\Delta}C_{t\ reference}$), which gives a $^{\Delta\Delta}C_t$ value. The third step was to calculate $2^{-\Delta\Delta Ct}$, which yielded the expression ratio (as a positive integer) for each individual sample. After performing the $2^{-\Delta\Delta Ct}$ calculation for each sample, we calculated the means for each group in addition to determining the standard deviation and standard error of the mean (SEM) thus providing a relative expression ratio (in arbitrary units) and variation between ratios. The expression ratio data were amenable to statistical tests such as analysis of variance (ANOVA) to the expression ratios.

2.2.18 Statistical analysis

Kaplan-Meier survival analysis was used to compare lifespan between groups; all other data were analyzed using student t-test or one-way ANOVA and graphed using GraphPad Prism 5.0 (GraphPad Software, Inc., San Diego, CA).

Results were expressed as group mean ± SEM. Difference in means were considered statistically significant when $p < 0.05$, unless otherwise stated. Analyses of qRT-PCR data were done using the Relative Expression Software Tool 2009 (REST2009), a Qiagen freeware.

3. Results

3.1 The response to hypoxia is time dependent

Hypoxia experiencing tissues show different types of responses, both at the morphological and the transcriptional level. The response to hypoxia is dose-dependent, meaning that increasing the time of treatment leads to higher overall treatment doses. To specify the most effective dose of hypoxia, which gives the optimal response while keeping most animals alive I did time course experiment with various time point and various concentrations of oxygen (O_2 1%, 5% and 0% O_2 - nitrogen only). Animals were confronted with these different doses of hypoxia for 0 hr, 1hr, 2 hr, 4 hr, 6hr, 8 hr 16 hr and 24 hr respectively, as shown in Figure 12. All experiments were performed with *Drosophila* third instar (L3) larvae and the matching controls (21% O_2).

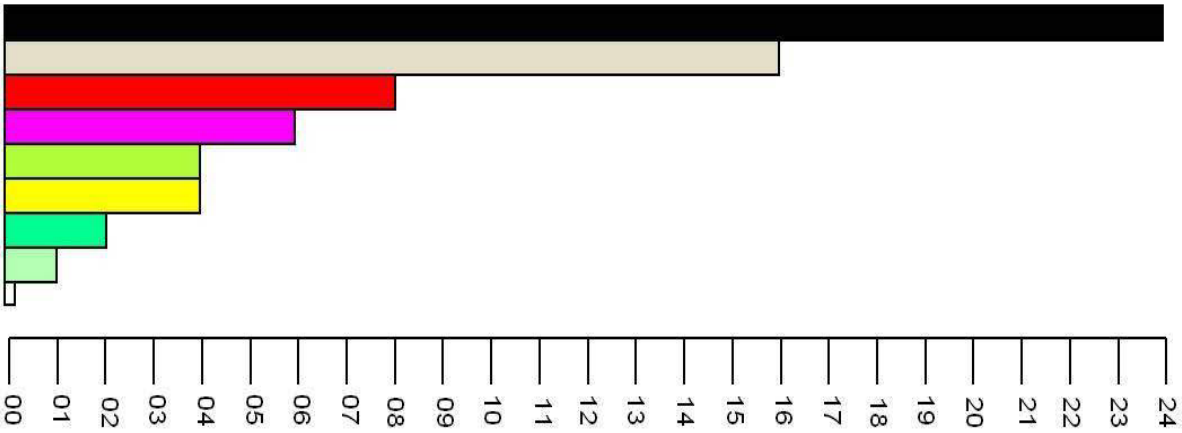

Figure 12: Time courses of hypoxia experiments.
Schematic diagram represents the periods of hypoxia treatment used in my experiments.

After the end of the experimental time, the animals were placed on 1XPBS and the trachea were prepared manually followed by mRNA isolation to quantify the *drosomycin* gene expression using qRT-PCR. I found that in cases of N_2 only (severe hypoxia) most of the animals died after one hour of treatment, thus I excluded treatment with N_2 for all future experiments. A very similar result was found in the case of 1% O_2, and I considered this also as very severe hypoxia

leading to severe damage and finally to death. *Drosomycin* expression increased after 1 hr of hypoxic treatment and reached its maximum after 4 hr and then declined gradually (figure 13).

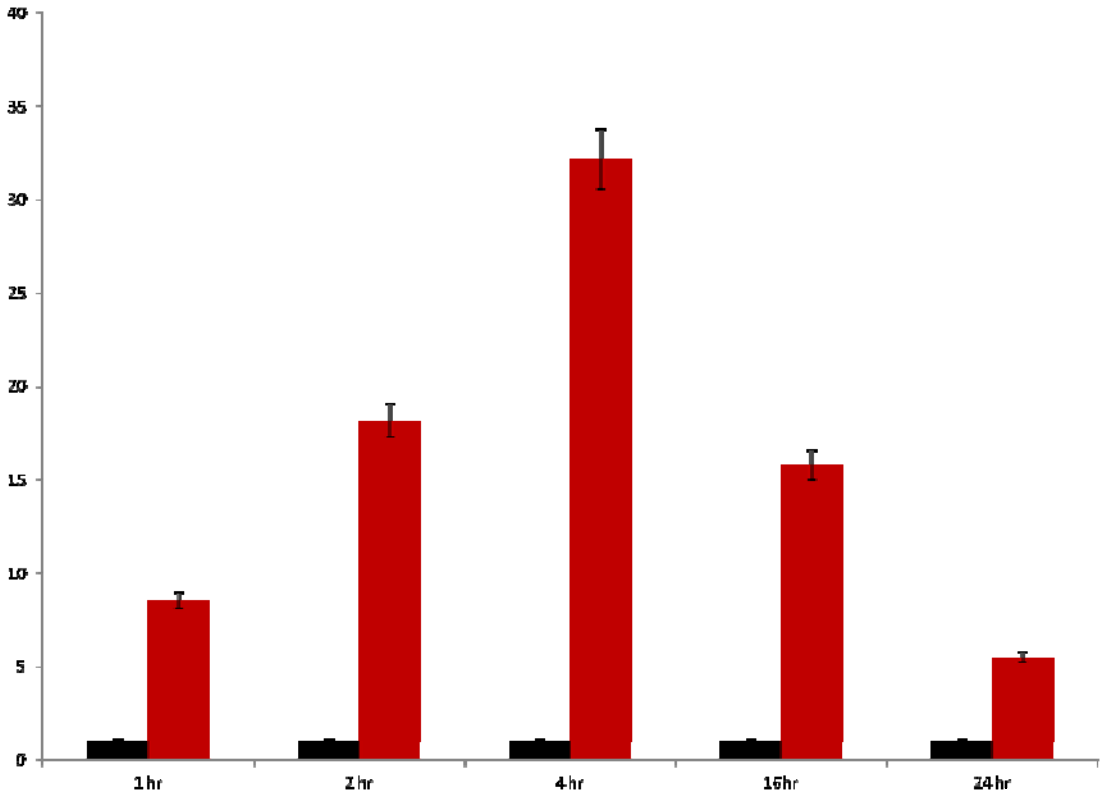

Figure 13: Hypoxia was applied for different periods.
Drosomycin mRNA levels were quantified at different time points (0, 1, 2, 4 and 24 hr) in hypoxia (5% oxygen) using wild-type animals (w^{1118}). The yellow column show the control samples; blue are those held in 5% oxygen.

3.2 Induced expression of *drosomycin* during hypoxia

Drosomycin is an inducible antifungal peptide of 44 amino acids initially isolated from bacteria-challenged *Drosophila melanogaster*. Using the *drosomycin-gfp* [yw (P(w-, drom-gfp)D4, P(ry+, dipt-lacZ)(162:7)2] as well as six other antimicrobial peptide-*gfp* reporter lines showed that only *drosomycin-gfp* is activated upon hypoxia in the airway of larvae and adults as depicted in Figure 14.

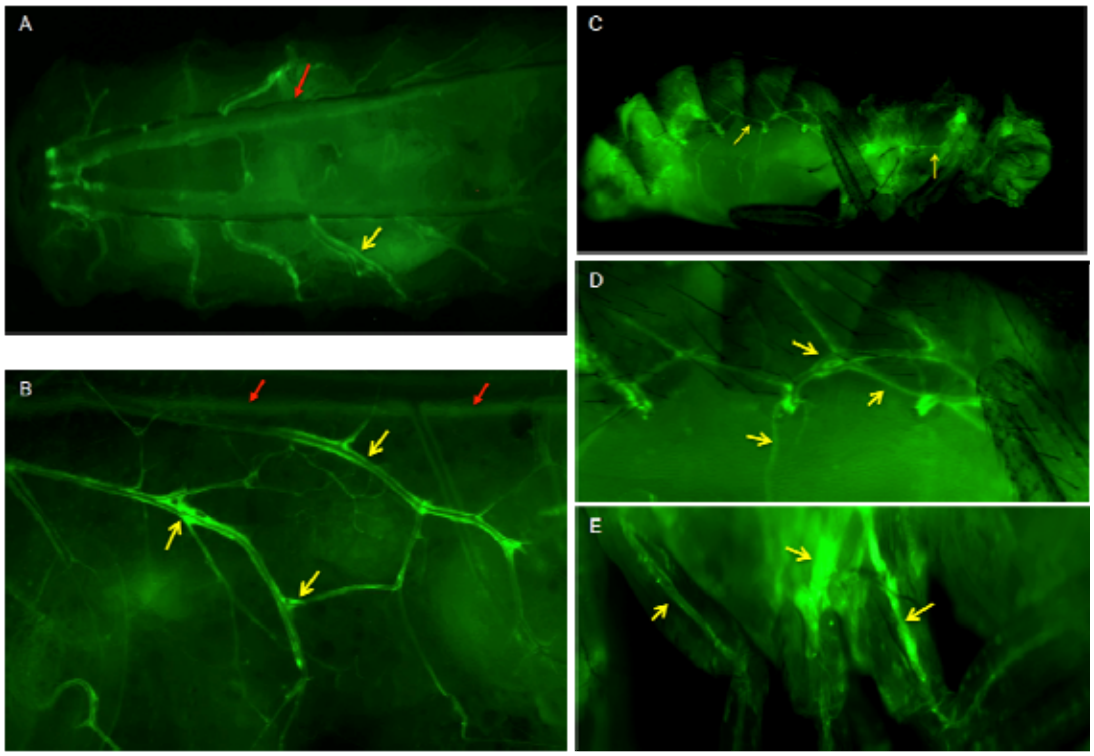

Figure 14: Induction of *drosomycin-gfp* expression upon hypoxia.
Hypoxia treatment of a *drosomycin* reporter (*drom-gfp*) induced expression of *gfp* in the airway epithelium only (A-E). In the overview (A); expression is confined to secondary and terminal branches of the airway system (yellow arrows), whereas the major trunks show no or little expression (red arrows). At a higher magnification (B), expression in especially secondary branches and terminal cells is even more evident. Using the same line, we could also observe the hypoxia-induced expression of the *drosomycin* reporter in the adult tracheal system (C-E). At low magnification, the peripheral tracheal system is visible through the cuticle (yellow arrows, C). At higher magnification, tracheal structures directly next to the spiracular openings (D) and within the legs (E) are easily visible.

3.3 Hypoxia induced structural changes in the airway epithelium

Upon mild hypoxia (5% O_2), an interesting phenomenon was observed. The thickness of primary, secondary and tertiary airway branches was significantly increased (Figure 15 C, D bottom panel). If compared with control regions (control: Fig 15 A and B upper panel), I was able to quantify this effect as the difference between both experimental groups as shown in Figure 15E. These results are in line with previous observation where animals were confronted with the bacteria *Erwinia carotovora.* They also show a remarkable increase in the thickness of the airway epithelium [65]. A comparable morphological modification was not observed in control animals, indicating that it represents a direct response to the strong and prolonged activation of stress

relevant systems. The general organization of the airways as a single cell-layered epithelium is not affected, because even in those parts of the airways, in which we observe this type of epithelial thickening, cell nuclei are organized in rows along the airway. In addition, animals expressing GFP as a marker in their airways (btl-gal4 X UAS-gfp) that experienced hypoxia show a high difference in the morphology of their terminal structures (figure 16). This indicates that hypoxia can induce morphogenesis of this subset of tracheal cell by increasing their number of branches in case of low oxygen.

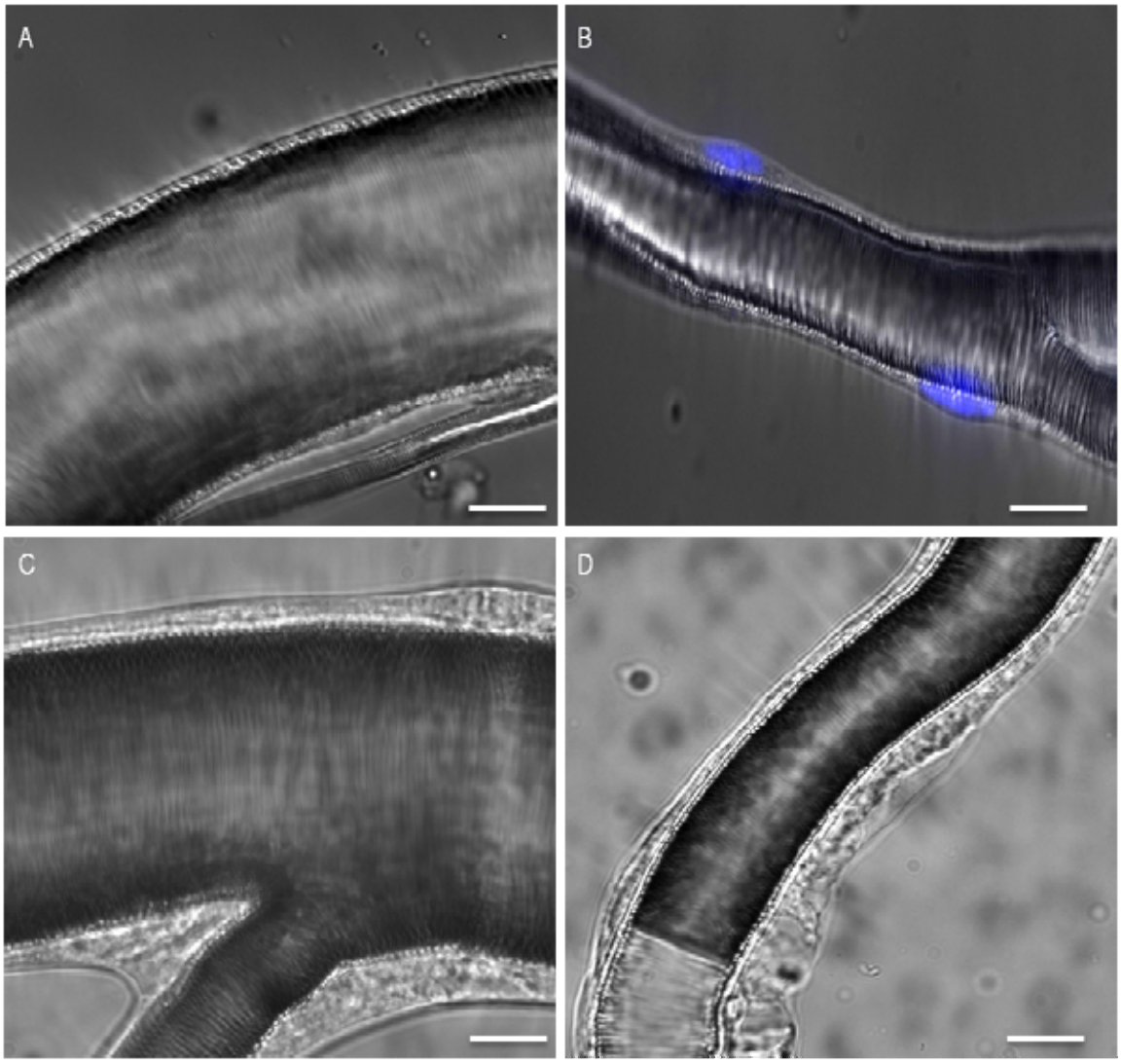

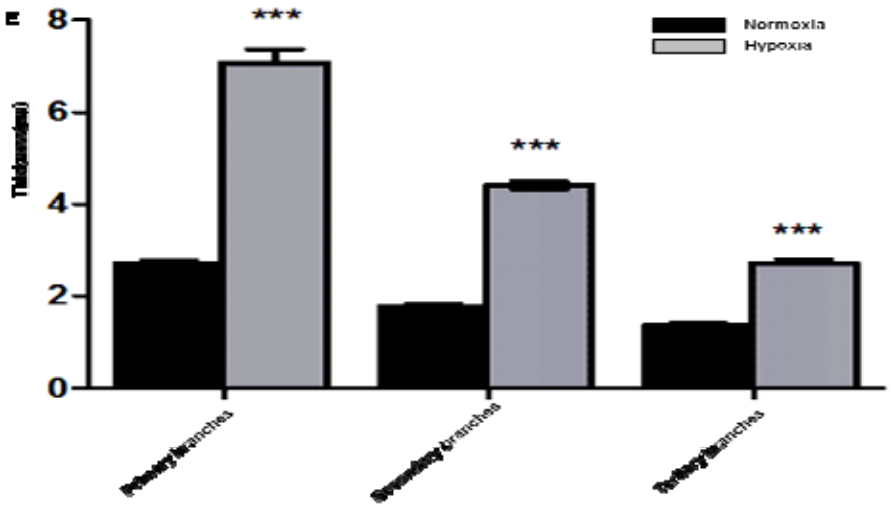

Figure 15: Changes in the morphology of the airway epithelium following hypoxia.
The upper panels show the primary (A) and secondary branches (B) of the trachea in normoxic condition with normal (thin) epithelium, while the lower panels show the primary (C) and secondary (D) branches of the tracheal system under hypoxia. B) Measurements of the primary secondary and tertiary tracheal branches, in normoxia (black bars) or hypoxia (gray bars). All values represent the means ± SD (*** $p<0.0001$).

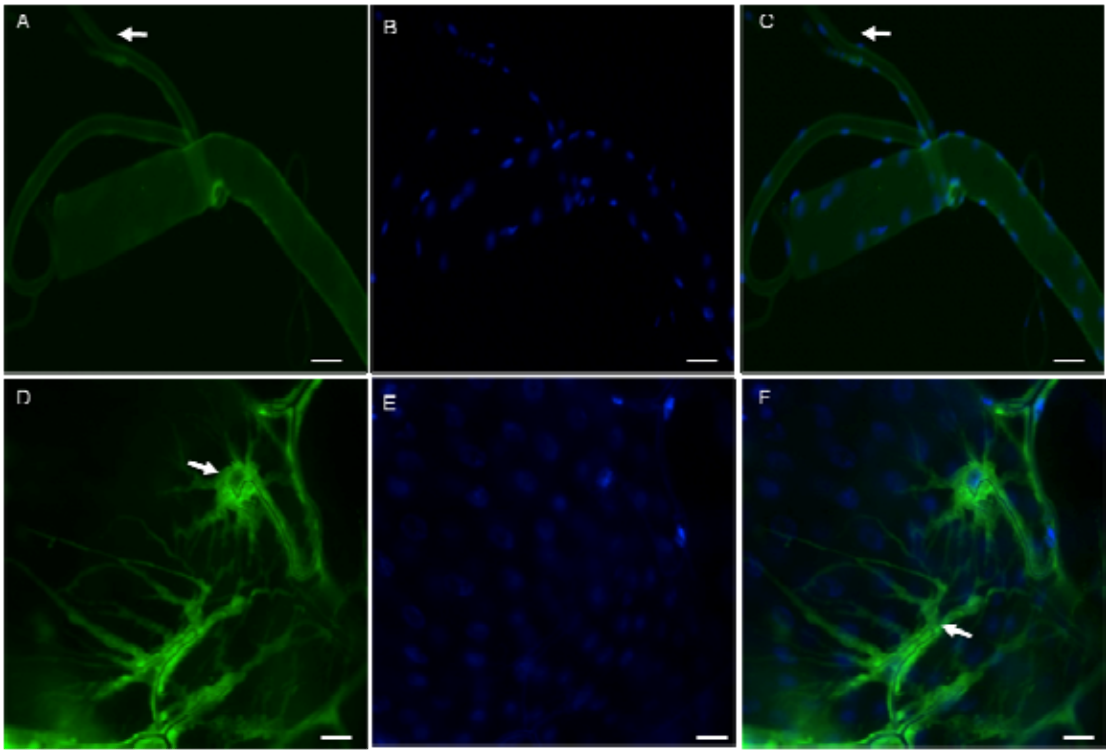

Figure 16: Structural changes of the airway epithelium following hypoxia treatment.
Terminal branches of the animals carrying the construct *Btl-gal4 X UAS-gfp* following hypoxia were photographed. Animals under normoxia in the upper panel (A-C) show the normal trachea architecture. Upon hypoxia extensive changes in the number of terminal branches were observed in the lower panels (D-F). A, D GFP channel, B, E DAPI channel, C, F overlay.

3.4 Translocation of HIF-1 upon hypoxia

For the design of a new Hypoxia Responsive Elements (HRE) reporter, the mammalian lactate dehydrogenase A (LDH-A) gene, which is hypoxia responsive and well conserved in flies was selected [115]. The mammalian LDH-A hypoxic enhancer includes two HREs separated by an 8-bp spacer and a cyclic AMP responsive element (CRE) located 16 bp further downstream. Both HREs and the CRE consensus sequences have been shown to be necessary for strong hypoxic induction in mammalian cells [115, 126]. Using an LDH-Gal4/UAS-nGFP reporter strain that induces nuclear expression of GFP under transcriptional control of the murine LDH-A enhancer [115], I could show that this reaction induces a highly reproducible hypoxic response primarily in the airway epithelium as depicted in Figure 17. This implied that the observed response of total larvae to hypoxia may reside primarily in the airway epithelium as a dominant response target for hypoxia.

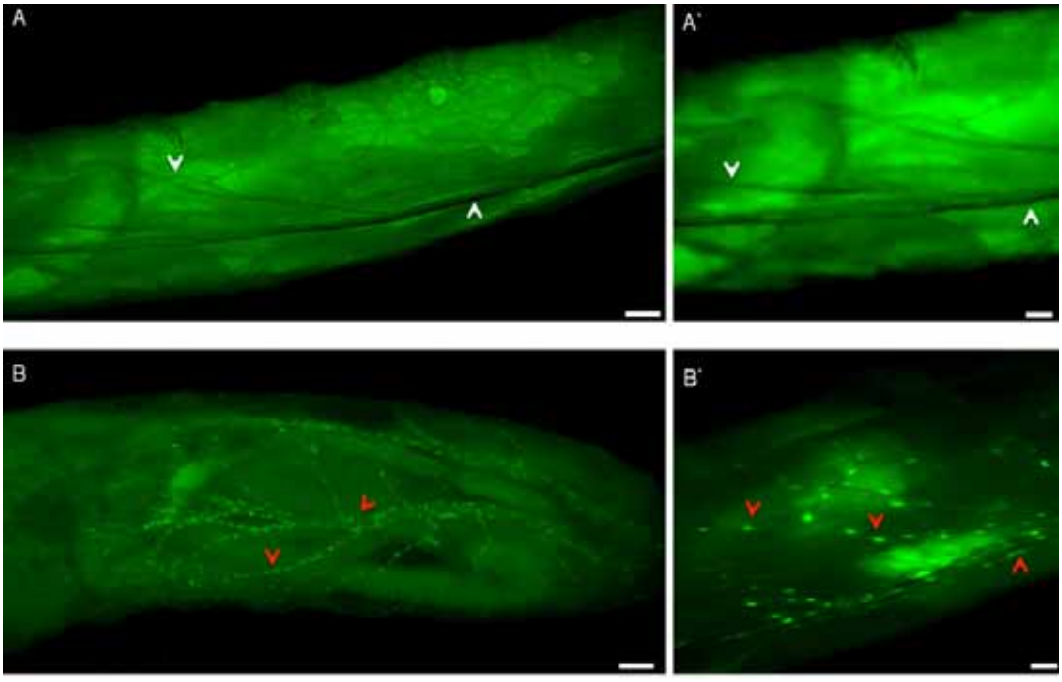

Figure 17: HIF nuclear translocation upon hypoxia treatment.
Expression of the LDH-Gal4/UAS-nGFP in normoxia and hypoxia of early third instar larvae. These larvae were subjected to a brief period of mild hypoxia (4h, 5% oxygen). Nuclear expression of GFP was observed in the airway epithelium only (red arrows). Background staining of the intestine is due to auto-fluorescence of ingested material.

3.5 dFoxO activation following hypoxia

To identify the underlying mechanism of induced *drosomycin* expression, I used transgenic animals, where XFP tagged transcription factors (UAS-*relish-yfp*, UAS-*dorsal-gfp*, UAS-*dif-cfp* [127], and UAS-*foxo-gfp* are ectopically expressed in the airways (driven by pkk4-Gal4, a tracheal epithelium specific driver line) [113] and subjected them to hypoxia. Neither Relish or Dif nor Dorsal showed any nuclear translocation following hypoxia (Fig. 18 A, B; It displayed is only UAS-dorsal, both other experimental setups yielded identical results). Under normoxic conditions, dFoxO-GFP is localized in the cytoplasm of the airway epithelial cells (Fig. 18C). In contrast, we observed an almost complete translocation of dFoxO following hypoxia (Fig. 18D, E). Using specific antibodies to dFoxO (GST-dFoxO) from Cosmo Bio Co., LTD, I observed a very similar reaction to hypoxic conditions. As observed for the expression of the antimicrobial peptide *drosomycin*, the reaction starts at the most terminal branches of the tracheal system and reactions in the major branches are seen only in few animals at later phases of the treatment. Even after the hypoxic treatment ended, dFoxO-GFP stayed for a certain time (usually more than one hour) in the nucleus before re-entering the cytoplasm. The time before re-entering the cytoplasm depended on the period of hypoxia, meaning that the longer the hypoxic treatment, the longer stayed dFoxO-GFP in the nucleus after return to normoxic conditions.

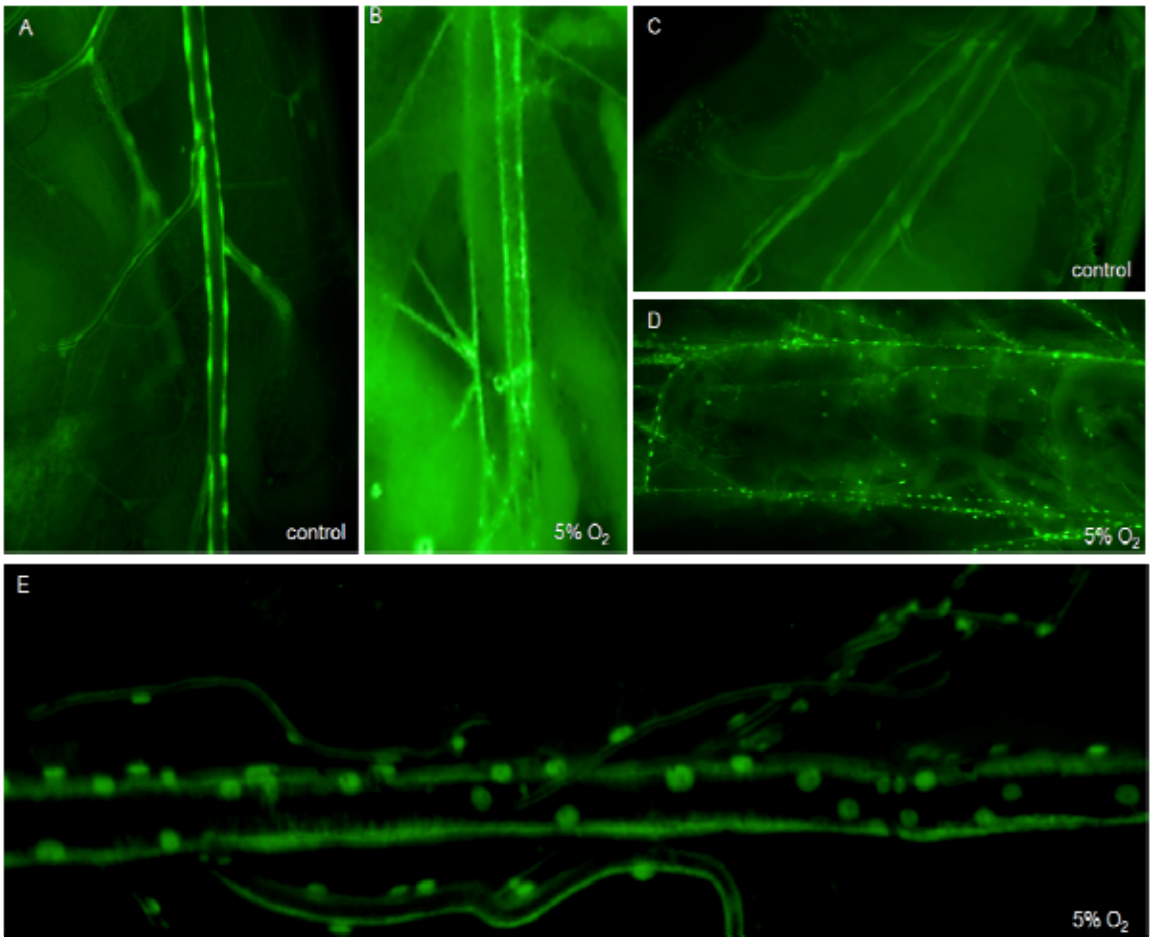

Figure 18: Role of transcription factors for the response to hypoxia.
Animals expressing GFP-tagged transcription factors were used for all experiments. *Dorsal-gfp*, either under normoxic conditions (A) or hypoxic conditions (B) didn't show any induced translocation into the nuclei of airway epithelial cells. Animals expressing *foxo-gfp* in the airway system also show a cytosolic expression during normoxia (C), whereas those subjected to hypoxia show a clear translocation (D, E). Fig. D shows an overview of a complete animal, whereas E shows an isolated trachea.

3.6 Hypoxia-induced AMP gene expression

To demonstrate the immune response of the tracheal system in response to hypoxia, we used the w^{1118} animals as wild-types to quantify the expression levels of antimicrobial peptide genes (AMPs). In this experiment, which the animals confronted with hypoxia (5% O_2) were compared to its parental control at normoxic condition (21% O_2). We analyzed the immune response of whole larvae using RT-qPCR, and found that the expression of *cecropin, attacin, drosocin* and

drosomycin were upregulated upon hypoxic treatment while the other three AMP genes *mechnikowin, defensin* and *diptericin* were downregulated as depicted in figure 19.

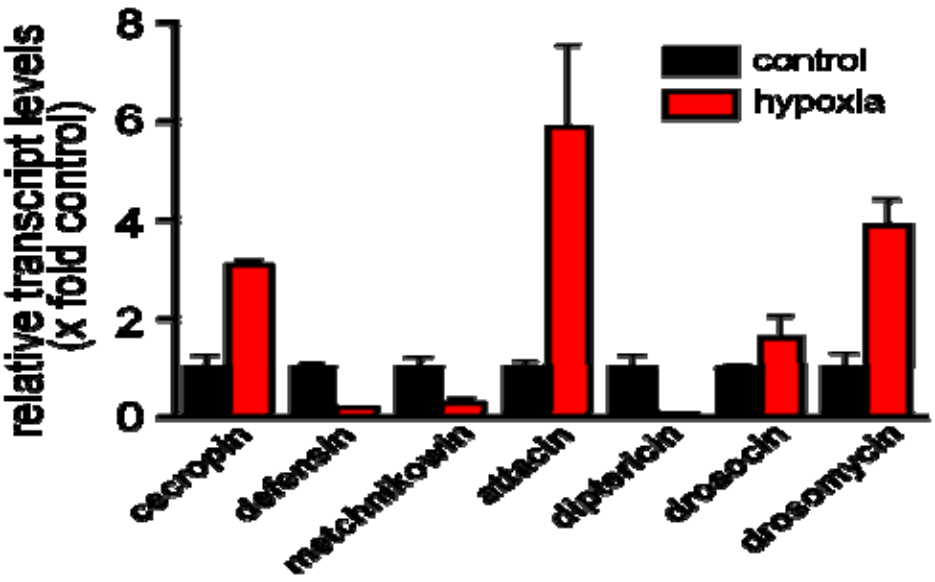

Figure 19: Antimicrobial peptides relative expression during hypoxia.
3rd instar larvae of wild-type flies (canton-S) were either subjected to hypoxia (red bars) or held under control conditions (black bars) and relative transcript levels of the antimicrobial peptide genes indicated were quantified using qRT-PCR. (Each experiment was performed at least three times in duplicate; * means $p<0.05$, data kindly given from K. Uliczka).

3.7 Induced expression of AMPs is dFoxO dependent

To dissect the molecular mechanism underlying the immune response to hypoxia, I used mutants defective in either the IMD-signalling pathway or those devoid of functional dFoxO proteins to quantify the regulation of *drosomycin*, as the most reliable readout, following hypoxia. IMD-deficient mutants, which are defective in the sole pathway of the fly's innate immune system converging onto activation of NF-κB factors operative in the airway epithelium [32, 41, 65], show a slightly reduced, but nevertheless, significant upregulation of drosomycin expression following hypoxia (represented in Figure 20). In addition, knockdown of SIMA, which is part of the HIF-machinery, does not impair this response completely, indicating that the hypoxia-

dependent increase in *drosomycin* expression does not depend on HIF-1 signaling. In contrast, animals defective in dFoxO ($foxo^{21}$/$foxo^{24}$ transheterozyotes) show no upregulation of *drosomycin* expression in response to hypoxia treatment, indicating that dFoxO is essential for this response (Fig. 20). Together, these data show that dFoxO can activate AMP expression independently of the NF-κB-dependent innate immune pathways.

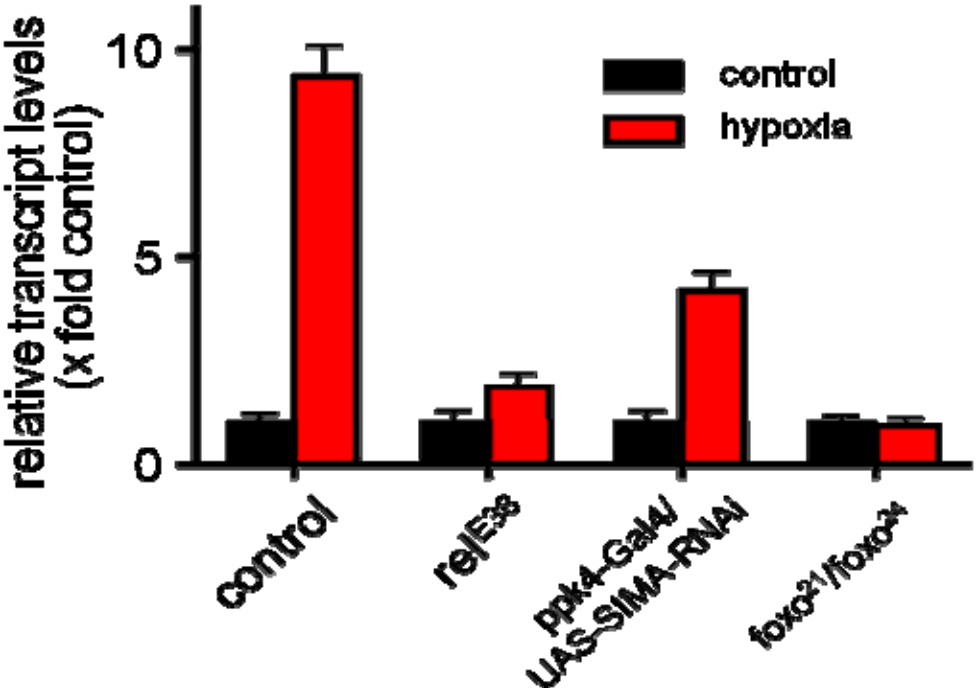

Figure 20: Analysis of the hypoxia induced immune response in the airway epithelium.
Quantitative real-time PCR using isolated airways from control animals (held under normoxia) and those that were subjected to hypoxia (4h, 5% oxygen). Values are means of at least three independent experiments. Mean control values (normoxia) were set as 1. Mean values ± S.D. are given.

To evaluate the possibility if dFoxO can directly induce *drosomycin* expression, I analysed the putative *drosomycin* promotor region for dFoxO binding sites *in silico*. This motif binding analysis for different genes on the promoter region of *drosomycin* showed that dFoxO has nine binding sites with the consensus sequence (gggctggggg) while there is no binding site for the Forkhead gene FKH (tctggccatg). In addition, the terminal JNK-pathway products Basket (gaccggaacg) and Puckered (ccgcaaagtc) have three and four binding sites, respectively. Concomitantly, the IMD core factor Relish has three motif binding sites (atcggcgccc) and finally insulin

receptors (InR) were defined by the consensus (gtcttcactg) has two binding sites as depicted in Figure 21. These data demonstrate that dFoxO-activation would be sufficient to induce *drosomycin* expression.

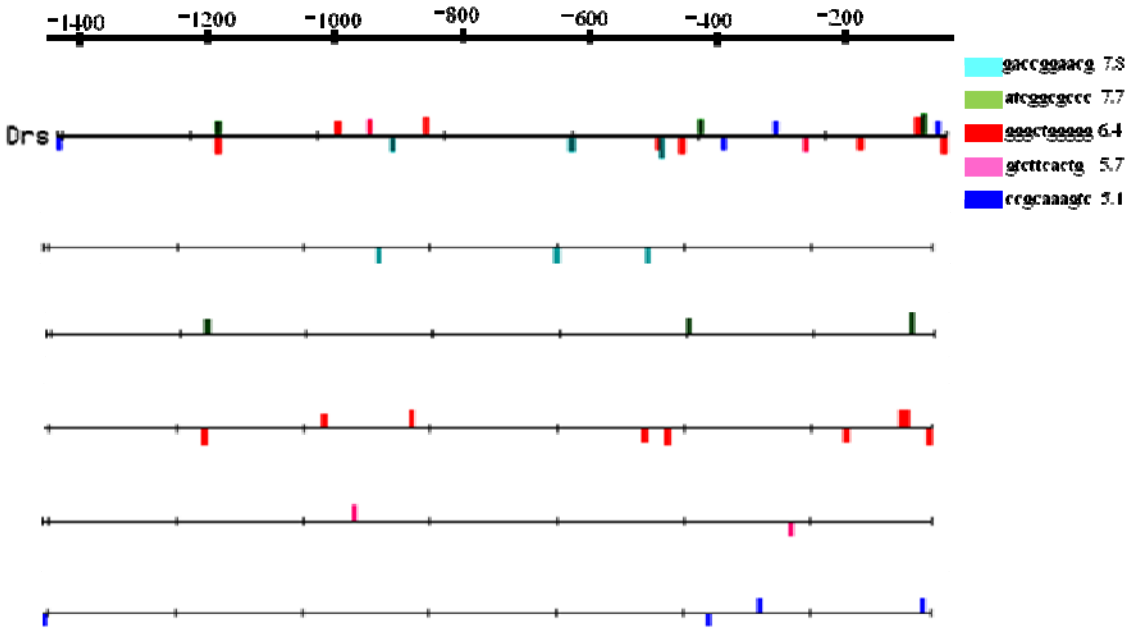

Figure 21: Motif binding sites on the *drosomycin* promoter region.
Bioinformatic analysis for the promotor region of *drosomycin* for various relevant transcription factors showed that different binding sites were identified for NF-κB (blue) and insulin responsive elements (green). On the other hand, there are no binding sites for the *Drosophila* fork head-A family member dFoxA (Orange; not shown), while the other representative family member dFoxO (red bars) is the most dominant one. As shown above, the upward bars indicate forward orientation; downward bars indicate reverse orientation. Analysis was done using the RSAT website (http://rsat.ulb.ac.be/).

3.8 Hypoxia induced immune responses are presumably mediated by JNK/dFoxO signaling

The JNK-pathway is activated by different types of stressor (e.g. UV irradiation). Previous studies using cell cultures suggested that JNK signaling might play an important role in the control of apoptosis after DNA damage [128-130]. To test the hypothesis whether JNK signaling is required for inducing *drosomycin* expression in the *Drosophila* trachea upon hypoxia, third instar larvae carrying a dominant negative basket allele (bsk^{DN}) were exposed to mild hypoxia (5% O_2), subsequently trachea were dissected and stained with the anti-dFoxO antibody. Com-

paring the nuclear translocation of dFoxO of those animals treated with hypoxia with their matching controls (21% O_2) showed no dFoxO translocation into the nucleus upon hypoxia in those animals expressing Basket^{DN} as shown in Figure 22.

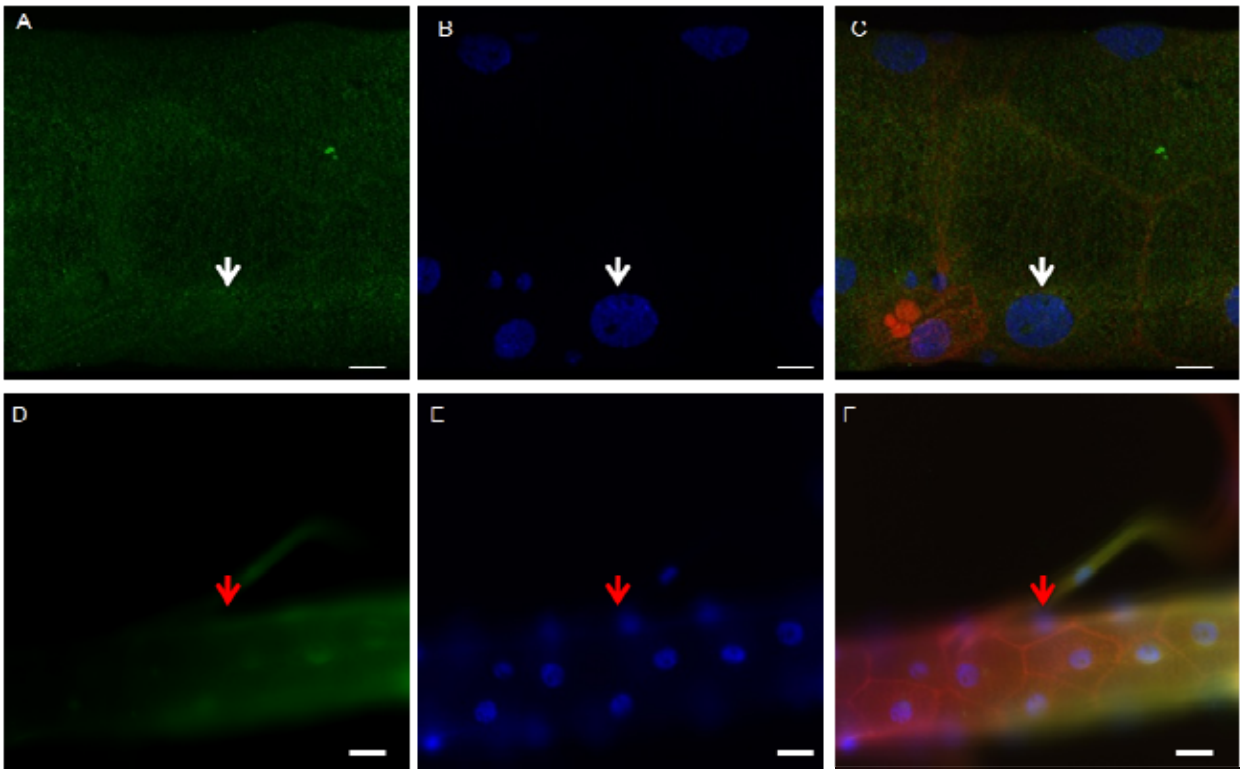

Figure 22: Nuclear translocation of dFoxO depends on JNK-signaling.
The upper panel A-C shows the pkk4-GAL4 X UAS-bsk^{DN} either under normoxia and stained with anti-dFoxO (green) and anti-*mmp1* antibodies (red) respectively. The comparison with those animals that experienced hypoxia (bottom panel D-F) revealed no translocation for dFoxO while induced expression of *mmp1* gene can be observed. A, D, anti-dFoxO - green, B, E, DAPI - blue, C, F merge + anti-MMP1 – red.

To confirm whether the JNK signaling activity can stimulate dFoxO *in vivo*, an additional JNK signaling output is expression of the puckered gene. Puc-GAL4 thus serves as a marker for JNK activation. Puckered-GAL4 (Puc^{E69}) animals were treated with hypoxia as previously and the level of gfp expression was monitored. The activation of the puckered promotor was clearly obvious if compared to those animals held under normoxic conditions (Figure 23).

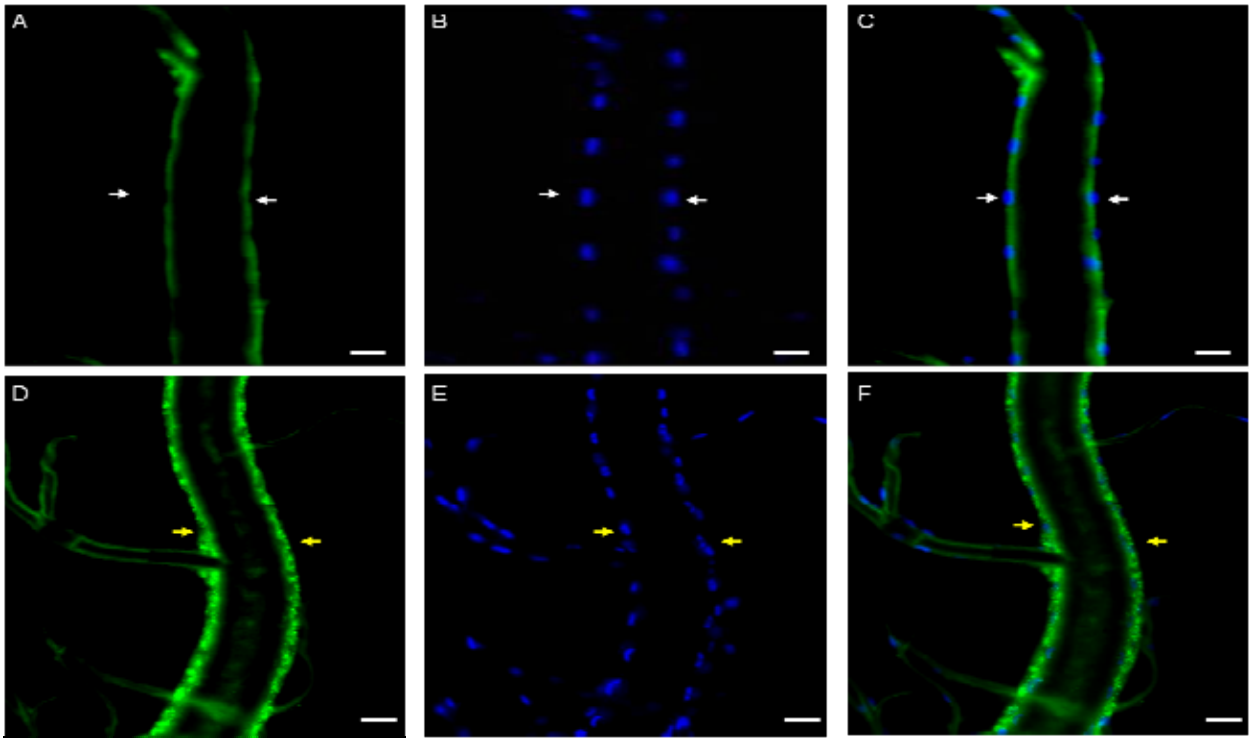

Figure 23: Activation of the JNK-pathway monitored by a puckered-Gal4 marker.
The puc^{E69} allele was crossed to UAS-GFP. The upper panel showed the trachea of the animals held under normoxia(A-C, white arrows). Upon hypoxia (4hrs at 5% O_2) gfp was expressed more strongly indicating activation of puckered expression in the airway epithelium (D-F; yellow arrows). A, D, GFP – green, B, E, DAPI – blue, C, F, merge.

3.9 dFoxO defective animals are less resistant to hypoxia

Performing life span assays is among the most powerful ways to elucidate the effect of a certain mutation at the animal level. In order to overcome technical problem I used second instar larvae for the survival assay. Twenty first instar larvae from both strains (w^{1118} and dFoxO defective mutants). Animals were transferred into special small vials (6 cm x 2 cm) supplemented with 1 cm of standard cornmeal media and allowed them to recover for twenty-four hours before using them for assays. Both strains were subjected to hypoxia (5% O_2) by placing them into the hypoxia chambers.

Different time points were chosen to monitor the larval health and counting the fraction of animals still alive. Survival rates were quantified at least three times independently. At 5% O_2

dFoxO mutant larvae have a significantly decreased survival rate in comparison to wild-types. All dFoxO defective animals were dead after 16h, whereas wild-types survived up to 24h (figure 24).

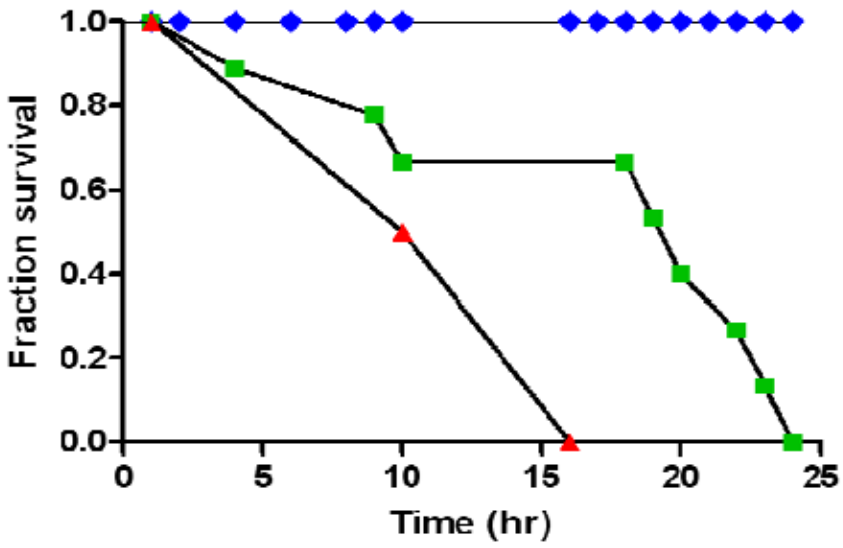

Figure 24: Predictive analysis of dFoxO mutant resistance to hypoxia.
Survival assay of w^{1118} under normoxic conditions (♦ blue) and hypoxia (■ Green). dFoxO transheterozygotes *foxo*$^{21/24}$ represented by (▲ red) under hypoxia, data of normoxic mutant dfoxo is not represented because it has the same values as wilde type.

3.10 Hypoxia-induced transcriptional regulation in dFoxO defective animals

For these experiments, both, w^{1118} as well as transheterozygotes *foxo*$^{21/24}$ were subjected to hypoxia. Following manual dissection of the trachea, this material was used as probes for DNA-microarray analyses. Transcripts were identified either as being induced or repressed following hypoxia. Data analyses were done using Acuity 4.0 Software (Applied Biosystems) and revealed a total of 1298 and 1041 transcripts as being induced or repressed following hypoxia. 426 genes were identified as significantly upregulated (±1.5 fold) in wild type animals while 106 genes in the mutant strains. I analyzed the expression of each of these genes by hierarchical clustering (Figure

25). Interestingly, dFoxO mutants exhibit a lower difference in hypoxia-induced genes that were regulated if compared with wild-type flies.

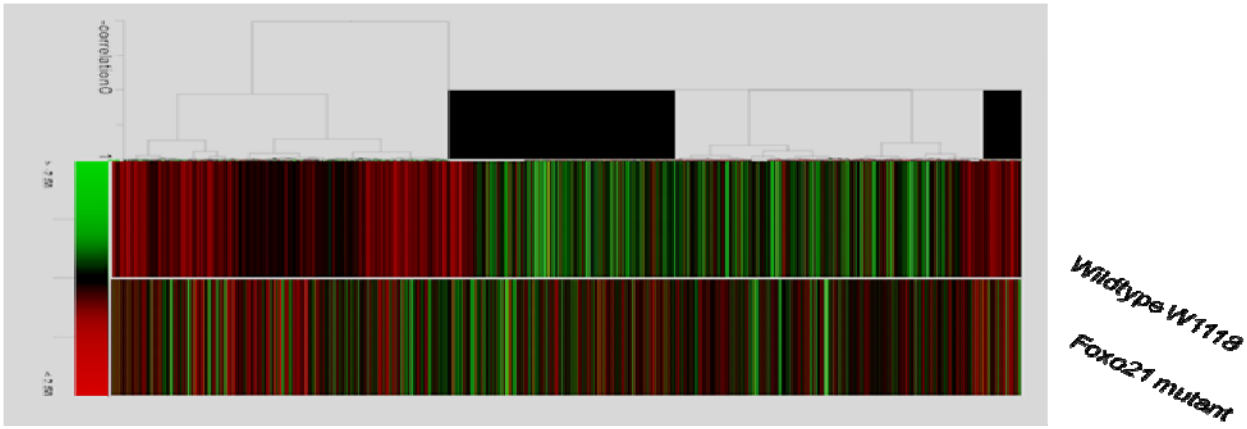

Figure 25: Hierarchical clustering of hypoxia in wild type and dFoxO mutant.
Hierarchical clustering of hypoxia modulated transcripts with significantly perturbed expression levels in wild type and mutant strain. Rows represent the average expression levels of transcripts from 3 biological replicates for the strain indicated in each column.

In order to identify immune-relevant genes among the regulated ones, I used Venn diagram analyses with a comprehensive list of immune relevant genes (Lemaitre lab – *http://lemaitrelab.epfl.ch/page-7757.html*) as depicted in figure 26 and table 1.

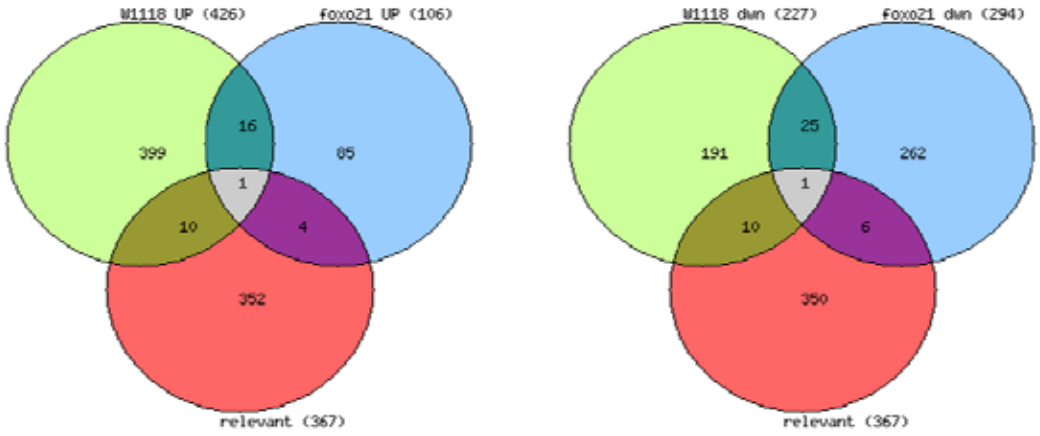

Figure 26: Venn-diagram analysis of wild type and dFoxO.
Venn diagrams comparing either up- or downregulated genes of wild-type flies (left), or dFoxO defective mutants (right) with the comprehensive list of immune relevant genes.

Table 1: List of immune relevant genes regulated upon hypoxia in wild-type and dfoxo^{21} mutant animals.

Gene ID	NAME	SYMBOL
Upregulated immune relevant genes in the dfoxo^{21} mutant strain		
CG14401	-	CG14401
CG31741	-	CG31741
CG7227	-	CG7227
CG9928	-	CG9928
Upregulated immune relevant genes in the wild-type strain		
CG10697	Dopa decarboxylase	Ddc
CG11159	-	CG11159
CG18108	Immune induced molecule 1	IM1
CG31764	virus-induced RNA 1	vir-1
CG4261	Helicase 89B	Hel89B
CG4432	Peptidoglycan recognition protein LC	PGRP-LC
CG4437	Peptidoglycan recognition protein LF	PGRP-LF
CG7496	PGRP-SD	PGRP-SD
CG7798	-	CG7798
CG8502	Cuticular protein 49Ac	Cpr49Ac
Counterpart upregulated genes in both, wild-type and dFoxO^{21}strain		
CG10563	lethal (2) 37Cd	l(2)37Cd
CG10747	-	CG10747
CG12667	-	CG12667
CG12732	-	CG12732
CG12820	Diacyl glycerol kinase	Dgk
CG14303	-	CG14303
CG17387	-	CG17387
CG17648	-	CG17648
CG32392	-	CG32392
CG32975	nicotinic Acetylcholine Receptor alpha34E	nAcRalpha 34E
CG33125	-	CG33125
CG33180	Ranbp16	Ranbp16
CG33255	-	CG33255
CG7200	-	CG7200
CG7236	-	CG7236
CG7257	-	Rpt4R
Common upregulated genes in immune relevant genes, wild-type and dFoxO^{21} strain		
CG7228	Peste	pes
Downregulated genes in wild-type and dFoxO^{21} strain		
CG10171	-	CG10171
CG10513	-	CG10513
CG11209	pickpocket 6	ppk6
CG11278	Syntaxin 13	Syx13

CG11686	-	CG11686
CG12072	Warts	wts
CG14117	-	CG14117
CG14395	-	CG14395
CG14506	-	CG14506
CG1801	-	CG1801
CG2973	Cuticular protein 23B	Cpr23B
CG31292	-	CR31292
CG32709	-	CG32709
CG3611	-	CG3611
CG4221	-	CG4221
CG4271	-	CG4271
CG4780	Membrin	membrin
CG5185	Twin of m4	Tom
CG6463	-	CG6463
CG7049	-	CG7049
CG7861	tubulin-specific chaperone E	tbce
CG8884	Synapse-associated protein 47kD	Sap47
CG9023	Drip	Drip
CG9030	-	CG9030
CG9682	-	CG9682
Downregulated immune relevant genes in the dfoxo^{21} mutant strain		
CG11313	-	CG11313
CG1697	rhomboid-4	rho-4
CG1851	Ady43A	Ady43A
CG4144	Gram-negative bacteria binding protein 2	GNBP2
CG7016	-	CG7016
CG9186	-	CG9186
Downregulated immune relevant genes in the wild-type strain		
CG1358	-	CG1358
CG13641	-	CG13641
CG13795	-	CG13795
CG15829	-	CG15829
CG16713	-	CG16713
CG31509	Turandot A	TotA
CG5909	-	CG5909
CG7417	TAK1-associated binding protein 2	Tab2
CG9434	Frost	Fst
CG9441	Punch	Pu
Counterpart downregulated genes between immune relevant genes,wild-type and the dFoxO^{21} mutant strain		
CG14841	-	CG14841
Commonly regulated genes of wild-type upregulated genes and dFoxO^{21} downregulated genes.		

CG17816	-	CG17816
CG39784	-	CG39784
CG5006	Odorant receptor 33c	Or33c
CG8580	Akirin	akirin
CG8874	Fps oncogene analog	Fps85D
Commonly regulated genes in downregulated genes in wild-type and upregulated genes in dFoxO[21]		
CG6937	-	CG6937

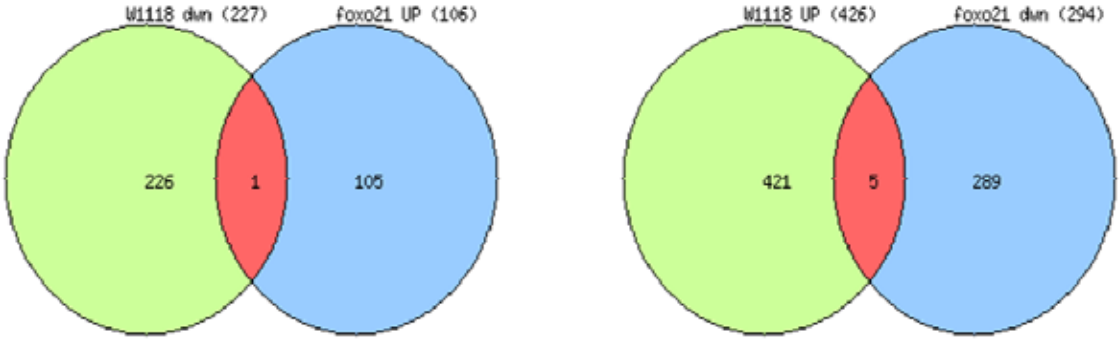

Figure 27: Analysis of regulated immune relevant genes.
Venn diagram analyses to compare the downregulated genes of wild-types with the upregulated genes of the dFoxo[21] mutant strain and *vice versa*. Analyses showed that a very small number of commonly regulated genes.

Gene functional annotation clustering showed higher indicative upregulation for immune responsive genes in the wild type in comparison to a relatively lower term-significance in case of dFoxo[21] mutant strain as shown in figure 28.

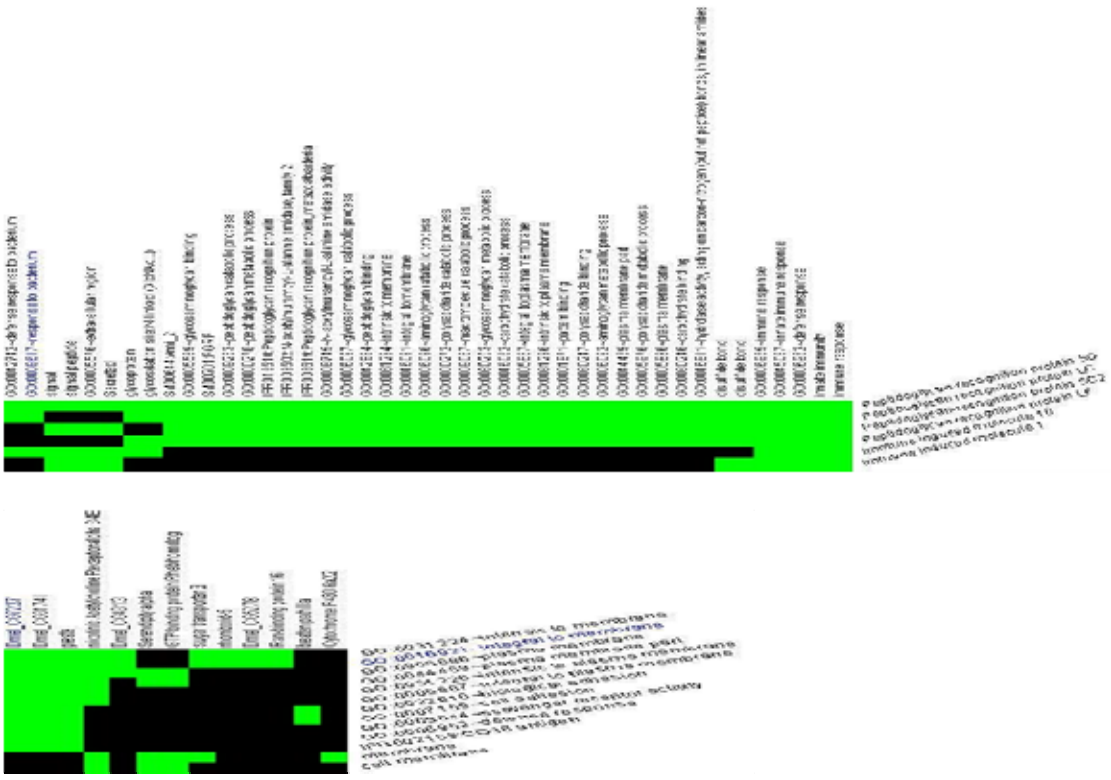

Figure 28: Cluster image of enriched genes within the different categories.
(■ Green) is the corresponding gene-term association positively reported while (■ black) is the corresponding gene-term association not reported yet.Upper panel showed the relevant immune genes represented in response to hypoxia in the wildtype animals while the lower panel represent the dfoxo[21] knockout animals.

Using FatiGO analysis for GO terms and pathways (KEGG), using a Fisher's exact test to compare the significant over-representation of annotations to the complete *Drosophila* genome [131]. This analysis showed a relevant upregulation for the glycerolphoslipid metabolic pathway followed by immune responsive genes (see table 2) in case of upregulated genes in wild-type animals, while no significance was found for dfoxo[21] defective animals as shown in Figure 28.

3.11 Transcriptional regulation of *Dm-mmp1*, dfoxo and relish

The matrix metalloproteinase MMP-1 is implicated to be relevant for various aspects of the fly's biology. In previous studies, an induction of *mmp1* expression following infection of the airways has already been shown (Christina Wagner, pers. commun.). In line with these earlier observations, I observed an induction of *mmp1* expression when larvae of wild-type animals (w^{1118}) were

treated with hypoxia (4h, 5% O_2). Furthermore, dFoxO protein levels were increased after hypoxia. This experiment showed that both genes, *dfoxo* and *relish* were induced upon hypoxia. Bioinformatic analyses of the promoter region of the *mmp1* gene (defined from -20800: -20570 with a total size of 231 bp) showed that this promotor contains only two consensus sites for dFoxO (CACAGGCGCCAC and CATCGGCGCC, a single Cis-Regulatory Element enriched Region (CRERs) of dFoxO in the region from -197 to -186), while consensus sequences for Relish (GGCGCC) are not present as shown in Figure 29.

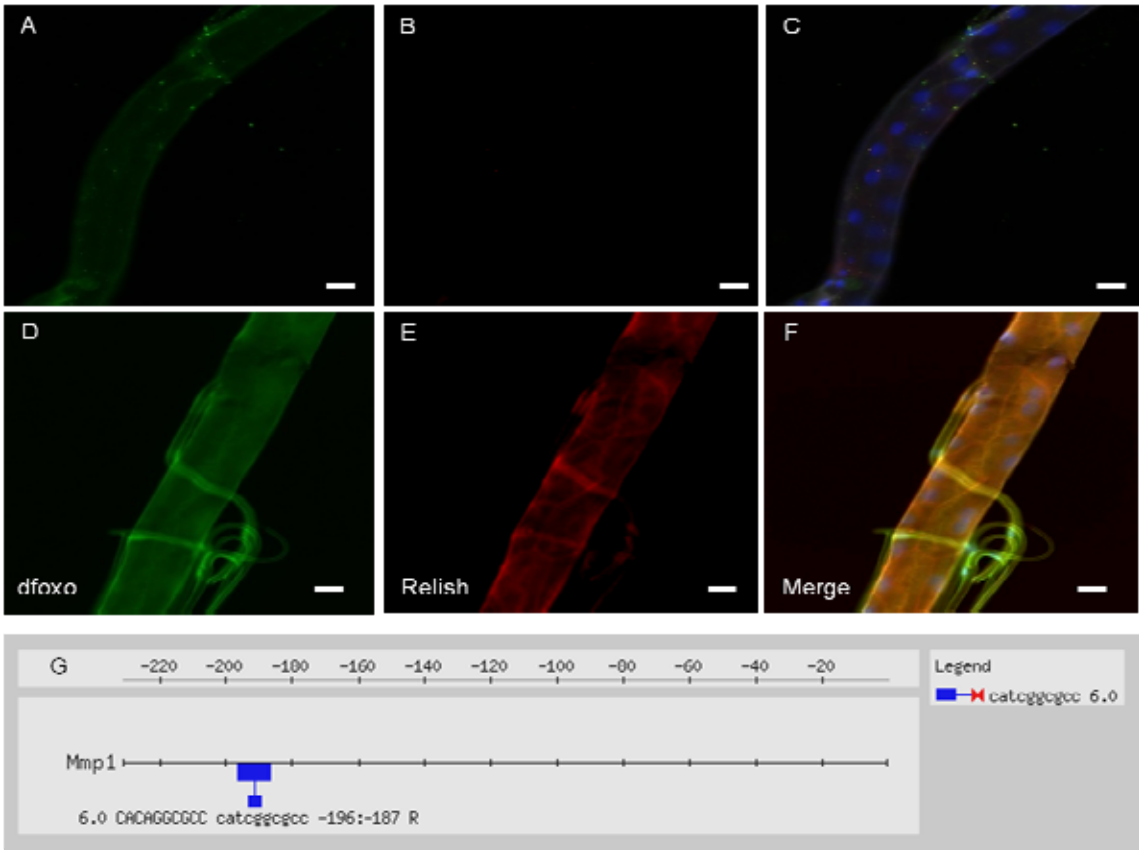

Figure 29: Regulations of dFoxO and Relish by hypoxia.
The upper panel shows wild-type animals ^{w1118} under normoxic conditions (A-C) or hypoxic conditions (D-F). The tracheae were stained with anti-dFoxO (A, D; green) and anti-relish (B, E; red), merge (C, F). The immunohisto-chemical studies showed the induction of the dFoxO and relish proteins upon hypoxia. The panel G represents a motif analysis of dFoxO and relish binding sites on the *mmp1* promotor.

3.12 Stress triggers *mmp1* expression

Previous study showed a notable increase of *mmp1* mRNA levels upon H_2O_2 treatment [132]. Here, I activated *mmp1* expression using the TARGET system [121]. The TARGET system uses a temperature-sensitive Gal80 to inhibit Gal4 at the permissive temperature. Combining this with the Gal4-UAS system in flies allows for temporal control of transgene expression. Temporal control is important for these experiments, as a constitutive expression of *mmp1* results in lethality. Upon shifting animals from 18°C to 30°C, the *mmp1* expression is induced (Figure 30). In addition, tracheal rearrangements, such as thickening of the airway epithelium can be identified.

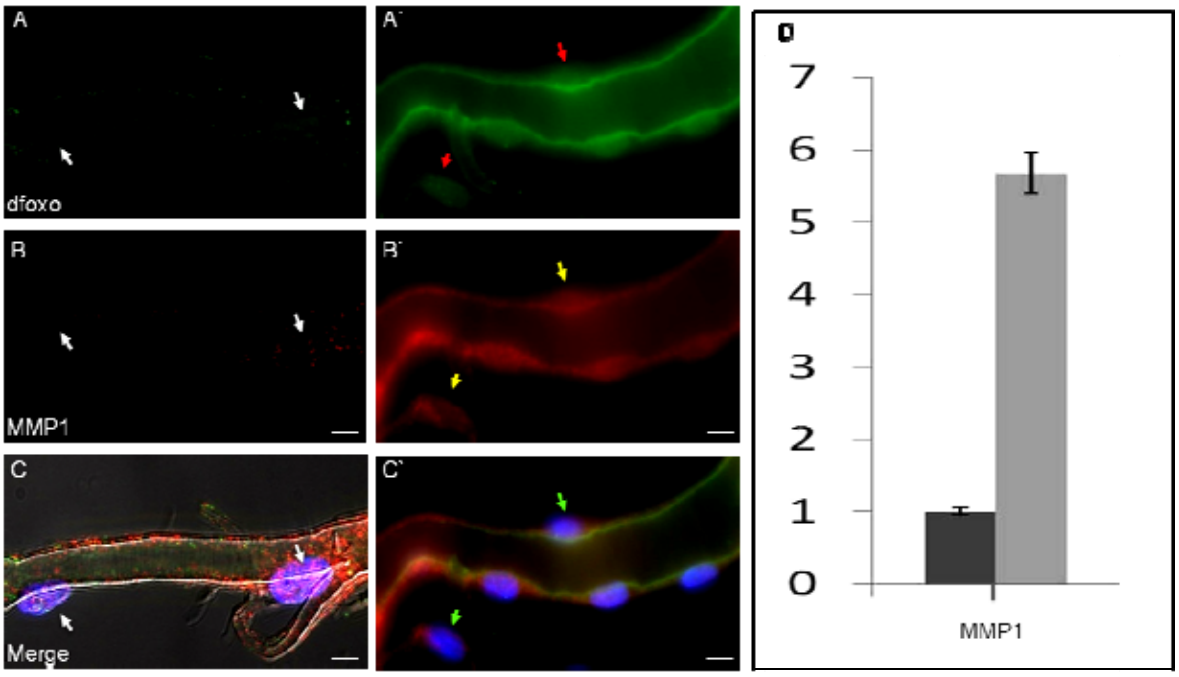

Figure 30: Ectopic activation of *mmp1* mutant strain.
Ectopic activation of *mmp1* gene in the trachea by crossing the temperature sensitive tracheal driver line PKK4-GAL4/GAL80 with *mmp1*-overexpression line (UAS-*mmp1*). Nuclear translocation of dFoxO (A` red arrows) and *mmp1* expression (B` yellows arrows) has been observed in animals shifted to 30°C from 18°C. The left panel show the parental control of this crossing at 18°C; no translocation were observed (A-C ;White arrows). mRNA levels of *mmp1* gene were quantified using the qRT-PCR as shown in figure D.

Additionally, animals overexpressing *mmp1* are crawling out of the lawn, a similar behavior as seen in animals experiencing hypoxia. Furthermore, *mmp1* downregulation is necessary for tracheal remodeling as well as for removal of the primary cuticle of the trachea after moulting.

Upon *mmp1* overexpression, the airway keeps the old cuticle within the new one, which may lead to severe problems during gas exchange along the animal body.

3.13 Infection induces Dm1-MMP activity and AMPs gene expression.

Recently it has been shown that infection with *Erwinia carotovora* can induce antimicrobial expression via a unique mechanism [41, 63, 65].

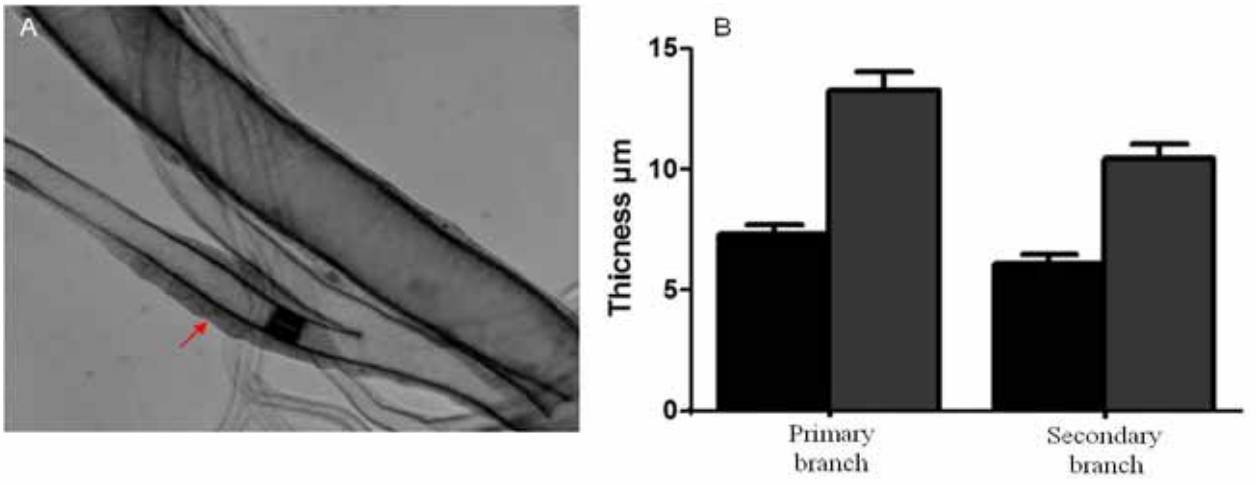

Figure 31: Remodeling of airway epithelia following infection.
Experiencing animals with infection (*Erwinia carotovora*) induces the remodeling of tracheal airways. Upon infection the thickeness of the airway epithelia increased in comparison to control epithelia as shown in A (narrated with red arrow). At least three experiments were used to quantify this phenomena as depicted in B for the primary and the secondary branches. All values represenad as means ± SEM

3.14 IMD pathway activation during hypoxia

To analyze by which mechanisms different challenges like hypoxia and infection direct *mmp1* overproduction I performed ectopic activation experiments. To unravel the role of Relish in regulation of *mmp1* expression, I stimulated the IMD-pathway in the *Drosophila* airway epithelium with hypoxia (5% O_2) for four hours while the control animals settle down in (21% O_2).

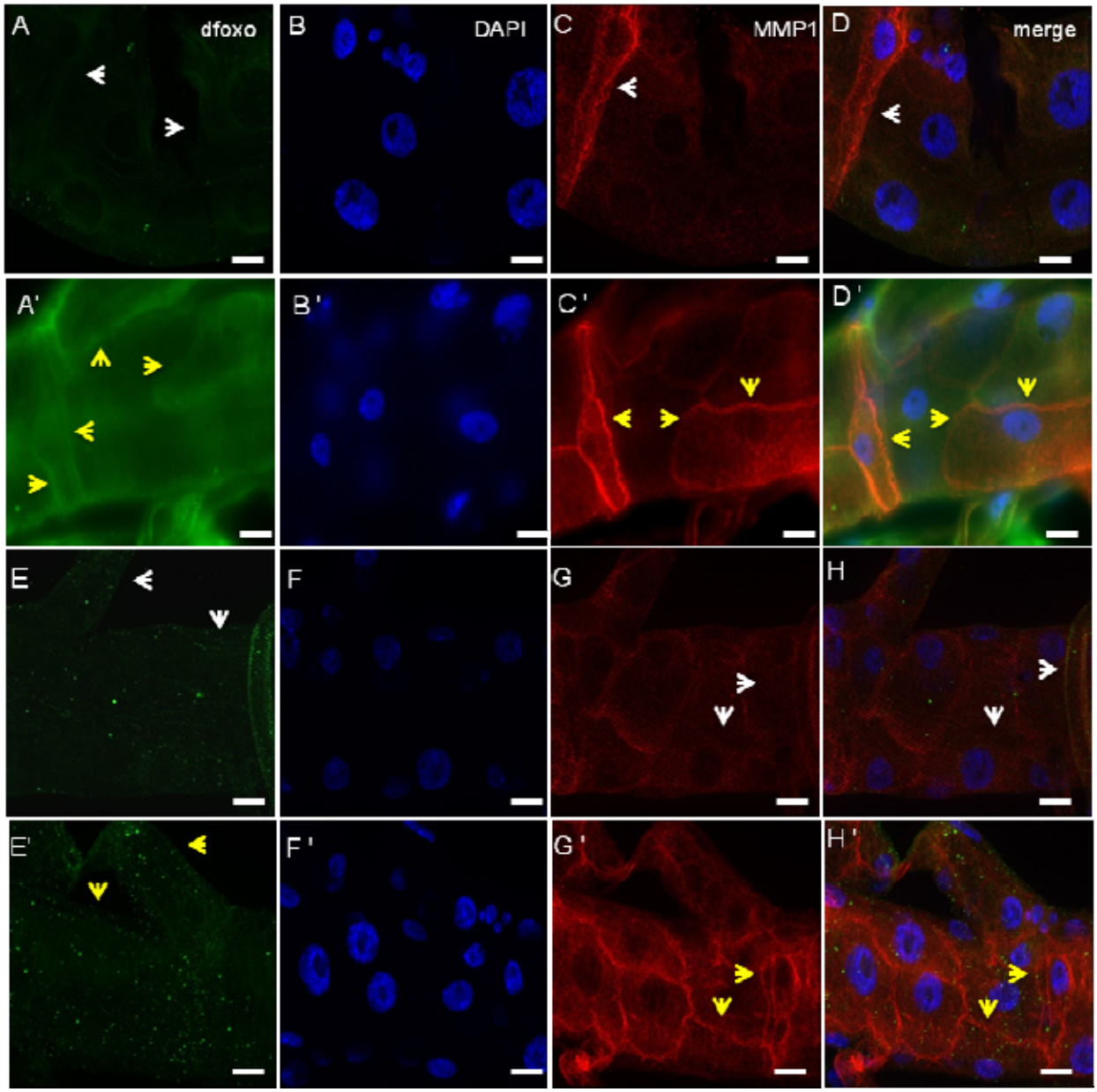

Figure 32: dFoxO and IMD pathways parallel modulate *mmp1* expression.
Crossing of the tracheal driver PKK4 GAL4, whether with the dFoxO^{TM} or UAS-PGRP-LC and further staining with anti-dFoxO (green) and anti-MMP1 (red) have been used. In the panels from A-D` can show the expression of both dFoxO (A, E, E') and MMP1 (C, G, G') proteins in the dFoxO$^{TM}$::PKKGAL4 upon hypoxia in comparison its parental control under normoxia. In the panels E-H`, the expression of *mmp1* proteins in the UASPGRPLC::PKKGAL4 upon hypoxia in comparison its parental control under normoxia has been, on the other hand; no dFoxO protein could be detected (E and E`). DAPI staining (B, E, E') used to show the localization of nuclei within the cells.

A weak signal of MMP1 in the trachea of control animals was detected, while the signal increased dramatically in those animals that were treated with hypoxia as shown in Figure 32.

These data conclude that the IMD pathway can regulate *mmp1* expression. Nevertheless, IMD pathway is not able to mediate the cell stress in a direct way, but it triggers the dFoxO using an additional cascade, which can stimulate the immune response and deteriorate the cell stress. This may be taken as a primary phase until the other cascades can be activated to realize the maximum protection for maintaining cell survival.

3.15 Dm-mmp1 confers an additional immune response

In these experiments I used the TARGET system [121] to induce *mmp1* expression. We maintain the mutant control animals at 18°C and upon shifting to 29°C the system is activated, and we can monitor the changes in the activated system. Activation of TARGET system by shifting to 29°C leads to slight upregulation of *dfoxo* (1,4 folds). Unexpectedly *relish* was downregulated six fold as shown in figure 33A.

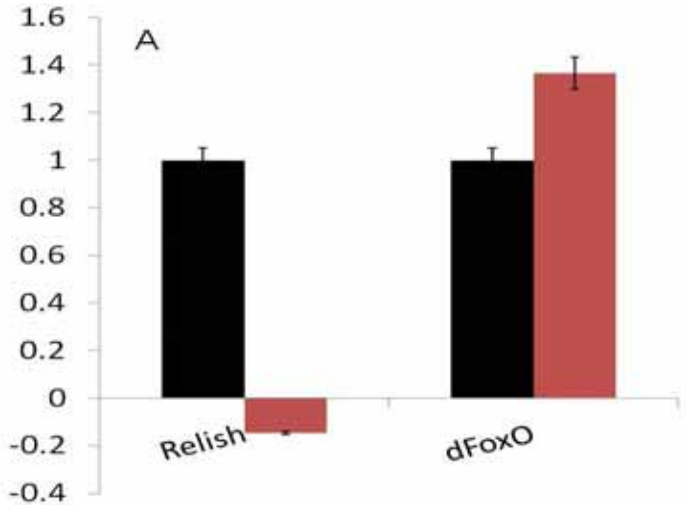

I also determined the gene expression of AMPs in ectopically activated *mmp1* in the airway epithelia. *Defensin, drosocin, drosomycin* and *metchnikowin* are significantly upregulated, whereas *attacin, cecropin* and *diptericin* are not (Fig. 33B).

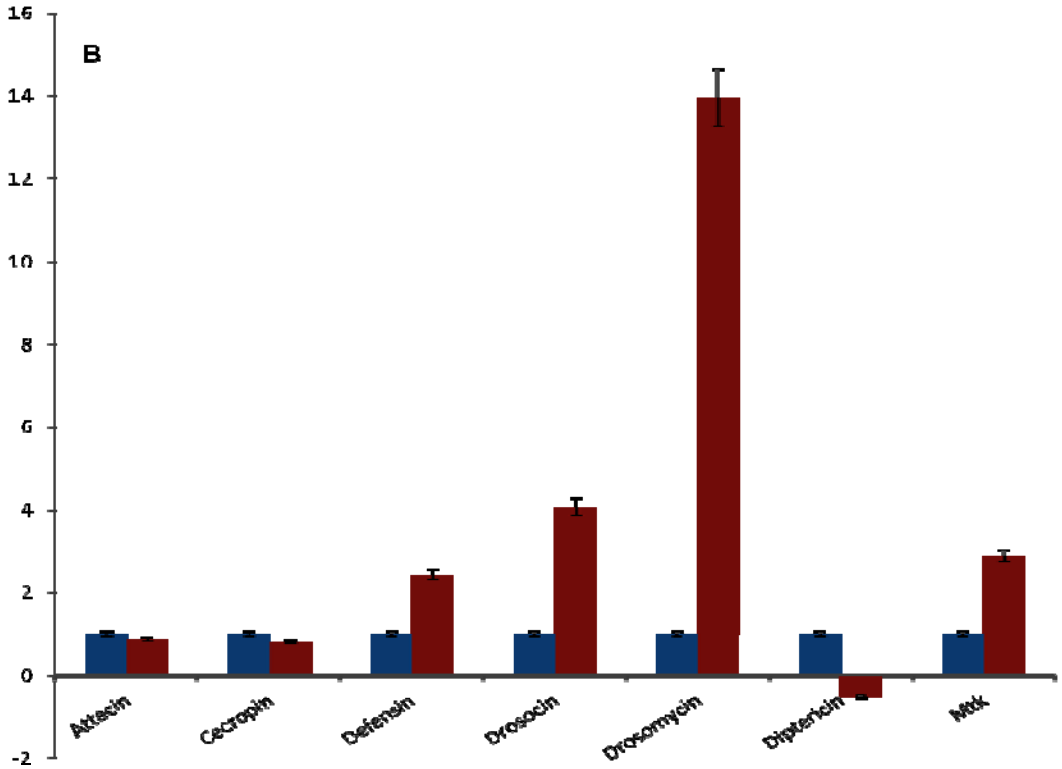

Figure 33: Additional immune activation may be induced by *mmp1* regulation.
qRT-PCR analysis of mRNA levels for antimicrobial peptide genes, dFoxO and relish. In this experiment, the TARGET systems were used to activate the F1 generation from crossings of the tracheal driver pkk4GAL4/GAL80 with the line overexpressing *mmp1* (UAS-*mmp1*). Panel A shows the induction of dfoxo and relish, while B represents the expression change for the AMP genes. Blue bars are from non-activated animals (set as one), red bars from those activated by shifting them to 29°C.

3.16 *Dm*-MMP1 production is JNK-dFoxO dependent

To explore the link between JNK signaling, dFoxO and their function for *mmp1* expression, the protein expression of MMP1 and dFoxO in JNK dominant-negative lines (JNK^{DN}) were consequently determined. Confronting animals with hypoxia (5% O_2) for four hours reveals that neither dFoxO, nor MMP1 protein levels were upregulated in those animals carrying the basket dominant negative isoform. Taken these observations together assume that JNK cannot directly induce the AMPs expression, but activate a downstream target dFoxO controlling diverse cellular reaction.

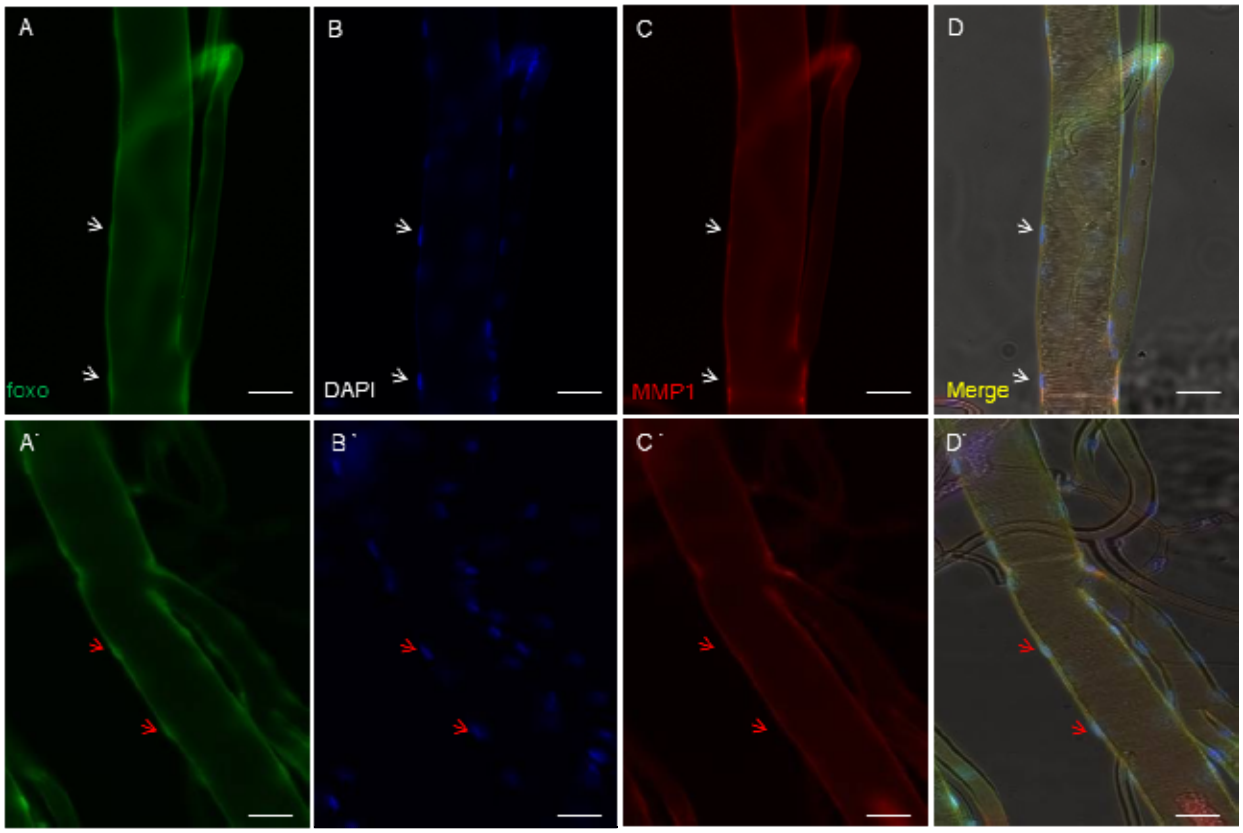

Figure 34: Induced expression of *Drosophila mmp1* is JNK/dFoxO dependent.
The dominant negative basket allele (bsk^{DN}) was crossed to the tracheal driver pkk4-GAL4. The larvae were treated with hypoxia (5% O_2, A'-D') or maintained under normoxia (21% O_2, A-D). Arrows show the location of nuclei. Staining with anti dFoxO (green, A, A'), DAPI (blue, B, B'), anti MMP1 (red, C, C') and the merge of A-C (D) and A'-C' (D').

3.17 dFoxO independently activates *Dm-mmp1* expression

In addition to of the previous results, I wanted to elucidate if dFoxO can induce *mmp1* expression without other inputs. For this purpose, Pkk4-Gal4 in a $dfoxo^{21}$ background were crossed to UAS-PGRP-LC in a $dfoxo^{24}$ background. As controls, $dfoxo^{-/-}$ defective lines were crossed to each other. Animals were analysed for expression of *mmp1* or *dfoxo* by using immunohistochemistry. As expected, dFoxO cannot be detected under any experimental condition as shown in figure 35. In addition, the MMP1 signal was not stronger in the hypoxia treated animals compared with normoxic controls.

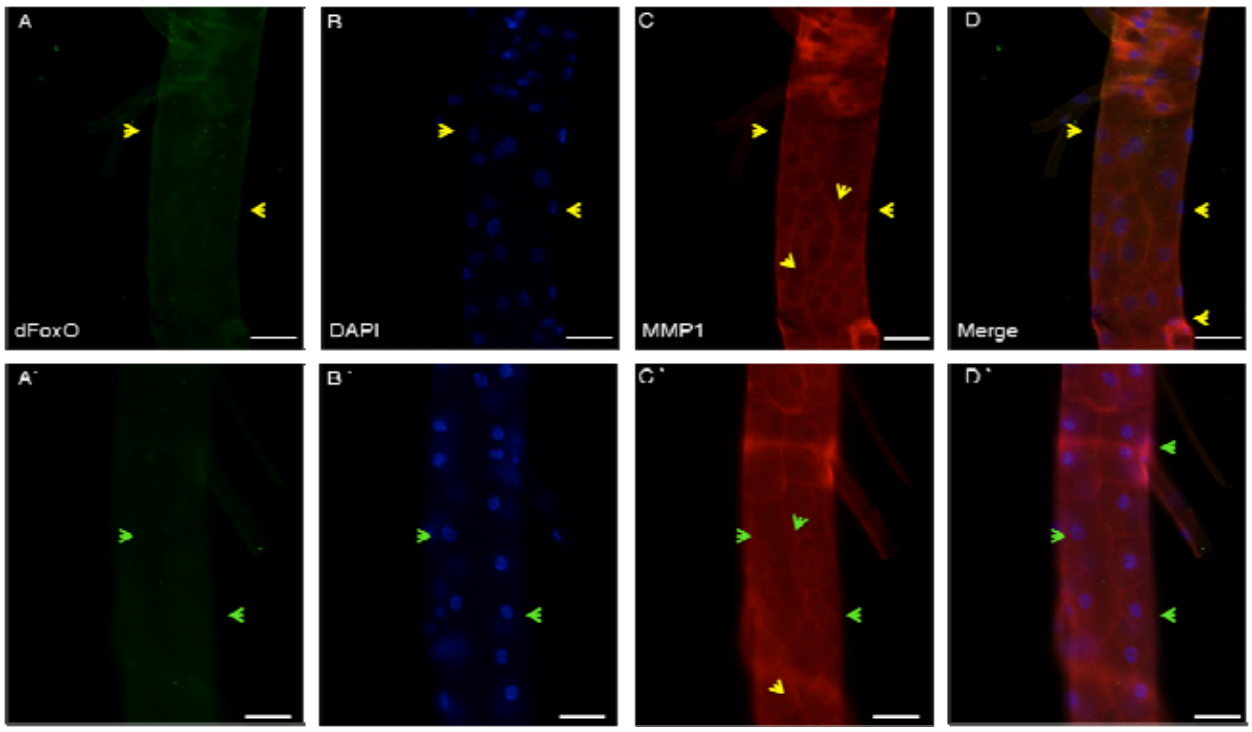

Figure 35: Activation of *Drosophila mmp1* is dFoxO-dependent.
The generated strain carrying the tracheal driver lines with a defective dFoxO allele (pkk4-gal4:: foxo^{21}) were crossed with overexpression lines, driving expression of PGRP-LC in dfoxo^{24} background (UAS-PGRP-LC::foxo^{24}). Larvae were treated with hypoxia (A'-D'. 5% O_2) or held under normoxia (A-D, 21% O_2). Staining with anti dFoxO (green, A, A'), DAPI (blue, B, B'), anti MMP1 (red, C, C') and the merge of A-C (D) and A'-C' (D').

3.18 Transcriptome analysis of *Drosophila mmp1* ectopic overexpression

To define if immune related genes were regulated in case of *mmp1* ectopic overexpression, Venn-diagram tests were performed including the set of known immune genes. Twenty genes were identified as being common between immune related genes and genes upregulated following ectopic *mmp1* overexpression. In addition, three genes are common between the respective groups of downregulated genes with immune related genes (figure 36).

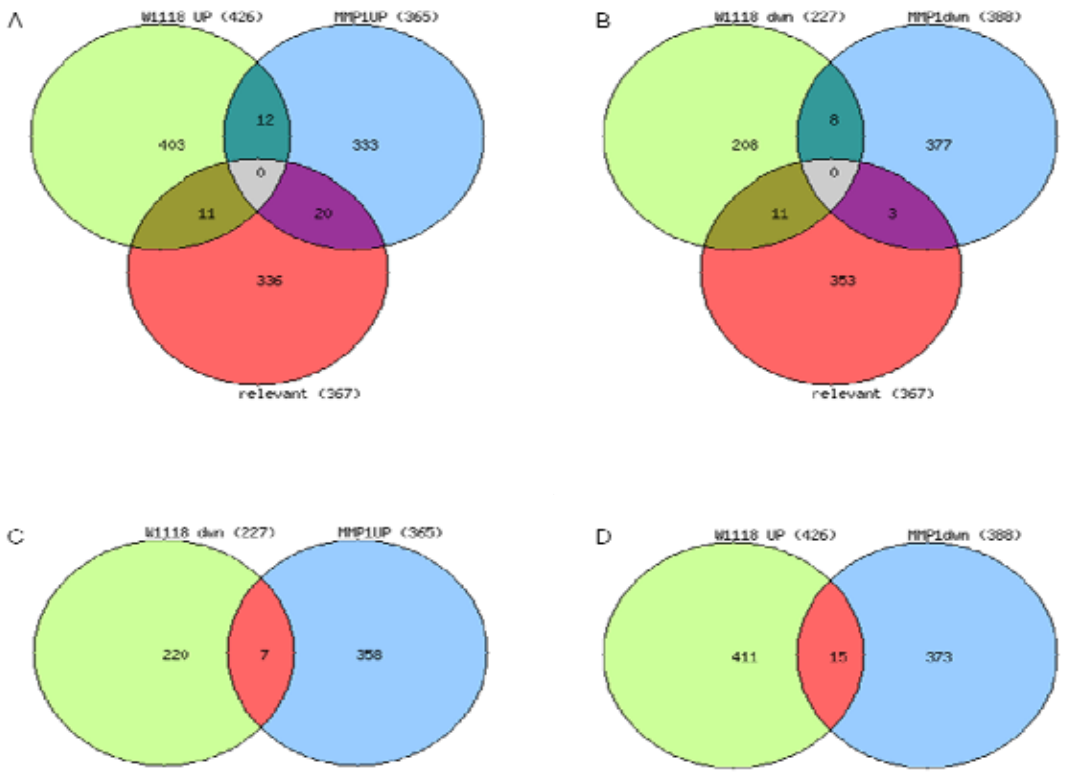

Figure 36: Comparison of regulated gene sets using Venn diagram analyses.
Relevant immune response genes (367 genes) were compared with regulated genes during hypoxia, both in wild type or *mmp1* ectopically activated strains. The comparison show 11 and 20 genes were identical between the upregulated genes in wild type, *mmp1* activated and relevant immune genes (A) While, 11 and 3 genes were the association between the downregulated genes in the wild type, *mmp1* activated and relevant immune genes (B). Seven genes and 15 were the counterpart between the downregulated genes from wild type and upregulated genes of *mmp1* activated (C) and vice versa (D).

Table 2: List of immune relevant genes regulated upon hypoxia in wild-type and *mmp1* ectopically activated strains.

Gene ID	NAME	SYMBOL
Commonly regulated genes between ectopically activated *mmp1* and wild-type experiencing hypoxia		
CG10001	Allatostatin Receptor 2	AR-2
CG12225	Spt6	Spt6
CG12820	Diacyl glycerol kinase	Dgk
CG13225	Odorant receptor 47a	Or47a
CG18107	-	CG18107
CG2010	-	CG2010
CG31872	-	CG31872
CG32118	-	CG32118
CG4181	Glutathione S transferase D2	GstD2
CG4533	lethal (2) essential for life	l(2)efl

CG6084	-	CG6084
CG8253	tungus	tun
Immune relevant genes upregulated in wild-type animals experiencing hypoxia		
CG10697	Dopa decarboxylase	Ddc
CG11159	-	CG11159
CG18108	Immune induced molecule 1	IM1
CG31764	virus-induced RNA 1	vir-1
CG4261	Helicase 89B	Hel89B
CG4432	Peptidoglycan recognition protein LC	PGRP-LC
CG4437	Peptidoglycan recognition protein LF	PGRP-LF
CG7228	peste	pes
CG7496	PGRP-SD	PGRP-SD
CG7798	-	CG7798
CG8502	Cuticular protein 49Ac	Cpr49Ac
Immune relevant genes upregulated in ectopically expressed *mmp1*		
CG10910	-	CG10910
CG13323	-	CG13323
CG13324	-	CG13324
CG13422	-	CG13422
CG1361	Andropin	Anp
CG15829	-	CG15829
CG16978	-	CG16978
CG18106	Immune induced molecule 2	IM2
CG18279	Immune induced molecule 10	IM10
CG5008	Gram-negative bacteria binding protein 3	GNBP3
CG5097	Metallothionein C	MtnC
CG5778	-	CG5778
CG6467	Jonah 65Aiv	Jon65Aiv
CG6687	Serpin 88Eb	Spn88Eb
CG8293	Inhibitor of apoptosis 2	Iap2
CG9080	Listericin	Listericin
CG9111	Lysozyme C	LysC
CG9116	Lysozyme P	LysP
CG9120	Lysozyme X	LysX
CG9976	Galactose-specific C-type lectin	Lectin-galC1
Commonly regulated genes in ectopically expressed *mmp1* (down) and wild-type animals experiencing hypoxia (up)		
CG10017	-	CG34340
CG10563	lethal (2) 37Cd	l(2)37Cd
CG11329	-	CG11329
CG1218	-	CG1218
CG13425	Bancal	bl
CG14958	-	CG14958

CG15345	-	CG15345
CG17386	-	CG17386
CG18783	Kruppel homolog 1	Kr-h1
CG31519	Odorant receptor 82a	Or82a
CG4005	Yorkie	yki
CG5893	Dichaete	D
CG8580	Akirin	akirin
CG9209	vacuolar peduncle	vap
CG9815	-	CG9815
Commonly regulated genes in ectopically expressed *mmp1* (up) and wild-type animals experiencing hypoxia (down)		
CG1079	Fire exit	Fie
CG11999	-	CG11999
CG1262	Accessory gland peptide 62F	Acp62F
CG14322	-	CG14322
CG15829	-	CG15829
CG4221	-	CG4221
CG5279	Rhodopsin 5	Rh5
Commonly downregulated genes between ectopically expressed *mmp1* and wild-type animals experiencing hypoxia		
CG12118	-	CG12118
CG14512	-	CG14512
CG1801	-	CG1801
CG31852	Two A-associated protein of 42kDa	Tap42
CG3739	-	CG3739
CG5451	-	CG5451
CG7861	tubulin-specific chaperone E	tbce
CG8007	-	CG42796
Immune relevant genes that are downregulated in wild-type animals experiencing hypoxia		
CG1358	-	CG1358
CG13641	-	CG13641
CG13795	-	CG13795
CG14841	-	CG14841
CG15829	-	CG15829
CG16713	-	CG16713
CG31509	Turandot A	TotA
CG5909	-	CG5909
CG7417	TAK1-associated binding protein 2	Tab2
CG9434	Frost	Fst
CG9441	Punch	Pu
Immune relevant genes downregulated in animals ectopically expressing *mmp1*		
CG15293	-	CG15293
CG18467	-	CG18467
CG3705	astray	aay

The comparison of the hierarchical clustering resulting from wild type strains microarray to those arrays from the *mmp1* ectopic overexpression showed the highest differential gene expression over high range of regulated gene sets as figured in 37.

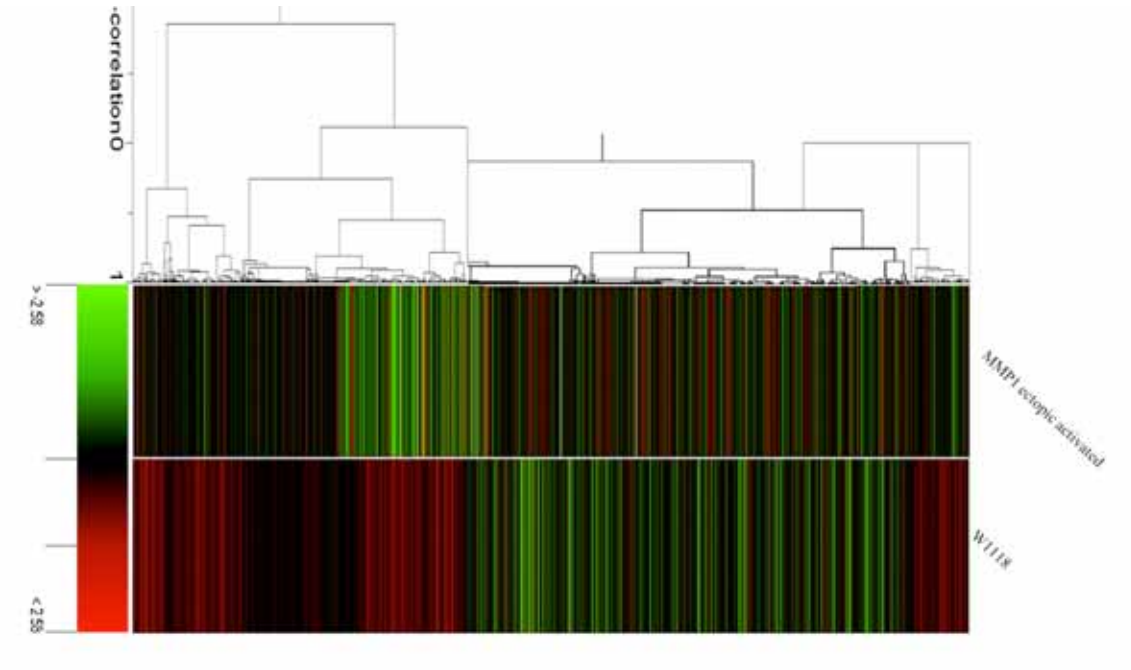

Figure 37: Hierarchical clustering of wildtype and ectopic activated *mmp1*.

4. Discussion

In multicellular animals, coordination between the metabolic processes and those systems, which supply oxygen, requires a full management to maintain oxygen homeostasis. In mammals, for example, local hypoxia is one of the major positive regulators of angiogenesis [133] acting via the hypoxia inducible factor (HIF) inducing expression of e.g. the vascular endothelial growth factor (VEGF), finally inducing ramification and sprouting of new projections [134, 135].

Hypoxia defines a situation of low oxygen tension that is lower than required to maintain a homeostatic balance between oxygen tissue supply and consumption. Usually, it occurs when the available oxygen concentration in a certain tissue is 5% or lower even lower. Hypoxia can be experienced during normal physiology (e.g. during embryogenesis or organ development) or in some pathological conditions such as myocardial infarction, sickle cell anaemia, and sleep apnea. [136, 137]. In addition, it comes along with various types of inflammation and is highly important for chronic lung diseases such as asthma and chronic obstructive pulmonary disease (COPD) [138]. Hypoxia can come in different flavours; it can be tissue specific or generalized, intermittent or constant. Otherwise, severe hypoxia can lead to cell death or injury, which may end up in severe organ damage or even in death of the organism [136].

Since these different hypoxic conditions are inextricably associated with a great variety of diseases, a better understanding of the cellular responses towards hypoxia is of great importance. Responses to hypoxia are highly context- and tissue-dependent, which is exemplified by the different reaction modes to intermittent and constant hypoxia [139]. The long-term effects of chronic hypoxia and the contribution of hypoxia to the disease phenotype in pathological states such as asthma or COPD are not well understood. Interestingly, we know very little about the reaction and role of those cells that are usually the first ones experiencing hypoxia, the airway epithelial cells. The airway epithelium, as the central structural component of the airway, is

devoted to all aspects associated with gas exchange. In addition, it has been shown that epithelia are able to mount an immune response if confronted with pathogens or pathogen associated molecular patterns [32, 41]. This type of response mainly depends on the innate immune system and should prevent bacterial colonization and/or invasion through the corresponding epithelia. Thus, two different modes of responses are operative following recognition of potential pathogens, the production and release of cytokines to recruit professional immune cells and the production and release of antimicrobial compounds such as antimicrobial peptides or reactive oxygen species [140, 141]. In the model used in the current work, the fruit fly *Drosophila melanogaster*, the latter type of response is apparently dominating [32, 41, 65].

Drosophila is a well-established model for various aspects of biomedical research [142]. Up to 70% of all human disease genes have counterparts in the fly, thus disclosing the full power of *Drosophila* genetics [143, 144] to elucidate their physiological and pathophysiological role. *Drosophila* shows a well-orchestrated response to hypoxia and has been used as a very informative model to study the reaction and adaptations towards it [145, 146]. The airway system of the fly shares common architectural and structural aspects with both, our lung and our circulatory system [41, 88]. Especially the reaction of the airway system of the fly (trachea) to hypoxia has a huge number of commonalities with hypoxia-induced angiogenesis observed in the mammalian circulatory system [70, 88]. Areas with local oxygen need induce matching growth of airways into these regions, a mechanism triggered by the branchless/breathless system (fibroblast growth factor/fibroblast growth factor receptor) that depends on HIF-1 [70, 88]. The response of the airway epithelium is cell autonomous, meaning that sensing of and reaction to hypoxia reside in these epithelial cells [70]. This point to the central role of airway epithelium in response to low oxygen tension (hypoxia). Here, I show that hypoxia itself is able to induce an immune response in the airway epithelium of the fly without any contact to pathogens or pathogen associated

molecular patterns. Interestingly, this reaction doesn't depend on the major player in the hypoxia field, namely HIF-1. Upon hypoxia treatment of third instar larvae, the antifungal peptide gene d*rosomycin* was the most prominent upregulated antimicrobial peptide gene. Others, such as *attacin* were also upregulated in complete larvae. In the airways, a similar type of response is obvious; indicating that at least some of these transcriptional responses can be attributed to the response in the airways. Taking into account that the airways represent only a very small portion of the entire animal, other organs in the larvae should also react to hypoxia with an immune response. Especially the increased expression of *drosomycin* is puzzling as it is usually induced in a Toll-dependent manner [1, 34, 147-149]. Only in epithelial immunity, this induction is Toll-independent and is induced via the IMD-pathway [41]. Interestingly, this response depends neither of the Toll- nor on the IMD-pathway. Another molecule has recently been identified in *Drosophila*, which has the ability to induce the production of AMPs (e.g., drosomycin) without requiring classical immune signaling. It is the *Drosophila* forkheadbox-O (dFoxO) protein, the sole representative of this family in the fly [150]. Under normal conditions, meaning in the presence of insulin or insulin-like growth factors the PI3K–Akt/SGK pathway is activated and dFoxO is, retained in the cytoplasm. In cases of starvation or hypoxia, when the insulin or corresponding growth factor signaling pathways are impaired or absent, FoxO transcription factors translocate to the nucleus. I could show that hypoxia is able to recapitulate this signaling, as it led to translocation of dFoxO into the nucleus of airway epithelial cells. This translocation triggers expression of dFoxO target genes, including some antimicrobial peptide genes, including *drosomycin*. This observation was made either using GFP reporter strains or by measuring the corresponding mRNA. This expression was not accompanied by translocation of either of the *Drosophila* NF-κB factors, namely relish, dorsal and dif, further supporting the hypothesis that expression of these antimicrobial peptide genes is not triggered by the conventional, NF-κB

dependent pathways. As observed for the expression of the antimicrobial peptide *drosomycin*, the reaction of the dFoxO translocation process starts at the most terminal structures of the tracheal system and reactions in the major branches are seen only in few animals at later phases of the treatment. Even after the hypoxic treatment ended, dFoxO-GFP stayed for a certain time (usually more than one hour) in the nucleus before re-entering the cytoplasm. The time before re-entering the cytoplasm depended on the period of hypoxia, meaning that the longer the hypoxic treatment, the longer stayed dFoxO-GFP in the nucleus after return to normoxic conditions.

Knockdown of SIMA, which is part of the HIF-machinery, does not impair this response completely, indicating that the hypoxia-dependent increase in *drosomycin* expression does also not depend on HIF-1 signaling. In contrast, animals defective in dFoxO ($foxo^{21}/foxo^{24}$ transheterozyotes) show no upregulation of *drosomycin* expression in response to hypoxia treatment, indicating that dFoxO is essential for this response. Together, these data show that dFoxO can activate AMP expression independently of the NF-κB-dependent innate immune pathways.

Different signaling cascades are able to modulate dFoxO signaling including JNK- and insulin-pathways [151, 152]. Recently, dFoxO activation has been shown to be responsible for a very special type of immune response. Upon starvation, dFoxO dependent activation of antimicrobial peptide gene expression can be detected in different organs of the fly. Those genes that are regulated upon starvation have dFoxO binding sited in their presumptive promotor regions [150]. These data indicate that dFoxO activation is an alternative way to induce an immune response in the fly (and presumably not only there). The reason for this unexpected response is yet not understood, especially as an immune response is launched without any contact to pathogen or activation of classical signal pathways involved in innate immunity. My results imply that this reaction is a response to cellular damages or severe cellular stress. dFoxO, as a terminal factor of various stress-related signaling pathways, is ideally suited for this purpose. Thus, this may be the

fly's way to react according to the vulnerability hypothesis, meaning that extensive stress leading to cell damage or impairment of cell function activate dFoxO, which induces in turn an immune response without activation of the classical signal transduction cascades devoted to immunity. The link between danger sensing and dFoxO activation followed by expression of antimicrobial peptide genes is not understood. Nevertheless, its may be the fly's equivalent to the danger hypothesis originally introduced by Polly Matzinger [153]. Damage of cells and the occurrence of danger related signals is according to this theory sufficient to induce a profound immune response. Mechanistically, one possibility to link oxygen sensing and insulin signalling has been shown in cultured *Drosophila* S2 cells [154]. Insulin signalling is able to induce Sima-dependent gene expression to similar extents as those observed following severe hypoxia. Here, PI3K- and TOR-dependent signalling appear to be essential for this interaction [155]. Whereas increased insulin signal induces hypoxia related responses via upregulation of Sima in S2 cells, dFoxO activation can be induced by decreased insulin signalling in the fly's airway epithelium. In addition, classical HIF-1 dependent signalling is apparently not involved in the hypoxia induced *drosomycin* expression. Alternatively, activation of other signalling systems such as the JNK system [156] may represent additional sensors in these cells. Thus, I identified a novel way how hypoxia regulates the physiological response of the airway epithelium, which, on the other hand, may represent a way how danger signalling operates in innate immunity.

Upon hypoxia, many structural changes can occur in the airway epithelia of *Drosophila*. These changes comprise, thickening of the epithelium outlining the trachea, via increasing the cell size but not its number. These changes match structural changes observed in asthma and/or COPD [65]. This reorganization might be the preparatory stage of metaplasia, meaning that the epithelial cells undergo a conversion to another, presumably different cell type. This result implies that prolonged and severe infections or, even more likely, strong local immune responses induce

remodeling of the airway epithelium, a situation that resembles the situation observed in chronically inflamed human airways [65].

In mammals, comparable structural changes are predominantly seen in the circulatory system. Both, the tracheal system of insects and the circulatory system of invertebrates are devoted to oxygen supply. Additional branches grow up of preexisting blood vessels in response to hypoxic stress. Such phenomena occur only in the superficial tissues of higher animals, because the circulatory system is the main transporter for the oxygen overall the body. Hence, this process is vital to increase the number of blood vessel, thus ensuring sufficient oxygen supply for peripheral tissue. In *Drosophila*, intensive increase in the number of the terminal branches in comparison to control animals was observed following hypoxia treatment in third instar larvae. The general structure of the tracheal systems in those animals is almost completed and fully functional. Only few cells are qualified for division and formation of branches and buds [70]. At normal oxygenation condition (normoxia), the structure of the airways is not changed and depends only on the genetic program realized during tracheal formation. Upon stimulation when facing low oxygen tension (hypoxia), HIF-1 is activated. FGF/Branchless in tissues experiencing hypoxic conditions binds the receptor breathless on tracheal cells. This complex is formed for several times, turned on and off in different locations depending on the oxygen tension, and finally inducing the sprouting of new projections in a way comparable to angiogenesis in mammalians [70, 105].

These processes, the production of new branches and the growths of terminal branches require additional mechanisms that enable them. Regarding certain of these aspects, this growth shares aspect also required for developmental processes such as molting. During embryonic morphogenesis, the epidermis and tubes of the internal respiratory organ are covered with a chitinous sheath. This cuticle barrier determines the ability of the organism to grow. During normal molt-

ing, the attached tracheal cuticular lining is forced externally through the spiracles, openings that link the tracheal tubes with the outer ambience as the larvae slithers out the earlier cuticle a new cuticle produced before shedding the elder one [157, 158]. The growth of airways occurs by increasing cell size and ploidity without increasing cell number. As tracheal elongation occurs in the presence of a cuticle, it seems to require cuticle remodeling. Previous reports have been shown that a *Drosophila* matrix metalloproteinase, MMP-1, is required for normal tracheal growth. In the mutant MMP-1 strains, the trachea become stretched and broken as the larva grows [159]. Other studies have reported that the MMP activity can be regulated at diverse ranks: proteolytic activation of the latent zymogen, interactions with endogenous inhibitors, and differential localization. In cultured cell lines another way to regulate of MMPs appears to be operational, namely direct regulation of secretion [160-162].

Numerous studies have studied the role of metalloproteinases in development and immunity [163, 164]. In the current study, I provide evidence that MMP-1 provide an auxiliary mechanism in boosting an appropriate innate immune defense against a bacterial infection. This finding is in agreement with recent observations in *Tribolium* MMP-1 [165]. Beetles defective in the corresponding MMP-1 were more susceptible to infection with enteropathogenic fungi [163]. In *Drosophila*, I found that additional MMP-1 can be found in response to mild stressing events such as hypoxia (incubation at 5% O_2). The underlying mechanism of MMP-1 activation, whether upon infection or following stress is still unknown. In this study, I dissected the pathways leading to activation of the MMP-1 production.

In a previous study, we reported an upregulation of AMP genes upon infection with the insect pathogen *Erwinia carotovora* [5]. Here, I give evidence that the expression of AMP genes can be regulated upon other environmental challenges such as hypoxia. This regulation was concomitant with higher levels on *mmp1* mRNA expression. On the other hand, overexpression of *mmp1* leads

to higher levels of AMP expression. Thus, we have a positive feedback loop that prolongs inflammatory processes in the airways. Consequently, induction of *mmp1* expression by stressors or infection may contribute substantially to the negative effects, e.g. the structural changes that are associated with these situations. The question which mechanism can induce upregulation of *mmp1* is still unresolved. *mmp1* upregulation can either be driven directly via induction of dFoxO or indirectly by activation of e.g. the IMD-Relish pathway. In the latter case, the activation of relish should induce JNK/TAK1 and finally orientates dephosphorylation and nuclear translocation of dFoxO via this pathway.

To tackle this question experimentally, I used epistatic analyses to unravel the connection between both pathways. Activation of the IMD-pathway way sufficient for induction of *mmp1* expression, but repeating this experiment in a dFoxO deficient background revealed that dFoxO is required for this response. My data indicate that IMD can activate *mmp1* expression presumably via the JNK pathway, while JNK can be stimulated by other ligands and activate its downstream target dFoxO, which finally bifurcates into two different functions: induction of *mmp1* expression and induction of AMP gene production. Data emerged from this study reported that neither dFoxO knocked out, nor BSK-dominant negative animals were able induce MMP1 protein in the *Drosophila* trachea upon hypoxia. Collectively, these two observations consummate that dFoxO is a substantial factor in regulation of *mmp1* expression, additionally dFoxO in case of mild environmental stress functions downstream of JNK. Thus, induction of *mmp1* upregulation is directed by a synergy between JNK, dFoxO and the IMD pathway. The study presented here thus illustrates an innovative signaling pathway for mutualistic action of the IMD-, JNK- and dFoxO-dependent signaling pathways in the regulation of *mmp1*.

The primary role of MMP-1 in this context is to enable growth of cells and building of new branches. MMP-1, as a metalloproteinase is able to degrade extracellular matrix molecules, thus

providing space for growth. Activation of an immune response may be an unwanted by-product of this activity. Proteases are able to activate the immune system non-specifically via cleavage of pattern recognition receptors. In *Drosophila*, this has already been reported [166]. A potential target for this is the central pattern recognition receptor of the IMD-pathway, PGRP-LC. Its cleavage is sufficient for triggering the IMD-pathway and therewith an immune response. The activated IMD pathway (via cleavage of PGRP-LC) activates TAK1 (presumably), which then stimulates IKK-dependent cleavage and activation of Relish, and the JNK pathway induced through TAK1. The JNK usually activates dFoxO during stages of increased stress. dFoxO activation provokes transcription of the *mmp1* and AMP genes, meanwhile JNK negatively regulates the transcription of relish. Thus, activation of dFoxO by stress is part of a negative feedback loop to reduce the levels of ROS in the cell environment.

Microarray analysis of the airway epithelium following ectopic *mmp1* expression showed upregulation of different types of genes; very interesting are the lysozymes, where lysozymes C, P and X are upregulated. Another molecule with relevance for the immune response is the listericin gene (CG9080), which is usually induced in response to *L. monocytogenes* infection. The listericin gene encodes a novel AMP-like protein whose induction is cooperatively regulated by PGRP-LE and the JAK-STAT pathway [167].

Another relevant molecule is metallothionein C (CG5097), which is evolutionarily conserved from mammals to insects. In *Drosophila,* expression of *metallothionein C* is metal-responsive transcription factor-1 (MTF-1) dependent. MTF-1 is a transcription factor that possesses DNA binding zinc fingers, which change conformation in response to fluctuations in cellular zinc concentrations [168]. Upon increase of metal ion levels in the cytoplasm, MTF-1 stimulates the transcription of *metallothionein* genes. Metallothioneins are tiny, cysteine-rich proteins that bind zinc under specific physiological conditions; they represent stress inducible genes with a diverse

array of functions. Metallothionein genes have also been shown to be transcribed in response to hypoxia in a MTF-1-dependent manner [169].

In conclusion, it can be said that the fly's airway system represents a very valuable model to study the general aspects of airway systems as the major architectural features of airway epithelia appear to be conserved throughout the animal kingdom. Usually, hypoxia induces a complex set of responses; most of them are believed to depend on HIF-1 like factors. In *Drosophila*, the major organ, where HIF-1 dependent gene expression in response to hypoxia could be observed is the airway epithelium itself [155, 170]. My observation that a potent immune response can be launched following hypoxia was unsuspected; especially that it apparently doesn't depend on HIF-1. The involvement of dFoxO in this response was also unexpected and may link locally action damage sensing with the induction of an immune response. In addition, the importance of dFoxO for the general response to hypoxia was further underpinned by the almost complete lack of common transcript signatures following hypoxia in wild-types and *dfoxo* deficient animals. This indicates that dFoxO is not only required to transduce the hypoxia-induced immune response but also a great number of different transcriptional responses. Presumably, this dFoxO dependent part of the reaction towards hypoxia may be the one that occurs in response to a more generalized impairment of cell homeostasis. This hypothesis is underpinned by previous work showing that dFoxO is activated during stressful situations in the fly's airway epithelium, where it is essential for cell survival [65]. This type of reaction is physiologically very meaningful as especially those regions of the airways (and only those) that experience damages should launch an appropriate transcriptional response. In addition, dFoxO appears to be also required to induce structural changes directly at the level of the airway epithelial cells including induced thickening as well as comparable structural adaptations.

On the other hand, the current data indicate that transcriptional regulation of *mmp1* is a crucial component to the hypoxia-induced immunity in flies. In this case, the JNK-responsive transcription factor dFoxO is also required for this response. Although activation of the IMD-pathway is sufficient for this response, it requires active dFoxO mediated signaling. MMP-1 is required to enable structural changes, but this increased induction is presumably paid by an unspecific activation of the innate immune response, mediated via cleavage of pattern recognition receptors. My data suggested that MMP-1 activation is part of a vicious cycle that enhances and prolongs inflammatory responses in the airway epithelium thus is may by concluded that comparable reactions are also relevant for inflammatory diseases of the lung including asthma und COPD.

5. Summary

The tracheal system of insects is a purely epithelial tissue that is primarily devoted to gas exchange. All airway epithelial cells of the fruit fly *Drosophila melanogaster* are immune-competent, meaning that they are able to mount an immune response if confronted with pathogens such as bacteria or fungi. Strong and prolonged activation of this epithelial immune response is able to elicit different responses including inflammation-like states and structural changes that are reminiscent to those observed in chronic inflammatory diseases of the human lung such as asthma or COPD (Chronic Obstructive Pulmonary Disease). The simplicity of the fly's airway system makes it to a credible candidate to examine the mechanisms underlying these inflammatory diseases.

Patient suffering from *Asthma bronchiale* or COPD often experience hypoxia and/or hypercapnia. The current study demonstrates that hypoxia can mount an immune response in the airway epithelium of the fruit fly, as shown by the induced expression of antimicrobial peptide genes. This response is triggered without any contact to pathogens or pathogen associated molecular patterns (PAMPs). Instead, this hypoxia-induced immune response depends on the transcription factor dFoxO. Translocation of dFoxO into the nuclei of airway epithelial cells precedes the expression of antimicrobial peptides under control of this transcription factor. Apparently, dFoxO mediates a danger-like response of the airway epithelium to this stressor.

In addition, I could show using microarray analyses, that dFoxO is not only necessary for the hypoxia induced immune activation, but also for a great variety of other hypoxia-induced transcriptomic responses. Comparing the transcriptomes between wild-type airway epithelia and those of animals lacking functional dFoxO revealed only a marginal overlap in the cohorts of genes regulated following hypoxia. Taken together, I have shown that dFoxO plays a much

larger role for hypoxia-induced gene regulation than it has previously been thought. In addition, I identified another dFoxO dependent process that is related to hypoxia-induced responses. Following hypoxia, the airways show structural changes including building of new terminal branches. To enable this, the matrix metalloproteinase MMP-1 is required to degrade the extra-cellular matrix around these structures. Expression of *mmp1* is induced following infection, but also following other stressors such as hypoxia. On the other hand, overexpression of *mmp1* in airway epithelia induces an immune response. Thus, MMP-1 apparently is part of a positive feedback loop leading to a prolonged and more severe immune response in the airway epithelium following an infection. Both, ectopic activation of the innate immune pathway IMD or of dFoxO are sufficient to induce *mmp1* expression. Epistatic analyses revealed that both responses critically depend on the presence of dFoxO, which in turn appears to be activated via the JNK-pathway.

The current study reveals that hypoxia induces a great number of unexpected responses in the airway epithelium that are mainly transduced via activation of dFoxO. These results are medically relevant because hypoxia is frequently experienced in different inflammatory diseases of the airways (e.g. Asthma and COPD). Apparently, dFoxO is, in addition to HIFs, a novel key molecule in the oxygen homeostasis, thus opening a new area for research in this field.

6. Zusammenfassung

Das tracheale System der Insekten ist ein rein epitheliales Gewebe, das primär dem Gasaustausch dient. Alle Atemwegsepithelzellen der Fruchtfliege sind immunkompetent, was bedeutet, dass sie nach Pathogenkontakt (z.B. mit Bakterien oder Pilzen), in der Lage sind, eine Immunantwort zu zeigen. Es hat sich gezeigt, dass eine sehr starke und langanhaltende Aktivierung des Immunsystems dazu führen kann, dass Entzündungs-ähnliche Zustände entstehen. Zusätzlich werden auch strukturelle Änderungen induziert, die denen entsprechen, die bei chronisch entzündlichen Erkrankungen der Lunge (z.B. Asthma oder COPD – *Chronic Obstructive Pulmonary Disease*) zu beobachten sind. Die strukturelle Einfachheit des Fliegensystems lässt es als ideales Modell für die Analyse der diesen Erkrankungen zugrunde liegenden Mechanismen erscheinen.

Patienten, die an *Asthma bronchiale* oder COPD leiden, erfahren oftmals hypoxische oder hyperkapnische Bedingungen. In der vorgelegten Arbeit konnte ich zeigen, dass Hypoxie in der Lage ist, eine Immunantwort des Atemwegsepithels zu induzieren. Diese Antwort wird ohne jeglichen Kontakt zu Pathogen oder Pathogen Assoziierten Molekularen Mustern (PAMPs) hervorgerufen. Diese induzierte Antwort beruht auf der Aktivität des Transkriptionsfaktors dFoxO. Hypoxie induziert dessen Translokation in den Kern, ein Prozess, der einer Expression antimikrobieller Peptidgene induziert. Offensichtlich vermittelt dFoxO eine sog. *Danger*-Antwort im Atemwegsepithel.

Außerdem konnte ich mit Hilfe von Microarray Analysen zeigen, dass dFoxO nicht nur für die Hypoxie-induzierte Immunantwort, sondern auch für eine Reihe anderer Antworten erforderlich ist. Ein Vergleich der Hypoxie-induzierten Genexpressionsmuster von Tracheen isoliert aus Wildtyp Larven mit den aus *dfoxo*-defizienten Larven ergab eine überraschend geringe

Übereinstimmung. Zusammenfassend kann gesagt werden, dass ich gezeigt habe, dass dFoxO eine sehr viel größere Rolle im Rahme der Hypoxie-vermittelten Antworten spielt als vorher angenommen wurde. Außerdem konnte ich einen weiteren dFoxO-abhängigen Prozess identifizieren, der direkte Bedeutung für Hypoxie-vermittelte Antworten hat. Hypoxie induziert in den Atemwegen strukturelle Änderungen, zu denen die Neubildung von terminalen Tracheenästen gehört. Um das zu ermöglichen, ist die Matrix-Metalloprotease MMP-1 erforderlich, die extrazelluläre Matrix Bestandteile verdaut. Die Expression der *mmp1* wird durch Infektion, aber auch durch Stressoren wie Hypoxie induziert. Andererseits induziert die ektopische Überexpression dieses Moleküls eine Immunantwort in den Tracheen. Demzufolge scheint MMP1 Teil einer positiven Rückkopplungsschleife zu sein, die dazu führt, dass Antworten auf Infektionen sehr viel stärker und länger in den Atemwegen persistieren. Epistasis Analysen konnten zeigen, dass die Aktivierung der mmp1-Expression von *dfoxo* abhängt und wahrscheinlich über den JNK-Signalweg vermittelt wird.

Die vorgelegte Arbeit zeigt, dass eine Vielzahl unerwarteter Antworten durch Hypoxie in den Atemwegen induziert wird und diese vornehmlich vom Transkriptionsfaktor dFoxO abhängen. Die Relevanz dieser Ergebnisse ist darin zu sehen, dass Hypoxie oft während entzündlicher Erkrankungen der Atemwege (Asthma oder COPD) erfahren wird und einen noch unbekannten Anteil an der Pathogenes dieser Erkrankungen einnimmt. Offensichtlich ist dFoxO, zusätzlich zu HIF-Faktoren von zentraler Bedeutung für die Hypoxie-Antwort des Atemwegsepithels.

7. Refernces

1. Lemaitre, B., Nicolas, E.,Michaut, L.,Reichhart, J. M.,Hoffmann, J. A.,, *The dorsoventral regulatory gene cassette spatzle/Toll/cactus controls the potent antifungal response in Drosophila adults.* Cell, 1996. **86**: p. 973-983.
2. Abdelsadik, A. and A. Trad, *Toll-like receptors on the fork roads between innate and adaptive immunity.* Hum Immunol, 2011. **72**(12): p. 1188-1193.
3. Roca, F.J., et al., *Evolution of the Inflammatory Response in Vertebrates: Fish TNF-α Is a Powerful Activator of Endothelial Cells but Hardly Activates Phagocytes.* The Journal of Immunology, 2008. **181**(7): p. 5071-5081.
4. Hultmark, D., *Drosophila immunity: paths and patterns.* Current Opinion in Immunology, 2003. **15**(1): p. 12-19.
5. Abdelsadik, A. and T. Roeder, *Chronic activation of the epithelial immune system of the fruit fly's salivary glands has a negative effect on organismal growth and induces a peculiar set of target genes.* BMC Genomics, 2010. **11**(1): p. 265-265.
6. Bulet, P., et al., *A novel inducible antibacterial peptide of Drosophila carries an O-glycosylated substitution.* Journal of Biological Chemistry, 1993. **268**(20): p. 14893-14897.
7. Ekengren, S. and D. Hultmark, *Drosophila cecropin as an antifungal agent.* Insect Biochemistry and Molecular Biology, 1999. **29**(11): p. 965-972.
8. Valanne, S., J.-H. Wang, and M. Rämet, *The Drosophila Toll Signaling Pathway.* The Journal of Immunology, 2011. **186**(2): p. 649-656.
9. West, A.P., A.A. Koblansky, and S. Ghosh, *Recognition and Signaling by Toll-Like Receptors.* Annu Rev Cell Dev Biol, 2006. **22**(1): p. 409-437.
10. Funderburg, N., et al., *Human -defensin-3 activates professional antigen-presenting cells via Toll-like receptors 1 and 2.* Proc Natl Acad Sci U S A, 2007. **104**(47): p. 18631-5.
11. Iwasaki, A. and R. Medzhitov, *Toll-like receptor control of the adaptive immune responses.* Nat Immunol, 2004. **5**(10): p. 987-95.
12. Reis e Sousa, C., *Toll-like receptors and dendritic cells: for whom the bug tolls.* Semin Immunol, 2004. **16**(1): p. 27-34.
13. Pasare, C. and R. Medzhitov, *Toll-like receptors: linking innate and adaptive immunity.* Adv Exp Med Biol, 2005. **560**: p. 11-8.
14. Sakaguchi, S., *Control of immune responses by naturally arising CD4+ regulatory T cells that express toll-like receptors.* J Exp Med, 2003. **197**(4): p. 397-401.
15. Anderson, K.V.a.C.N.-V., *"Information for the dorsal-ventral pattern of the Drosophila embryo is stored as maternal mRNA.* Nature, 1984. **311**(5983): p. 223-227.
16. Medzhitov, R. and C.A. Janeway, *Innate Immunity: The Virtues of a Nonclonal System of Recognition.* Cell, 1997. **91**(3): p. 295-298.
17. Shen, B., et al., *Physical and functional interactions between Drosophila TRAF2 and Pelle kinase contribute to Dorsal activation.* PNAS, 2001. **98**: p. 8596-8601.
18. Kim, T.-W., W. H. Pettingell, et al. , *Endoproteolytic Cleavage and Proteasomal Degradation of Presenilin 2in Transfected Cells.* 1997. **272**: p. 11006-11010.

19. Lu, Y., L. P. Wu, et al. , *The antibacterial arm of the Drosophila innate immune response requires an I{kappa}B kinase.* 2001. **15**(104-110).
20. Silverman, N., et al., *A Drosophila IkappaB kinase complex required for Relish cleavage and antibacterial immunity.* Genes Dev, 2000. **14**: p. 2461.
21. Cociancich, S., et al., *Novel Inducible Antibacterial Peptides from a Hemipteran Insect, the Sap-Sucking Bug Pyrrhocoris-Apterus.* Biochemical Journal, 1994. **300**: p. 567-575.
22. Sun, S.C., B. Asling, and I. Faye, *Organization and Expression of the Immunoresponsive Lysozyme Gene in the Giant Silk Moth, Hyalophora-Cecropia.* Journal of Biological Chemistry, 1991. **266**(10): p. 6644-6649.
23. Reichhart, J.M., et al., *Insect immunity: developmental and inducible activity of the Drosophila diptericin promoter.* EMBO J., 1992. **11**: p. 1469.
24. Engstrom, Y., et al., *kappaB-like motifs regulate the induction of immune genes in Drosophila.* J. Mol. Biol, 1993. **232**: p. 327.
25. Coutinho, A., et al., *Thymic commitment of regulatory T cells is a pathway of TCR-dependent selection that isolates repertoires undergoing positive or negative selection.* Curr Top Microbiol Immunol, 2005. **293**: p. 43-71.
26. Stoven, S., et al., *Activation of the Drosophila NF-[kappa]B factor Relish by rapid endoproteolytic cleavage.* EMBO Rep., 2000. **1**: p. 347-352.
27. Silverman, N. and T. Maniatis, *NF-{kappa}B signaling pathways in mammalian and insect innate immunity.* Genes Dev., 2001. **15**(18): p. 2321-2342.
28. Naitza, S., *The Drosophila immune defense against gram-negative infection requires the death protein dFADD.* Immunity, 2002. **17**: p. 575-581.
29. Kaneko, T. and N. Silverman, *Bacterial recognition and signalling by the Drosophila IMD pathway*. 2005. p. 461-469.
30. Leclerc, V. and J.-M. Reichhart, *The immune response of Drosophila melanogaster.* Immunological Reviews, 2004. **198**(1): p. 59-71.
31. Naitza, S. and P. Ligoxygakis, *Antimicrobial defences in Drosophila: the story so far.* Molecular Immunology, 2004. **40**(12): p. 887-896.
32. Tzou, P., Ohresser, S., Ferrandon, D., Capovilla, M., Reichhart, Jean-Marc., Lemaitre, B., Hoffmann, J. A., Imler, Jean-Luc.,, *Tissue-Specific Inducible Expression of Antimicrobial Peptide Genes in Drosophila Surface Epithelia.* Immunity, 2000. **13**(5): p. 737-748.
33. Hoffmann, J.A. and J.-M. Reichhart, *Drosophila innate immunity: an evolutionary perspective.* Nat Immunol, 2002. **3**(2): p. 121-126.
34. Lemaitre, B.a.H., Jules, *The Host Defense of Drosophila melanogaster.* Annual Review of Immunology, 2007. **25**(1): p. 697-743.
35. Tzou, P., J.M. Reichhart, and B. Lemaitre, *Constitutive expression of a single antimicrobial peptide can restore wild-type resistance to infection in immuno-deficient Drosophila mutants.* Proc. Natl. Acad. Sci. USA, 2002. **99**: p. 2152.
36. Sondarva, G., et al., *TRAF2-MLK3 interaction is essential for TNF-[alpha]-induced MLK3 activation.* Cell Res, 2009. **20**(1): p. 89-98.
37. Darnell, J.J., *STATs and gene regulation.* Science, 1997(277): p. 1630-1635.
38. Agaisse, H. and N. Perrimon, *The roles of JAK/STAT signaling in Drosophila immune responses.* Immunological Reviews, 2004. **198**(1): p. 72-82.

39. Binari, R., Perrimon N, *Stripe-specific regulation of pair-rule genes by hopscotch, a putative Jak family tyrosine kinase in Drosophila.* Genes Dev, 1994. **8**: p. 300-312.
40. Senger, K., K. Harris, and M. Levine, *GATA factors participate in tissue-specific immune responses in Drosophila larvae.* Proceedings of the National Academy of Sciences, 2006. **103**(43): p. 15957-15962.
41. Wagner, C., Isermann, K., Fehrenbach, H., Roeder, T.,, *Molecular architecture of the fruit fly's airway epithelial immune system.* BMC Genomics, 2008. **9**: p. 446.
42. Silverman, N., et al., *Immune Activation of NF-κB and JNK Requires Drosophila TAK1.* Journal of Biological Chemistry, 2003. **278**(49): p. 48928-48934.
43. Bond, D. and E. Foley, *A Quantitative RNAi Screen for JNK Modifiers Identifies Pvr as a Novel Regulator of Drosophila Immune Signaling.* PLoS Pathog, 2009. **5**(11): p. e1000655.
44. Dhanasekaran, D.N.R., E. P., *JNK signaling in apoptosis.* Oncogene, 2008. **27**(48): p. 6245-6251.
45. Guntermann, S. and E. Foley, *The Protein Dredd Is an Essential Component of the c-Jun N-terminal Kinase Pathway in the Drosophila Immune Response.* Journal of Biological Chemistry, 2011. **286**(35): p. 30284-30294.
46. Huang, C., K. Jacobson, and M.D. Schaller, *MAP kinases and cell migration.* J Cell Sci, 2004. **117**(20): p. 4619-4628.
47. Park, J., et al.,, *Targeting of TAK1 by the NF-κB protein Relish regulates the JNK-mediated immune response in Drosophila.* Genes Dev, 2004. **18**(5): p. 584-594.
48. Park, J.M., et al., *Targeting of TAK1 by the NF-κB protein Relish regulates the JNK-mediated immune response in Drosophila.* Genes & Development, 2004. **18**(5): p. 584-594.
49. Tanji, T. and Y.T. Ip, *Regulators of the Toll and Imd pathways in the Drosophila innate immune response.* Trends in Immunology, 2005. **26**(4): p. 193-198.
50. Karin, M. and A. Lin, *NF-kappa B at the crossroads of life and death.* Nature Immunology, 2002. **3**(3): p. 221-227.
51. Tang, G., et al., *Inhibition of JNK activation through NF-[kappa]B target genes.* Nature, 2001. **414**(6861): p. 313-317.
52. De Smaele, E., et al., *Induction of gadd45[beta] by NF-[kappa]B downregulates pro-apoptotic JNK signalling.* Nature, 2001. **414**(6861): p. 308-313.
53. Sakon, S., et al., *NF-kappa B inhibits TNF-induced accumulation of ROS that mediate prolonged MAPK activation and necrotic cell death.* Embo Journal, 2003. **22**(15): p. 3898-3909.
54. Onfelt, T., and E.Engstrom, Y. , *The imd gene is required for local Cecropin expression in Drosophila barrier epithelia.* EMBO Rep, 2001. **2**: p. 239-243.
55. Ha, E.M., et al., *A direct role for dual oxidase in Drosophila gut immunity.* Science, 2005. **310**: p. 847.
56. Ha, E.M., et al., *An antioxidant system required for host protection against gut infection in Drosophila.* Dev. Cell, 2005. **8**: p. 125.

57. Ryu, J.-H., et al., *An essential complementary role of NF-[kappa]B pathway to microbicidal oxidants in Drosophila gut immunity.* Embo J, 2006. **25**(15): p. 3693-3701.
58. Scherfer, C., *Haemolymph clotting in Drosophila melanogaster and Galleria mellonella*. 2004, Universitätsbibliothek: Gießen.
59. Goto, A., T. Kadowaki, and Y. Kitagawa, *Drosophila hemolectin gene is expressed in embryonic and larval hemocytes and its knock down causes bleeding defects.* Dev Biol, 2003. **264**(2): p. 582-591.
60. Scherfer, C., et al., *The Toll immune-regulated Drosophila protein Fondue is involved in hemolymph clotting and puparium formation.* Dev Biol, 2006. **295**(1): p. 156-163.
61. Brinkmann, V., et al., *Neutrophil Extracellular Traps Kill Bacteria.* Science, 2004. **303**(5663): p. 1532-1535.
62. Govind, S., *Innate immunity in Drosophila: Pathogens and pathways.* Insect Science, 2008. **15**(1): p. 29-43.
63. Basset, A., et al., *The phytopathogenic bacteria Erwinia carotovora infects Drosophila and activates an immune response.* Proceedings of the National Academy of Sciences, 2000. **97**(7): p. 3376-3381.
64. Zaidman-Rémy, A., et al., *The Drosophila Amidase PGRP-LB Modulates the Immune Response to Bacterial Infection.* Immunity, 2006. **24**(4): p. 463-473.
65. Wagner, C., Isermann, K., Roeder, T.,, *Infection induces a survival program and local remodeling in the airway epithelium of the fly.* Faseb J, 2009. **23**(7): p. 2045-54.
66. Ritsick, D., Edens WA, et al. , *The use of model systems to study biological functions of Nox/Duox enzymes.* Biochem. Soc. Symp, 2004: p. 85-96.
67. Zhou, D., et al., *Mechanisms underlying hypoxia tolerance in Drosophila melanogaster: hairy as a metabolic switch.* PLoS Genet, 2008. **4**(10): p. e1000221.
68. Baird, N.A., D.W. Turnbull, and E.A. Johnson, *Induction of the heat shock pathway during hypoxia requires regulation of heat shock factor by hypoxia-inducible factor-1.* J Biol Chem, 2006. **281**(50): p. 38675-81.
69. Semenza, G.L., *Hypoxia-inducible factor 1 (HIF-l) pathway.* Sci STKE, 2007. **cm8**.
70. Centanin, L., Dekanty, Andrés., Romero, N., Irisarri, M., G., Thomas, A., Wappner, P.,, *Cell Autonomy of HIF Effects in Drosophila: Tracheal Cells Sense Hypoxia and Induce Terminal Branch Sprouting.* Dev Cell, 2008. **14**(4): p. 547-558.
71. Kewley, R.J., M.L. Whitelaw, and A. Chapman-Smith, *The mammalian basic helix-loop-helixlPAS family of transcriptional regulators.* Int J Biochem Cell Bioi, 2004(36): p. 189-204.
72. Stockmann, C., and J. Fandrey, *Hypoxia-induced erythropoietin production: a paradigm for oxygen-regulated gene expression.* Clin Exp Pharmacol Physiol., 2006(33): p. 968-979.
73. Centanin, L., P.J. Ratcliffe, and P. Wappner, *Reversion of lethality and growth defects in Fatiga oxygen-sensor mutant flies by loss of hypoxia-inducible factor-alpha/Sima.* EMBO Rep, 2005. **6**(11): p. 1070-5.

74. Brunet, A., L.B. Sweeney, l.F. Sturgill, K.F. Chua, P.L. Greer, Y. Lin, H. Tran, S.E., R.M. Ross, H.Y. Cohen, L.S. Hu, H.L. Cheng, M.P. Jedrychowski, S.P., and D.A.S. Gygi, F.W. Alt, and M.E. Greenberg, *Stress-dependent regulation of FOXO transcription factors by the SIRTI deacetylase.* Science, 2004. **303** p. 2011-2015.
75. Bakker, W.J., 1.S. Harris, and T.W. Mak, *FOXO3a is activated in response to hypoxic stress and inhibits HIFl-induced apoptosis via regulation ofCITED2.* Mol.Cell., 2007(28): p. 941-953.
76. Chen, F., V. Castranova, X. Shi, and L.M. Demers. , *New insights into the role of nuclear factor-kappaB, a ubiquitous transcription factor in the initiation of diseases.* Clin Chem Lab Med, 1999(45): p. 7-17.
77. Minakhina, S., and R. Steward, *Nuclear factor-kappa B pathways in Drosophila.* Oncogene, 2006(25): p. 6749-6757.
78. Chandel, N.S., W.C. Trzyna, D.S. McClintock, and P.T. Schumacker, *Role of oxidants in NF-kappa B activation and TNF-alpha gene transcription induced by hypoxia and endotoxin.* J Immunol, 2000(165): p. 1013-1021.
79. Koong, A.C., E.Y Chen, and A.J. Giaccia, *Hypoxia causes the activation of nuclear factor kappa B through the phosphorylation of I kappa B alpha on tyrosine residues.* Cancer Res, 1994(54): p. 1425-1430.
80. Galkin, A., A. Higgs, and S. Moncada, *Nitric oxide and hypoxia.* Essays Biochem, 2007(43): p. 29-42.
81. Wingrove, J.A. and P.H. O'Farrell, *Nitric oxide contributes to behavioral, cellular, and developmental responses to low oxygen in Drosophila.* Cell, 1999. **98**(1): p. 105-14.
82. Liu, G., Roy, J., Johnson, E. A.,, *Identification and function of hypoxia-response genes in Drosophila melanogaster.* Physiol Genomics, 2006. **25**(1): p. 134-41.
83. Maxwell, P.H., *The tumour suppressor protein VHL targets hypoxia-inducible factors for oxygen-dependent proteolysis.* Nature, 1999. **399**: p. 271-275.
84. Cao, Y., et al., *Update on therapeutic neovascularization.* Cardiovascular Research, 2005. **65**(3): p. 639-648.
85. Notter, R.H., *Lung surfactants: basic science and clinical applications*. 2000, New York: Marcel Dekker.
86. Bungeroth, U., *Pulmologie Basics*. 2005, München: Urban & Fischer.
87. Ruhle, H., *Das larvale Tracheensystem von Drosophila melanogaster Meigen und seine Variabilität.* Z. Wiss. Zool., 1932. **141**: p. 159.
88. Ghabrial, A., Luschnig, S.,Metzstein, M. M.,Krasnow, M. A.,, *Branching morphogenesis of the Drosophila tracheal system.* Annual review of cell and developmental biology, 2003. **19**: p. 623-47.
89. Samakovlis, C., et al., *Genetic control of epithelial tube fusion during Drosophila tracheal development.* Development, 1996. **122**: p. 3531.
90. Storch, V.W.U., *Kurzes Lehrbuch der Zoologie. 7 Auflage*. Spektrum Verlag. 2003.
91. Hochachka, P.W., *Defense strategies against hypoxia and hypothermia* Science, 1986. **231**: p. 234-241.

92. Hochachka, P.W., L.T. Buck, and S.C.L. C.J. Doll, *Unifying theory of hypoxia tolerance: molecular/metabolic defense and rescue mechanisms for surviving oxygen lack.* Proc. Natl. Acad. Sci. USA, 1996. **93** p. 9493-9498.
93. Carmeliet, P., et al., *Role of HIF-1[alpha] in hypoxia-mediated apoptosis, cell proliferation and tumour angiogenesis.* Nature, 1998. **394**(6692): p. 485-490.
94. Folkman, J.a.K., M.,, *Angiogenic factors.* Science, 1987. **235** p. 442-447.
95. Pugh, C.W., and Ratcliffe,P.J., , *Regulation of angiogenesis by hypoxia: role of the HIF system.* Nat. Med, 2003. **9**: p. 677-684.
96. Bacon, N.C., Wappner, P., O'Rourke, J. F., Bartlett, S. M.,Shilo, B.,Pugh, C. W.,Ratcliffe, P. J., *Regulation of the Drosophila bHLH-PAS protein Sima by hypoxia: functional evidence for homology with mammalian HIF-1 alpha.* Biochem Biophys Res Commun, 1998. **249**(3): p. 811-6.
97. Nambu, J.R., et al., *The Drosophila melanogaster similar bHLH-PAS gene encodes a protein related to human hypoxia-inducible factor 1 alpha and Drosophila single-minded.* Gene, 1996. **172**(2): p. 249-54.
98. Ma, E. and G. Haddad, *A Drosophila CDK5alpha-like molecule and its possible role in response to O(2) deprivation.* Biochem Biophys Res Commun, 1999. **261**(2): p. 459-63.
99. Ohshiro, T. and S. K, *Transcriptional regulation of breathless FGF receptor gene by binding of TRACHEALESS/dARNT heterodimers to three central midline elements in Drosophila developing trachea.* Development, 1997. **124**: p. 3975.
100. Burmester, T. and T. Hankeln, *The respiratory proteins of insects.* J Insect Physiol, 2007. **53**(4): p. 285-294.
101. Affolter, M., et al., *Tube or Not Tube: Remodeling Epithelial Tissues by Branching Morphogenesis.* Dev Cell, 2003. **4**(1): p. 11-18.
102. Ghabrial, A., et al., *BRANCHING MORPHOGENESIS OF THE DROSOPHILA TRACHEAL SYSTEM.* Annu Rev Cell Dev Biol, 2003. **19**(1): p. 623-647.
103. Samakovlis, C., et al., *Development of the Drosophila tracheal system occurs by a series of morphologically distinct but genetically coupled branching events.* Development, 1996. **122**: p. 1395.
104. Klambt, C., G. L, and S. BZ, *breathless, a Drosophila FGF receptor homolog, is essential for migration of tracheal and specific midline glial cells.* Genes Dev., 1992. **6**: p. 1668.
105. Sutherland, D., S. C, and K. MA, *branchless encodes a Drosophila FGF homolog that controls tracheal cell migration and the pattern of branching.* Cell, 1996. **87**: p. 1091.
106. Guillemin, K., et al., *The pruned gene encodes the Drosophila serum response factor and regulates cytoplasmic outgrowth during terminal branching of the tracheal system.* Development, 1996. **122**: p. 1353.
107. Metzger, R. and K. MA, *Genetic control of branching morphogenesis.* Science, 1999. **284**: p. 1635.
108. Jarecki, J., J. E, and K. MA, *Oxygen regulation of airway branching in Drosophila is mediated by branchless FGF.* Cell, 1999. **99**: p. 211.
109. Rosato, E. and C.P. Kyriacou, *Analysis of locomotor activity rhythms in Drosophila.* Nat. Protocols, 2006. **1**(2): p. 559-568.

110. Ferrandon, D., et al., *A drosomycin-GFP reporter transgene reveals a local immune response in Drosophila that is not dependent on the Toll pathway.* EMBO J, 1998. **17**(5): p. 1217-27.
111. Takehana, A., et al., *Overexpression of a pattern-recognition receptor, peptidoglycan-recognition protein-LE, activates imd/relish-mediated antibacterial defense and the prophenoloxidase cascade in Drosophila larvae.* Proc Natl Acad Sci U S A, 2002. **99**(21): p. 13705-10.
112. Hayashi, S., et al., *GETDB, a database compiling expression patterns and molecular locations of a collection of Gal4 enhancer traps.* Genesis, 2002. **34**(1-2): p. 58-61.
113. Liu, L., W.A. Johnson, and M.J. Welsh, *Drosophila DEG/ENaC pickpocket genes are expressed in the tracheal system, where they may be involved in liquid clearance.* Proc Natl Acad Sci U S A, 2003. **100**(4): p. 2128-33.
114. Aubert, B., et al., *Measurement of D{0}-D[-over]{0} mixing from a time-dependent amplitude analysis of D{0}-->K+pi{-}pi{0} decays.* Phys Rev Lett, 2009. **103**(21): p. 211801.
115. Lavista-Llanos, S., Centanin L.,Irisarri, M.,Russo, DM.,Gleadle, JM.,, *Control of the hypoxic response in Drosophila melanogaster by the basic helix-loop-helix PAS protein similar.* Mol. Cell. Biol., 2002. **22**: p. 6842.
116. Brand, A.H.a.N.P., *Targeted gene expression as a means of altering cell fates and generating dominant phenotypes.* Development, 1993. **118**: p. 401-415.
117. Fanny, S.N., Michelle M. Tangredi, and F.R. Jackson, *Glial Cells Physiologically Modulate Clock Neurons and Circadian Behavior in a Calcium-Dependent Manner.* Current biology : CB, 2011. **21**(8): p. 625-634.
118. Liu, Y.a.L.M., 2008. , *A genomic response to the yeast transcription factor GAL4 in Drosophila.* Fly (Austin), 2008. **2**(2).
119. Hartley, K.e.a., *Targeted gene expression in transgenic Xenopus using the binary Gal4-UAS system.* Proc Natl Acad Sci UAS 2002. **99**(3): p. 1377-82.
120. Davison, J.e.a., *ransactivation from Gal4-VP16 transgenic insertions for tissue-specific cell labeling and ablation in zebrafish.* Developmental Biology 2007. **304**(2): p. 811-824.
121. McGuire, S.E., et al., *Spatiotemporal Rescue of Memory Dysfunction in Drosophila.* Science, 2003. **302**(5651): p. 1765-1768.
122. McGuire, S., Roman G, Davis RL, *Gene expression systems in Drosophila: a synthesis of time and space.* Trends Genet, 2004(20): p. 384-91.
123. Johnston, S., Daniel, *The art and design of genetic screens: Drosophila melanogaster.* Nat Rev Genet, 2002. **3**(3): p. 176-188.
124. Eberwine, J., Yeh, H., Miyashiro, K., Cao, Y., Nair, S., Finnell, R., Zettel, M., and Coleman, P, *Analysis of Gene Expression in Single Live Neurons.* PNAS, 1992. **89**: p. 3010-3014.
125. Pfaffl, M., *A new mathematical model for relative quantification in real-time RT-PCR.* Nucleic Acids Res, 2001(29): p. e45.
126. Firth, J.D., B.L. Ebert, and P.J. Ratcliffe, *Hypoxic Regulation of Lactate Dehydrogenase A:INTERACTION BETWEEN HYPOXIA-INDUCIBLE FACTOR 1 AND cAMP RESPONSE ELEMENTS* Journal of Biological Chemistry, 1995. **270**(36): p. 21021-21027.

127. Bettencourt, R., et al., *Hemolymph-dependent and -independent responses in Drosophila immune tissue.* Journal of cellular biochemistry, 2004. **92**(4): p. 849-63.
128. Hamdi, M., et al., *DNA damage in transcribed genes induces apoptosis via the JNK pathway and the JNK-phosphatase MKP-1.* Oncogene, 2005. **24**: p. 7135-7144.
129. Puig, O., et al., *Control of cell number by Drosophila FOXO: downstream and feedback regulation of the insulin receptor pathway.* Genes Dev, 2003. **17**: p. 2006-2020.
130. van Dam, H., et al., *ATF-2 is preferentially activated by stress-activated protein kinases to mediate c-jun induction in response to genotoxic agents.* Embo J, 1995. **14**: p. 1798-1811.
131. Al-Shahrour, F., R. Diaz-Uriarte, and J. Dopazo, *FatiGO: a web tool for finding significant associations of Gene Ontology terms with groups of genes.* Bioinformatics, 2004. **20**(4): p. 578-580.
132. Kang, K.A., et al., *Inhibitory Effects of Triphlorethol-A on MMP-1 Induced by Oxidative Stress in Human Keratinocytes via ERK and AP-1 Inhibition.* Journal of Toxicology and Environmental Health, Part A, 2008. **71**(15): p. 992-999.
133. Klagsbrun, M., Knighton, D., Folkman, J. ,, *Tumor Angiogenesis Activity in Cells Grown in Tissue Culture.* Cancer Res, 1976. **36**(1): p. 110-114.
134. Shweiki, D., et al., *Vascular endothelial growth factor induced by hypoxia may mediate hypoxia-initiated angiogenesis.* Nature, 1992. **359**(6398): p. 843-845.
135. Shweiki, D., et al., *Induction of vascular endothelial growth factor expression by hypoxia and by glucose deficiency in multicell spheroids: implications for tumor angiogenesis.* Proceedings of the National Academy of Sciences, 1995. **92**(3): p. 768-772.
136. Michiels, C., *Physiological and pathological responses to hypoxia.* The American journal of pathology, 2004. **164**(6): p. 1875-82.
137. Steinke, J.W., C.R. Woodard, and L. Borish, *Role of hypoxia in inflammatory upper airway disease.* Current opinion in allergy and clinical immunology, 2008. **8**(1): p. 16-20.
138. Nizet, V. and R.S. Johnson, *Interdependence of hypoxic and innate immune responses.* Nature reviews. Immunology, 2009. **9**(9): p. 609-17.
139. Neubauer, J.A., *Invited review: Physiological and pathophysiological responses to intermittent hypoxia.* Journal of applied physiology, 2001. **90**(4): p. 1593-9.
140. Forteza, R., Salathe, M., Miot, F., Conner, G. E.,, *Regulated hydrogen peroxide production by Duox in human airway epithelial cells.* American journal of respiratory cell and molecular biology, 2005. **32**(5): p. 462-9.
141. Bals, R., Wang, X., Zasloff, M., Wilson, J. M.,, *The peptide antibiotic LL-37/hCAP-18 is expressed in epithelia of the human lung where it has broad antimicrobial activity at the airway surface.* Proc Natl Acad Sci U S A, 1998. **95**(16): p. 9541-6.
142. Pandey, U.B. and C.D. Nichols, *Human Disease Models in Drosophila melanogaster and the Role of the Fly in Therapeutic Drug Discovery.* Pharmacological reviews, 2011. **63**(2): p. 411-36.

143. Venken, K.J.T. and H.J. Bellen, *Transgenesis upgrades for Drosophila melanogaster.* Development, 2007. **134**(20): p. 3571-3584.
144. Venken, Koen J.T., Julie H. Simpson, and Hugo J. Bellen, *Genetic Manipulation of Genes and Cells in the Nervous System of the Fruit Fly.* Neuron, 2011. **72**(2): p. 202-230.
145. Zhou, D., Visk, D. W.,Haddad, G. G.,, *Drosophila, a golden bug, for the dissection of the genetic basis of tolerance and susceptibility to hypoxia.* Pediatric research, 2009. **66**(3): p. 239-47.
146. Haddad, G.G., *Enhancing our understanding of the molecular responses to hypoxia in mammals using Drosophila melanogaster.* Journal of applied physiology, 2000. **88**(4): p. 1481-7.
147. Lafaille, J.J., et al., *Junctional sequences of T cell receptor gamma delta genes: implications for gamma delta T cell lineages and for a novel intermediate of V-(D)-J joining.* Cell, 1989. **59**(5): p. 859-70.
148. Lemaitre, B., Kromer-Metzger, E.,Michaut, L.,Nicolas, E.,Meister, M.,, *A recessive mutation, immune deficiency (imd), defines two distinct control pathways in the Drosophila host defense.* Proc. Natl. Acad. Sci. USA, 1995. **92**: p. 9365.
149. Lemaitre, B., J. Reichhart, and J. Hoffmann, *Drosophila host defense: differential induction of antimicrobial peptide genes after infection by various classes of microorganisms.* Proc. Natl. Acad. Sci. USA, 1997. **94**: p. 14614.
150. Becker, T., Loch, G., Beyer, M. Zinke., I.Aschenbrenner, A. C., Carrera, P.Inhester., T.Schultze, J. L., Hoch, M.,, *FOXO-dependent regulation of innate immune homeostasis.* Nature, 2010. **463**(7279): p. 369-73.
151. van der Horst, A. and B.M. Burgering, *Stressing the role of FoxO proteins in lifespan and disease.* Nature reviews. Molecular cell biology, 2007. **8**(6): p. 440-50.
152. Wang, M.C., Bohmann, D., Jasper, H.,, *JNK Extends Life Span and Limits Growth by Antagonizing Cellular and Organism-Wide Responses to Insulin Signaling.* Cell, 2005. **121**(1): p. 115-125.
153. Matzinger, P., *The danger model: a renewed sense of self.* Science, 2002. **296**(5566): p. 301-5.
154. Dekanty, A., Lavista-Llanos, S., Irisarri, M., Oldham, S., Wappner, P.,, *The insulin-PI3K/TOR pathway induces a HIF-dependent transcriptional response in Drosophila by promoting nuclear localization of HIF-alpha/Sima.* Journal of cell science, 2005. **118**(Pt 23): p. 5431-41.
155. Romero, N.M., A. Dekanty, and P. Wappner, *Cellular and developmental adaptations to hypoxia: a Drosophila perspective.* Methods Enzymol, 2007. **435**: p. 123-44.
156. Wu, H., M.C. Wang, and D. Bohmann, *JNK protects Drosophila from oxidative stress by trancriptionally activating autophagy.* Mech Dev, 2009. **126**(8-9): p. 624-37.
157. Beitel, G.J., Krasnow, M.A.,, *Genetic control of epithelial tube size in the Drosophila tracheal system.* Development, 2000. **127**: p. 3271-3282.
158. Manning, G. and M.A. Krasnow, *Development of the Drosophila tracheal system.* M. Bate, A. Martinez Arias (Eds.), The Development of Drosophila

melanogaster,, 1993. **Cold Spring Harbor Laboratory Press, Plainview, New York**: p. 609-685.

159. Page-McCaw, A., et al., *Drosophila Matrix Metalloproteinases Are Required for Tissue Remodeling, but Not Embryonic Development.* Dev Cell, 2003. **4**(1): p. 95-106.
160. Glasheen, B.M., et al., *A matrix metalloproteinase mediates airway remodeling in Drosophila.* Developmental Biology, 2010. **344**(2): p. 772-783.
161. Sbai, O., et al., *Vesicular trafficking and secretion of matrix metalloproteinases-2, -9 and tissue inhibitor of metalloproteinases-1 in neuronal cells.* Molecular and Cellular Neuroscience, 2008. **39**(4): p. 549-568.
162. Tanaka, M., et al., *The C-terminus of ephrin-B1 regulates metalloproteinase secretion and invasion of cancer cells.* J Cell Sci, 2007. **120**(13): p. 2179-2189.
163. Knorr, E., H. Schmidtberg, and A. Vilcinskas, *MMPs Regulate both Development and Immunity in the Tribolium Model Insect.* PLoS ONE, 2009. **4**(3): p. e4751.
164. Miller, C.M., A. Page-McCaw, and H.T. Broihier, *Matrix metalloproteinases promote motor axon fasciculation in the Drosophila embryo.* Development, 2008. **135**(1): p. 95-109.
165. Cronin, S.J.F., et al., *Genome-Wide RNAi Screen Identifies Genes Involved in Intestinal Pathogenic Bacterial Infection.* Science, 2009. **325**(5938): p. 340-343.
166. Schmidt, R.L., et al., *Infection-induced proteolysis of PGRP-LC controls the IMD activation and melanization cascades in Drosophila.* The FASEB Journal, 2008. **22**(3): p. 918-929.
167. Goto, A., et al., *Cooperative Regulation of the Induction of the Novel Antibacterial Listericin by Peptidoglycan Recognition Protein LE and the JAK-STAT Pathway.* Journal of Biological Chemistry, 2010. **285**(21): p. 15731-15738.
168. Li, Y., T.,, J.B. Kimura, and G.K. Andrews, *The zinc-sensing mechanism of mouse MTF-l involves linker peptides between the zinc fingers.* Mol.Cell. Biol, 2006(26): p. 5580-5587.
169. Zhang, B., O. , Georgiev, M. Hagmann, C., Gunes, M., Cramer, P., Faller, M., Vasak, and W. Schaffner, *Activity of metal-responsive transcription factor 1 by toxic heavy metals and H202 in vitro is modulated by metallothionein.* Mol Cell Biol, 2003(23): p. 8471-8485.
170. Gorr, T.A., Tomita, T., Wappner, P., Bunn, H. F.,, *Regulation of Drosophila hypoxia-inducible factor (HIF) activity in SL2 cells: identification of a hypoxia-induced variant isoform of the HIFalpha homolog gene similar.* J Biol Chem, 2004. **279**(34): p. 36048-58.

8. Appendix

Table 3: List of upregulated genes upon hypoxia in the wild type strain w^{1118}

Gene ID	Ratio of medians	Name
CG33309	16,486	-
CG5193	16,486	Transcription factor IIB
CG14869	16,208	CG14869
CG5006	16,208	Odorant receptor 33c
CG12836	16,202	CG12836
CG17907	16,202	Acetylcholine esterase
CG1869	16,202	CG1869
CG31415	9,210	CG31415
CG7457	8,119	CG7457
CG3971	7,136	Baldspot
CG4432	5,963	Peptidoglycan recognition protein LC
CG8548	5,759	-
CG9847	5,335	Fkbp13
CG3213	4,759	CG3213
CG30259	4,734	CG30259
CG32677	4,707	CG32677
CG7440	4,505	Twiggy
CG32720	4,499	CG32720
CG31519	4,456	Odorant receptor 82a
CG7082	4,258	CG7082
CG17962	4,250	Z600
CG11761	4,221	Translin
CG18258	3,926	CG18258
CG32036	3,783	CG32036
CG32372	3,727	CG32372
CG13388	3,701	A kinase anchor protein 200
CG4261	3,613	Helicase 89B
CG9168	3,613	CG9168
CG16944	3,592	stress-sensitive B
CG2125	3,470	cubitus interruptus
CG18783	3,461	Kruppel homolog 1
CG31005	3,450	CG31005
CG2297	3,433	Obp44a
CG6052	3,433	CG6052
CG14323	3,408	CG14323
CG18107	3,370	CG18107
CG7496	3,316	PGRP-SD

CG8253	3,264	Tungus
CG8918	3,236	CG8918
CG3528	3,216	CG3528
CG8629	3,208	CG8629
CG12269	3,198	CG12269
CG9784	3,177	CG9784
CG116411	3,096	-
CG3588	3,085	CG3588
CG31932	3,073	Gustatory receptor 22f
CG12317	3,041	JhI-21
CG326873	3,025	-
CG14303	3,019	CG14303
CG10563	2,997	CG10563
CG1832	2,986	CG1832
CG15207	2,977	CG15207
CG5705	2,929	CG5705
CG1674	2,927	CG1674
CG15663	2,914	-
CG10732	2,912	CG10732
CG14715	2,912	CG14715
CG6391	2,906	Aps
CG10017	2,890	CG10017
CG8453	2,878	Cyp6g1
CG7923	2,836	Fad2
CG1728	2,824	Tim8
CG39784	2,802	-
CG32315	2,773	discs lost
CG17370	2,762	CG17370
CG11550	2,736	CG11550
CG7928	2,725	-
CG13252	2,721	CG13252
CG8483	2,719	-
CG31176	2,714	CG31176
CG4533	2,707	lethal (2) essential for life
CG7761	2,696	Parcas
CG1331	2,683	Ccp84Af
CG15227	2,674	CG15227
CG3078	2,667	CG3078
CG12140	2,666	CG12140
CG18212	2,650	CG18212
CG9509	2,631	CG9509

CG5893	2,628	Dichaete
CG2682	2,592	d4
CG15623	2,590	CG15623
CG11211	2,570	CG11211
CG31297	2,551	CG31297
CG6116	2,551	CG6116
CG5835	2,550	CG5835
CG7402	2,538	CG7402
CG9472	2,525	CG9472
CG30145	2,523	Odorant-binding protein 57e
CG11280	2,508	Tartan
CG31764	2,473	virus-induced RNA 1
CG8536	2,461	-
CG15533	2,409	CG15533
CG30464	2,408	CG30464
CG172287	2,397	-
CG10799	2,379	CG10799
CG8640	2,375	CG8640
CG17840	2,366	CG17840
CG7122	2,352	RhoGAP16F
CG17964	2,335	Pangolin
CG33045	2,335	-
CG31116	2,319	CG31116
CG13958	2,299	CG13958
CG13350	2,292	CG13350
CG13425	2,291	Bancal
CG33291	2,291	CG33291
CG17608	2,285	fu12
CG8671	2,280	CG8671
CG7487	2,278	RecQ4
CG30374	2,273	CG30374
CG1530	2,255	CG1530
CG8197	2,248	CG8197
CG4181	2,243	Glutathione S transferase D2
CG10353	2,234	CG10353
CG14087	2,230	CG14087
CG18039	2,219	KaiRIA
CG32975	2,219	-
CG8695	2,203	Larval visceral protein L
CG7236	2,198	CG7236
CG7257	2,182	CG7257

CG39152	2,178	-
CG1827	2,177	CG1827
CG8853	2,177	CG8853
CG7011	2,168	CG7011
CG12334	2,165	Autophagy-specific gene 8b
CG18340	2,160	Ucp4B
CG9593	2,160	CG9593
CG8582	2,158	-
CG33180	2,145	Ranbp16
CG40192	2,138	-
CG31916	2,132	-
CG12896	2,127	CG12896
CG4005	2,124	CG4005
CG8580	2,119	-
CG15442	2,117	-
CG12162	2,113	CG12162
CG11106	2,112	CG11106
CG16735	2,108	CG16735
CG17242	2,108	CG17242
CG30289	2,093	CG30289
CG8151	2,089	Tfb1
CG32406	2,088	CG32406
CG9245	2,086	CG9245
CG15893	2,085	CG15893
CG7692	2,083	CG7692
CG33125	2,067	CG33125
CG4827	2,064	CG4827
CG4459	2,060	CG4459
CG14636	2,058	CG14636
CG17064	2,058	Mars
CG18108	2,057	Immune induced molecule 1
CG11512	2,051	Glutathione S transferase D4
CG31872	2,051	CG31872
CG33278	2,051	CG33278
CG9795	2,045	CG9795
CG1090	2,039	CG1090
CG31021	2,039	-
CG5499	2,038	Histone H2A variant
CG17386	2,037	CG17386
CG5862	2,037	CG5862
CG8635	2,035	CG8635

CG11579	2,027	Armadillo
CG15312	2,023	CG15312
CG32429	2,018	-
CG11159	2,011	CG11159
CG171772	2,009	-
CG4185	2,008	-
CG15133	2,006	CG15133
CG9589	2,000	CG9589
CG17816	1,999	CG17816
CG7200	1,996	CG7200
CG6939	1,991	SET domain binding factor
CG9323	1,991	CG9323
CG3209	1,988	CG3209
CG7196	1,986	CG7196
CG32033	1,984	CG32033
CG14997	1,983	CG14997
CG1221	1,969	Miple
CG17584	1,968	Odorant receptor 49b
CG30499	1,965	CG30499
CG1152	1,961	Glucose dehydrogenase
CG7228	1,959	CG7228
CG1838	1,958	Myoglianin
CG4437	1,956	Peptidoglycan recognition protein LF
CG9815	1,955	CG9815
CG6708	1,951	Oxysterol binding protein
CG13897	1,946	CG13897
CG7262	1,946	CG7262
CG15437	1,942	modifier of rpr and grim
CG8478	1,942	CG8478
CG8444	1,931	CG8444
CG16826	1,930	-
CG33255	1,926	-
CG5124	1,921	Adipose
CG8909	1,917	CG8909
CG33105	1,914	CG33105
CG11190	1,908	CG11190
CG18302	1,907	CG18302
CG13766	1,904	CG13766
CG17104	1,904	CG17104
CG7098	1,904	Diskette
CG303440	1,903	-

CG3308	1,903	CG3308
CG12667	1,895	CG12667
CG32392	1,895	CG32392
CG31713	1,892	CG31713
CG3558	1,886	CG3558
CG33057	1,879	CG33057
CG17299	1,878	-
CG15345	1,876	CG15345
CG32150	1,876	CG32150
CG6084	1,875	CG6084
CG6410	1,870	CG6410
CG8320	1,870	CG8320
CG11044	1,862	-
CG30377	1,859	CG30377
CG8337	1,859	-
CG18788	1,855	CG18788
CG1669	1,851	-
CG17784	1,850	CG17784
CG11836	1,848	CG11836
CG15387	1,846	CG15387
CG4450	1,845	CG4450
CG18641	1,842	CG18641
CG1216	1,841	Mrityu
CG9735	1,830	Tryptophanyl-tRNA synthetase
CG13834	1,826	CG13834
CG14080	1,824	Mitogen-activated protein kinase phosphatase 3
CG13225	1,823	Odorant receptor 47a
CG8830	1,822	CG8830
CG4033	1,819	RNA polymerase I 135kD subunit
CG5719	1,819	-
CG5813	1,817	Chiffon
CG14684	1,814	CG14684
CG10747	1,812	CG10747
CG11811	1,809	CG11811
CG10080	1,805	CG10080
CG8401	1,803	CG8401
CG8823	1,803	Lip3
CG31955	1,799	CG31955
CG1213	1,797	CG1213
CG17261	1,797	CG17261
CG31673	1,791	CG31673

CG6623	1,790	CG6623
CG10001	1,788	Allatostatin Receptor 2
CG12338	1,788	CG12338
CG13120	1,785	CG13120
CG31857	1,780	CG31857
CG8237	1,775	CG8237
CG32364	1,774	CG32364
CG10627	1,773	CG10627
CG17387	1,770	CG17387
CG17680	1,767	CG17680
CG12587	1,766	CG12587
CG11329	1,762	CG11329
CG14820	1,762	CG14820
CG9195	1,762	-
CG18186	1,759	CG18186
CG3803	1,759	CG3803
CG7115	1,759	CG7115
CG7705	1,759	CG7705
CG15504	1,757	doublesex-Mab related 99B
CG2457	1,757	inaF
CG8181	1,756	CG8181
CG10139	1,750	CG10139
CG10339	1,750	CG10339
CG9046	1,748	Vitelline membrane 26Ab
CG31037	1,747	-
CG1480	1,744	Bottleneck
CG12820	1,736	CG12820
CG1690	1,736	CG1690
CG18193	1,735	CG18193
CG9200	1,733	CG9200
CG10233	1,728	CG10233
CG12732	1,726	CG12732
CG31353	1,726	CG31353
CG14235	1,725	CG14235
CG17743	1,725	Pleiohomeotic
CG14187	1,724	CG14187
CG15023	1,723	CG15023
CG8789	1,721	CG8789
CG8890	1,720	GDP-mannose 4
CG30273	1,716	CG30273
CG15514	1,715	CG15514

CG17086	1,715	CG17086
CG6333	1,714	CG6333
CG10435	1,713	CG10435
CG31501	1,712	nuclear export factor 4
CG31058	1,707	CG31058
CG10246	1,706	Cytochrome P450-6a9
CG40169	1,706	-
CG4960	1,705	CG4960
CG6126	1,705	CG6126
CG6696	1,703	CG6696
CG15671	1,702	crossveinless 2
CG1512	1,699	cul-2
CG66050	1,698	-
CG8481	1,696	CG8481
CG8922	1,692	-
CG18324	1,690	CG18324
CG14842	1,682	CG14842
CG18572	1,682	Rudimentary
CG15786	1,681	CG15786
CG14958	1,679	CG14958
CG6747	1,679	Inwardly rectifying potassium channel
CG3939	1,676	CG3939
CG9731	1,671	CG9731
CG12019	1,670	Cdc37
CG15438	1,670	CG15438
CG4729	1,668	CG4729
CG10396	1,667	CG10396
CG7179	1,665	CG7179
CG31315	1,662	CG31315
CG31745	1,658	CG31745
CG17648	1,657	CG17648
CG9776	1,657	CG9776
CG5660	1,654	CG5660
CG8874	1,654	Fps oncogene analog
CG31311	1,653	-
CG12225	1,652	Spt6
CG31709	1,651	CG31709
CG15314	1,649	CG15314
CG1736	1,649	-
CG4168	1,648	CG4168
CG1307	1,646	CG1307

CG8403	1,644	SP2353
CG17268	1,643	-
CG17610	1,643	Gurken
CG10638	1,642	CG10638
CG40195	1,642	-
CG10369	1,641	Inwardly rectifying potassium channel 3
CG9366	1,638	rho-like
CG12045	1,637	CG12045
CG6154	1,637	CG6154
CG8340	1,631	-
CG11656	1,629	CG11656
CG1131	1,627	-
CG2530	1,626	Corto
CG14499	1,625	-
CG18132	1,625	CG18132
CG15218	1,624	Cyclin K
CG9280	1,624	Glutactin
CG12600	1,621	-
CG15329	1,621	hold'em
CG2292	1,617	CG2292
CG31098	1,616	CG31098
CG31371	1,615	CG31371
CG12236	1,614	CG12236
CG8219	1,613	CG8219
CG41041	1,608	-
CG12802	1,606	CG12802
CG17626	1,606	-
CG12094	1,603	CG12094
CG14516	1,599	-
CG51300	1,598	-
CG5295	1,597	CG5295
CG31925	1,596	CG31925
CG4220	1,595	elbow B
CG2201	1,593	CG2201
CG10486	1,592	CG10486
CG10801	1,592	CG10801
CG14223	1,592	CG14223
CG2574	1,592	CG2574
CG7127	1,592	exo70
CG3278	1,590	-
CR31485	1,590	-

CG9526	1,586	CG9526
CG14014	1,585	CG14014
CG9057	1,581	-
CG2010	1,580	CG2010
CG12259	1,579	CG12259
CG7798	1,579	CG7798
CG5571	1,578	-
CG32246	1,576	CG32246
CG32356	1,575	Ecdysone-inducible gene E1
CG9209	1,572	vacuolar peduncle
CG1218	1,571	CG1218
CG12654	1,571	CG12654
CG10090	1,569	Tim17a1
CG14871	1,566	CG14871
CG6700	1,566	CG6700
CG11513	1,565	Armitage
CG4900	1,565	Iron regulatory protein 1A
CG4212	1,562	Rab-protein 14
CG2899	1,561	kinase suppressor of ras
CG32750	1,561	CG32750
CG32118	1,558	CG32118
CG14151	1,557	CG14151
CG18327	1,557	CG18327
CG31874	1,557	CG31874
CG5412	1,556	CG5412
CG10205	1,549	CG10205
CG31772	1,549	CG31772
CG8258	1,547	CG8258
CG6875	1,546	abnormal spindle
CG18811	1,544	CG18811
CG3897	1,543	bloated tubules
CG31050	1,542	CG31050
CG17489	1,539	-
CG5400	1,539	Eclosion hormone
CG8161	1,538	Rlb1
CG3953	1,537	lethal (3) IX-14
CG9541	1,536	CG9541
CG8502	1,535	CG8502
CG6454	1,534	CG6454
CG10697	1,533	Dopa decarboxylase
CG31900	1,532	CG31900

CG14503	1,531	CG14503
CG30033	1,531	CG30033
CG30424	1,531	CG30424
CG40113	1,530	-
CG7404	1,530	estrogen-related receptor
CG31012	1,529	CG31012
CG14317	1,528	CG14317
CG7085	1,525	lethal (2) s5379
CG18518	1,524	CG18518
CG11120	1,522	CG11120
CG12081	1,522	CG12081
CG32561	1,522	xmas-1
CG6401	1,518	CG6401
CG3561	1,517	CG3561
CG9390	1,516	Acetyl Coenzyme A synthase
CG6695	1,511	CG6695
CG31732	1,506	-
CG12153	1,505	Hira
CG12855	1,505	CG12855
CG10711	1,502	CG10711

Table 4: List of downregulated genes upon hypoxia in the wild type strain w^{1118}

Gene ID	Ratio of medians	Name
CG6653	-6,731	Ugt86De
CG32830	-6,198	CG32830
CG12118	-5,460	CG12118
CG13339	-4,918	CG13339
CG1801	-4,899	-
CG2837	-4,602	CG2837
CG12752	-4,582	NTF2-related export protein 1
CG31195	-4,561	CG31195
CG5451	-4,420	CG5451
CG31852	-4,402	Two A-associated protein of 42kDa
CG14379	-4,104	CheA87a
CG6937	-4,062	CG6937
CG3162	-4,052	CG3162
CG3539	-4,042	SLY-1 homologous
CG7847	-3,987	stripe
CG12072	-3,978	warts
CG14117	-3,973	CG14117
CG1129	-3,965	CG1129
CG10971	-3,863	CG10971

CG11278	-3,789	Syntaxin 13
CG5274	-3,752	CG5274
CG4771	-3,652	CG4771
CG13116	-3,646	CG13116
CG7084	-3,642	CG7084
CG9682	-3,627	CG9682
CG17633	-3,617	CG17633
CG13545	-3,561	CG13545
CG7502	-3,487	CG7502
CG9997	-3,339	CG9997
CG4342	-3,290	CG4342
CG11048	-3,249	CG11048
CG9023	-3,248	Drip
CG6148	-3,230	Putative Achaete Scute Target 1
CG16716	-3,225	CG16716
CG1982	-3,218	Sorbitol dehydrogenase 1
CG14312	-3,173	CG14312
CG31069	-3,162	spindle D
CG8532	-3,087	liquid facets
CG13869	-3,071	CG13869
CR30298	-3,065	-
CG31812	-3,060	CG31812
CG11404	-3,005	CG11404
CG2224	-2,965	CG2224
CG30105	-2,952	CG30105
CG10670	-2,931	XPG-like endonuclease
CG15128	-2,931	CG15128
CG127892	-2,929	-
CG3523	-2,926	CG3523
CG15657	-2,872	CG15657
CG1656	-2,869	lectin-46Ca
CG12661	-2,862	CG12661
CG10249	-2,859	CG10249
CG4720	-2,839	Protein kinase at 92B
CG15279	-2,819	CG15279
CG10874	-2,817	CG10874
CG12091	-2,782	CG12091
CG9503	-2,770	CG9503
CG9470	-2,739	Metallothionein A
CG9434	-2,734	Frost
CG4584	-2,733	Deoxyuridine triphosphatase

CG1637	-2,708	CG1637
CG30016	-2,685	CG30016
CG14167	-2,660	insulin-like peptide 3
CG3060	-2,660	morula
CG11555	-2,645	CG11555
CG3265	-2,644	Eb1
CG31509	-2,638	Turandot A
CG10171	-2,624	CG10171
CG13091	-2,611	CG13091
CG2194	-2,605	Rhythmically expressed gene 3
CG5803	-2,594	Fasciclin 3
CG11958	-2,588	Calnexin 99A
CG15001	-2,583	-
CG15538	-2,571	Osiris 23
CG2973	-2,546	CG2973
CG17369	-2,529	Vacuolar H
CG6189	-2,505	lethal (1) 1Bi
CG11614	-2,501	naked cuticle
CG9030	-2,501	CG9030
CG10531	-2,480	CG10531
CG11999	-2,479	CG11999
CG14841	-2,420	CG14841
CG14506	-2,397	CG14506
CG31292	-2,394	CG31292
CG5185	-2,390	Twin of m4
CG6975	-2,389	gigas
CG11398	-2,381	CG11398
CG11552	-2,377	-
CG9426	-2,377	CG9426
CG18660	-2,367	Nckx30C
CG32676	-2,354	CG32676
CG33478	-2,322	Odorant receptor 46a
CG1079	-2,305	CG1079
CG7077	-2,296	CG7077
CG10694	-2,283	CG10694
CG14322	-2,278	CG14322
CG11693	-2,269	CG11693
CG7417	-2,265	Tab2
CG10513	-2,236	CG10513
CG3739	-2.205	CG3739
CG3671	-2.186	Malvolio

CG7756	-2,168	Heat shock protein cognate 2
CG10725	-2,162	CG10725
CG9569	-2,158	-
CG38110	-2,153	-
CG32709	-2,142	CG32709
CG7438	-2,138	Myosin 31DF
CG7497	-2,137	-
CG10516	-2,127	CG10516
CG7595	-2,127	crinkled
CG11105	-2,117	CG11105
CG32031	-2,111	Arginine kinase
CG30038	-2,084	CG30038
CG3920	-2,076	lethal (2) k16918
CG7861	-2,066	CG7861
CG8617	-2,065	CG8617
CG7899	-2,059	Acid phosphatase 1
CG15829	-2,053	CG15829
CG13349	-2,051	CG13349
CG32114	-2,051	CG32114
CG7057	-2,043	AP-50
CG7587	-2,042	CG7587
CG10324	-2,036	CG10324
CG32158	-2,035	CG32158
CG32380	-2,032	-
CG12496	-2,027	CG12496
CG14885	-2,021	Guanylyl cyclase at 89Da
CG5333	-2,013	CG5333
CG2508	-2,004	cdc23
CG40484	-2,002	-
CG64462	-1,998	-
CG3880	-1,993	CG3880
CG5909	-1,978	CG5909
CG7935	-1,973	moleskin
CG5279	-1,961	Rhodopsin 5
CG5327	-1,957	-
CG9018	-1,950	CG9018
CG16713	-1,945	CG16713
CG32945	-1,945	CG32945
CG8008	-1,927	CG8008
CG16704	-1,918	CG16704
CG14395	-1,898	CG14395

CG81200	-1,893	-
CG8335	-1,893	CG8335
CG31821	-1,889	CG31821
CG30178	-1,884	CG30178
CG13791	-1,877	CG13791
CG9921	-1,871	CG9921
CG3008	-1,865	CG3008
CG7704	-1,852	TBP-associated factor 5
CG15141	-1,841	CG15141
CG12674	-1,840	CG12674
CG4221	-1,835	CG4221
CG5929	-1,824	CG5929
CG10655	-1,807	lethal (2) 37Bb
CG30432	-1,807	CG30432
CG4372	-1,806	CG4372
CG15509	-1,805	-
CG5310	-1,799	nmdyn-D6
CG15658	-1,798	CG15658
CG1358	-1,795	CG1358
CG16747	-1,766	Ornithine decarboxylase antizyme
CG31815	-1,757	CG31815
CG78755	-1,752	-
CG3183	-1,741	-
CG3323	-1,740	CG3323
CG12212	-1,731	pebbled
CG14492	-1,730	CG14492
CG5156	-1,727	CG5156
CG5958	-1,725	CG5958
CG13548	-1,724	CG13548
CG4780	-1,717	CG4780
CG17367	-1,715	Lnk
CG4271	-1,713	CG4271
CG16834	-1,708	lectin-33A
CG3764	-1,703	CG3764
CG1877	-1,700	lin-19-like
CG7728	-1,682	CG7728
CG4918	-1,678	Ribosomal protein LP2
CG8908	-1,674	CG8908
CG10536	-1,669	crossbronx
CG7498	-1,668	CG7498
CG13840	-1,656	CG13840

CG15261	-1,654	CG15261
CG12825	-1,652	CG12825
CG17244	-1,651	CG17244
CG4573	-1,650	CG4573
CG13321	-1,649	CG13321
CG2070	-1,648	CG2070
CG4781	-1,648	CG4781
CG2685	-1,647	CG2685
CG32171	-1,638	Limpet
CG304186	-1,631	-
CG10105	-1,627	CG10105
CG1262	-1,627	Accessory gland peptide 62F
CG15370	-1,619	CG15370
CG3661	-1,619	Ribosomal protein L23
CG8884	-1,615	Synapse-associated protein 47kD
CG9441	-1,609	Punch
CG6194	-1,605	CG6194
CG6463	-1,600	-
CG1737	-1,597	CG1737
CG4371	-1,586	Glutathione S transferase D7
CG11686	-1,582	CG11686
CG31064	-1,578	CG31064
CG5854	-1,578	CG5854
CG7059	-1,578	CG7059
CG3611	-1,575	CG3611
CG18468	-1,565	CG18468
CG6817	-1,562	fear-of-intimacy
CG8007	-1,557	CG8007
CG18104	-1,553	arginase
CG32691	-1,548	CG32691
CG7049	-1,544	-
CG16974	-1,543	CG16974
CG13641	-1,540	CG13641
CG14053	-1,536	CG14053
CG1273	-1,531	CG1273
CG32582	-1,526	CG32582
CG7848	-1,523	CG7848
CG14512	-1,517	-
CG13795	-1,515	CG13795
CG11209	-1,511	pickpocket 6
CG5656	-1,510	CG5656

CG15924	-1,509	CG15924
CG31104	-1,508	CG31104
CG10585	-1,502	CG10585

Table 5: List of upregulated genes upon hypoxia in the dFoxO mutant strain foxo[21]

Gene ID	Ratio of medians	Name
CG6751	5,750	CG6751
CG17957	4,070	-
CG33180	3,446	Ranbp16
CG11170	3,362	CG11170
CG6937	3,345	CG6937
CG12732	3,305	CG12732
CG32392	3,001	CG32392
CG10563	2,975	CG10563
CG4721	2,904	CG4721
CG17888	2,811	PAR-domain protein 1
CG33125	2,793	CG33125
CG32513	2,741	bves
CG7236	2,638	CG7236
CG15173	2,613	CG15173
CG7145	2,608	CG7145
CG1442	2,597	CG1442
CG12184	2,591	CG12184
CG6654	2,541	CG6654
CG13652	2,486	CG13652
CG32106	2,350	CG32106
CG11450	2,287	net
CG10761	2,229	CG10761
CG3168	2,213	CG3168
CG34010	2,206	-
CG8786	2,201	CG8786
CG13917	2,184	CG13917
CG12680	2,173	CG12680
CG4313	2,161	CG4313
CG8245	2,115	CG8245
CG14303	2,112	CG14303
CG18180	2,110	CG18180
CG32069	2,105	CG32069
CG1081	2,104	-
CG14493	2,096	-
CG18568	2,079	CG18568

CG32488	2,059	CG32488
CG14334	2,035	beaten path IIa
CG33304	2,028	rhomboid-5
CG1776	2,006	CG1776
CG3715	1,997	SHC-adaptor protein
CG4756	1,972	CG4756
CG3955	1,934	CG3955
CG12667	1,925	CG12667
CG18031	1,921	CG18031
CG4694	1,920	hermaphrodite
CG8818	1,919	CG8818
CG13567	1,897	CG13567
CG7227	1,891	CG7227
CG7200	1,880	CG7200
CG1394	1,873	CG1394
CG7228	1,867	CG7228
CG31103	1,857	CG31103
CG40413	1,815	-
CG17258	1,810	CG17258
CG7097	1,807	CG7097
CG15010	1,804	archipelago
CG10014	1,803	CG10014
CG10240	1,792	Cyp6a22
CG17387	1,778	CG17387
CG31741	1,772	CG31741
CG9928	1,762	CG9928
CG10747	1,754	CG10747
CG13162	1,751	CG13162
CG17648	1,743	CG17648
CG14687	1,738	CG14687
CG31397	1,735	CG31397
CG15710	1,718	CG15710
CG32445	1,717	CG32445
CG5278	1,714	CG5278
CG6744	1,701	CG6744
CG8005	1,691	CG8005
CG17443	1,682	-
CG6232	1,682	CG6232
CG32504	1,679	CG32504
CG13459	1,677	-
CG33255	1,663	-

CG17976	1,661	sugar transporter 3
CG12165	1,657	Inner centromere protein
CG6386	1,655	ballchen
CG31723	1,644	CG31723
CG10855	1,640	CG10855
CG14309	1,634	CG14309
CG12820	1,630	CG12820
CG31179	1,620	CG31179
CG7229	1,610	CG7229
CG3743	1,596	MTF-1
CR32747	1,594	-
CG7257	1,593	CG7257
CG3143	1,587	forkhead box
CG10756	1,583	TBP-associated factor 13
CG3587	1,581	CG3587
CG10192	1,576	CG10192
CG3595	1,573	spaghetti squash
CG11820	1,572	CG11820
CG17028	1,564	CG17028
CG31251	1,562	CG31251
CG31953	1,553	CG31953
CG14865	1,543	lethal (3) neo43
CG3324	1,543	cGMP-dependent protein kinase 21D
CG32975	1,538	-
CG2278	1,531	CG2278
CG6325	1,531	CG6325
CG11089	1,512	CG11089
CG9084	1,512	CG9084
CG14401	1,508	CG14401
CG6478	1,505	CG6478

Table 6: List of downregulated genes upon hypoxia in the dFoxO mutant strain foxo[21]

Gene ID	Ratio of medians	Name
CG12700	-8,341	skpD
CG10177	-6,717	CG10177
CG17946	-6,704	Male-specific RNA 84Da
CG11248	-5,781	CG11248
CG32043	-5,422	CG32043
CG4447	-4,921	CG4447
CG13830	-4,728	CG13830
CG12923	-4,503	CG12923
CG32709	-4,441	CG32709
CG8885	-4,338	CG8885
CG13875	-4,206	CG13875
CG1801	-3,960	-

CG13170	-3,919	CG13170
CG8836	-3,904	CG8836
CG14463	-3,816	CG14463
CG2233	-3,564	CG2233
CG14841	-3,527	CG14841
CG1774	-3,438	CG1774
CG1402	-3,432	CG1402
CG11981	-3,422	-
CG30353	-3,405	CG30353
CG33454	-3,369	-
CG31292	-3,302	CG31292
CG11175	-3,240	CG11175
CG8580	-3,215	-
CG32743	-3,205	Smg1
CG9653	-3,190	brinker
CG4631	-3,171	CG4631
CG2956	-3,142	twist
CG27742	-3,120	-
CG13807	-3,08	CG13807
CG15642	-3,082	CG15642
CG32719	-3,080	CG32719
CG15742	-3,058	CG15742
CG4598	-3,033	CG4598
CG8090	-3,031	CG8090
CG4208	-2,988	XRCC1
CG16785	-2,959	frizzled 3
CR40474	-2,928	-
CG7931	-2,923	janus B
CG3267	-2,880	CG3267
CG11259	-2,864	MICAL-like
CG6953	-2,853	fat-spondin
CG32715	-2,827	CG32715
CG17280	-2,784	CG17280
CG4103	-2,757	CG4103
CG11873	-2,731	CG11873
CG17190	-2,710	CG17190
CG18026	-2,705	-
CG9539	-2,696	-
CG11024	-2,681	-
CG14290	-2,643	CG14290
CG4673	-2,631	CG4673
CG5055	-2,619	bazooka
CG5554	-2,616	CG5554
CG32983	-2,605	CG32983
CG32044	-2,570	CG32044
CG119880	-2,561	-
CG12128	-2,543	CG12128
CG32568	-2,543	CG32568
CG13064	-2,527	-
CG11313	-2,523	CG11313
CG18109	-2,519	CG18109
CG4207	-2,515	bonsai
CG14237	-2,506	CG14237

CG8977	-2,493	-
CG13980	-2,491	CG13980
CG40470	-2,490	-
CG3611	-2,483	CG3611
CG4535	-2,456	FK506-binding protein FKBP59
CG1697	-2,432	rhomboid-4
CG10513	-2,424	CG10513
CG14894	-2,423	CG14894
CG7516	-2,411	CG7516
CG18648	-2,409	-
CG7049	-2,406	-
CG4206	-2,397	Minichromosome maintenance 3
CG7614	-2,391	Mat1
CG6545	-2,384	ladybird early
CG13271	-2,381	Ugt36Bb
CG4426	-2,378	asteroid
CG2973	-2,365	CG2973
CG325915	-2,364	-
CG15690	-2,362	CG15690
CG9186	-2,357	CG9186
CG40127	-2,352	-
CG31620	-2,342	Gustatory receptor 39b
CG31738	-2,342	CG31738
CG6988	-2,332	Protein disulfide isomerase
CG11906	-2,328	CG11906
CG14032	-2,324	Cyp4ac1
CG4140	-2,312	CG4140
CG7861	-2,311	CG7861
CG4780	-2,306	CG4780
CG1851	-2,305	Ady43A
CG13855	-2,296	CG13855
CG9079	-2,292	CG9079
CG2204	-2,291	-
CG8223	-2,291	CG8223
CG17525	-2,267	Glutathione S transferase E4
CG2244	-2,265	MTA1-like
CG40182	-2,260	-
CG4699	-2,253	CG4699
CG4453	-2,252	Nup153
CG4183	-2,248	Heat shock protein 26
CG6686	-2,246	CG6686
CG8585	-2,243	-
CG3943	-2,223	kraken
CG4362	-2,216	CG4362
CG18678	-2,212	CG18678
CG32613	-2,208	CG32613
CG9384	-2,178	CG9384
CG4205	-2,174	Ferredoxin
CG9590	-2,158	CG9590
CG39540	-2,136	-
CG11236	-2,129	CG11236
CG14047	-2,127	CG14047
CG7069	-2,127	CG7069

CG30027	-2,109	-
CG11757	-2,100	CG11757
CG10759	-2,087	Odorant receptor 7a
CG12993	-2,079	CG12993
CG15369	-2,072	CG15369
CG12508	-2,058	CG12508
CG4110	-2,036	-
CG6490	-2,032	CG6490
CG14117	-2,029	CG14117
CG16971	-2,025	-
CG13924	-2,022	CG13924
CG17601	-2,014	CG17601
CG10171	-2,013	CG10171
CG14395	-2,010	CG14395
CG32633	-2,008	CG32633
CG4590	-2,007	innexin 2
CG4520	-1,993	CG4520
CG7476	-1,987	methuselah-like 7
CG6944	-1,980	Lamin
CG32955	-1,973	-
CG2984	-1,972	Protein phosphatase 2C
CG30430	-1,963	CG30430
CG12061	-1,959	-
CG15862	-1,954	cAMP-dependent protein kinase R2
CG17746	-1,953	CG17746
CG3108	-1,953	CG3108
CG11994	-1,952	Adenosine deaminase
CG33044	-1,949	-
CG6424	-1,942	CG6424
CG4271	-1,932	CG4271
CG30398	-1,931	CG30398
CG8613	-1,912	CG8613
CG6406	-1,911	CG6406
CR32730	-1,911	-
CG13476	-1,910	CG13476
CG12656	-1,904	CG12656
CG32226	-1,896	CG32226
CG6515	-1,896	Tachykinin-like receptor at 86C
CG12072	-1,894	warts
CG17745	-1,887	CG17745
CG31274	-1,883	-
CG9023	-1,880	Drip
CG9841	-1,877	EfSec
CG7691	-1,871	CG7691
CG31835	-1,868	CG31835
CG4677	-1,868	-
CG5185	-1,858	Twin of m4
CG7622	-1,857	Ribosomal protein L36
CG17765	-1,853	CG17765
CG7676	-1,851	CG7676
CG9030	-1,850	CG9030
CG13129	-1,848	CG13129
CG31605	-1,832	Basigin

CG7429	-1,832	CG7429
CG5308	-1,820	dpr5
CG17368	-1,818	CG17368
CG14909	-1,810	CG14909
CG13393	-1,808	CG13393
CG9705	-1,800	CG9705
CG31244	-1,791	CG31244
CG7046	-1,791	CG7046
CG2691	-1,781	CG2691
CG3107	-1,781	CG3107
CG9019	-1,781	dissatisfaction
CG17461	-1,778	Kif3C
CG11333	-1,771	CG11333
CG31373	-1,771	CG31373
CG6226	-1,765	FK506-binding protein 1
CG8861	-1,765	CG8861
CG5880	-1,762	CG5880
CG32642	-1,761	CG32642
CG31876	-1,759	CG31876
CG18581	-1,755	CG18581
CG12169	-1,752	CG12169
CG31472	-1,752	CG31472
CG1644	-1,750	Cyp6t1
CG7459	-1,750	Copper transporter 1B
CG2616	-1,747	CG2616
CG4672	-1,742	TMS1
CG17905	-1,738	CG17905
CG10346	-1,736	Grip71
CG11209	-1,735	pickpocket 6
CG3032	-1,724	CG3032
CG12865	-1,717	CG12865
CG17816	-1,717	CG17816
CG31033	-1,717	CG31033
CG32462	-1,715	CG32462
CG17698	-1,711	-
CG18557	-1,710	CG18557
CG8966	-1,708	CG8966
CG8884	-1,700	Synapse-associated protein 47kD
CG4726	-1,692	CG4726
CG9682	-1,691	CG9682
CG11601	-1,689	CG11601
CG8870	-1,689	CG8870
CG32686	-1,681	CG32686
CG7028	-1,678	CG7028
CG16998	-1,677	CG16998
CG7564	-1,675	CG7564
CG17009	-1,674	CG17009
CG7166	-1,674	CG7166
CG32611	-1,672	CG32611
CG11686	-1,671	CG11686
CG4887	-1,669	CG4887
CG6296	-1,666	CG6296
CG13681	-1,665	CG13681

CG11278	-1,661	Syntaxin 13
CG6289	-1,661	CG6289
CG14160	-1,660	CG14160
CG14367	-1,660	CG14367
CG1721	-1,654	Phosphoglyceromutase
CG30438	-1,654	CG30438
CG8620	-1,653	CG8620
CG9159	-1,649	Kruppel homolog 2
CG8874	-1,644	Fps oncogene analog
CG13062	-1,643	CG13062
CG30416	-1,638	CG30416
CG32589	-1,638	-
CG6463	-1,628	-
CG14724	-1,626	Cytochrome c oxidase subunit Va
CG12936	-1,624	CG12936
CG12427	-1,620	CG12427
CG30158	-1,619	CG30158
CG15547	-1,617	CG15547
CG1994	-1,614	lethal (1) G0020
CG12740	-1,612	Ribosomal protein L28
CG6999	-1,605	CG6999
CG33277	-1,604	CG33277
CG3926	-1,604	Serine pyruvate aminotransferase
CG14506	-1,598	CG14506
CG39784	-1,597	-
CG4221	-1,593	CG4221
CG13935	-1,592	CG13935
CG31141	-1,588	CG31141
CG18768	-1,584	SP2523
CG6174	-1,584	Actin-related protein 87C
CG7267	-1,584	CG7267
CG8435	-1,575	CG8435
CG15400	-1,574	CG15400
CG14834	-1,573	CG14834
CG18582	-1,573	mushroom bodies tiny
CG4329	-1,571	CG4329
CG8072	-1,571	CG8072
CG7016	-1,569	CG7016
CG14408	-1,567	CG14408
CG7467	-1,563	osa
CG17906	-1,561	CG17906
CG13059	-1,558	CG13059
CG18085	-1,556	sevenless
CG7054	-1,556	CG7054
CG14291	-1,554	CG14291
CG18271	-1,554	CG18271
CG41106	-1,554	-
CG33350	-1,552	CheB42c
CG5093	-1,549	Dorsocross3
CG14394	-1,545	CG14394
CG18476	-1,543	CG18476
CG32496	-1,541	CG32496
CG4144	-1,538	Gram-negative bacteria binding protein 2

CG9907	-1,538	paralytic
CG13616	-1,536	CG13616
CG13390	-1,531	CG13390
CG5006	-1,531	Odorant receptor 33c
CG5370	-1,527	Death caspase-1
CG30322	-1,526	-
CG7023	-1,525	CG7023
CG32172	-1,522	noe
CG10700	-1,520	CG10700
CG12895	-1,519	CG12895
CG3719	-1,518	CG3719
CG6914	-1,513	CG6914
CG15918	-1,510	CG15918
CG17051	-1,507	dodo
CG4226	-1,507	--
CG3382	-1,501	Organic anion transporting polypeptide 58Db
CG13050	-1,500	-

Table 7: List of upregulated genes upon ectopically activated metalloproteinase-1strain (Dm-mmp1)

Gene ID	Ratio of medians	Name
CG13380	8.064	CG13380
CG8223	6.652	CG8223
CG13155	5.781	CG13155
CG31513	5.634	CG31513
CG1361	4.838	Andropin
CG9074	4.822	Male-specific RNA 57Da
CG3018	4.674	-
CG2665	4.653	Protein ejaculatory bulb II
CG18064	4.568	Met75Cb
CG18628	4.532	CG18628
CG9108	4.414	Regulator of G-protein signalling 7
CG10712	4.242	Chromator
CG31061	4.236	Gustatory receptor 98d
CG14645	4.209	CG14645
CG11192	4.117	CG11192
CR32911	4.105	-
CG18778	4.08	CG18778
CG5465	3.859	Mediator complex subunit 16
CG9120	3.855	Lysozyme X
CG31033	3.711	CG31033
CG13933	3.66	CG13933
CG11999	3.654	CG11999
CG17673	3.554	Accessory gland peptide 70A
CG9153	3.526	CG9153

CG1262	3.51	Accessory gland peptide 62F
CG15464	3.485	CG15464
CG16762	3.464	CG16762
CG1691	3.404	IGF-II mRNA-binding protein
CG15528	3.386	CG15528
CG5683	3.372	Adult enhancer factor 1
CR32899	3.354	-
CG18646	3.353	CG18646
CG8424	3.328	CG8424
CG31762	3.287	arrest
CG5556	3.262	CG5556
CG13225	3.241	Odorant receptor 47a
CG10910	3.237	CG10910
CG31056	3.236	Accessory gland-specific peptide 98AB
CG14560	3.199	male-specific opa containing gene
CG14000	3.144	CG14000
CG13324	3.131	CG13324
CG8779	3.102	neuromusculin
CG13097	3.087	CG13097
CG15394	3.087	CG15394
CG13375	3.055	CG13375
CG15068	3.05	CG15068
CG1265	3.043	CG1265
CG7715	3.035	CG7715
CG32950	3.002	-
CR32893	2.97	-
CG9920	2.965	CG9920
CG8579	2.954	Jonah 44E
CG9111	2.897	-
CG15874	2.882	CG15874
CG14676	2.875	CG14676
CG9116	2.872	Lysozyme P
CG32800	2.853	-
CG31747	2.839	Gustatory receptor 36a
CG9335	2.838	CG9335
CG31369	2.834	CG31369
CG32569	2.822	CG32569
CG12524	2.814	CG12524
CG31872	2.803	CG31872
CG31412	2.801	CG31412
CG10724	2.733	CG10724

CG3532	2.718	CG3532
CG9166	2.716	312
CG6283	2.715	CG6283
CG13702	2.693	allatostatin C receptor 2
CG7160	2.685	CG7160
CG18030	2.68	Jonah 99Fi
CG5097	2.655	Metallothionein C
CG9029	2.65	CG9029
CG6084	2.648	CG6084
CG12902	2.611	CG12902
CG30473	2.602	Odorant-binding protein 51a
CG9976	2.601	Galactose-specific C-type lectin
CG2010	2.595	CG2010
CG13223	2.591	CG13223
CG10154	2.585	CG10154
CG13003	2.582	CG13003
CG5008	2.58	Gram-negative bacteria binding protein 3
CG4181	2.575	Glutathione S transferase D2
CG4894	2.563	-
CG5399	2.557	CG5399
CG8343	2.54	CG8343
CG7144	2.538	CG7144
CG13510	2.536	CG13510
CG17389	2.529	CG17389
CG4649	2.515	Sorbitol dehydrogenase-2
CG7470	2.511	CG7470
CG32302	2.51	CG32302
CG17012	2.498	CG17012
CG4755	2.493	RhoGAP92B
CG8569	2.487	CG8569
CG9080	2.478	CG9080
CG3411	2.471	blistered
CG6919	2.468	octopamine receptor 2
CG1079	2.467	CG1079
CG7245	2.466	-
CG3656	2.462	Cytochrome P450-4d1
CG5815	2.452	CG5815
CG17063	2.446	inx6
CG10852	2.422	Accessory gland peptide 63F
CG8228	2.414	CG8228
CG13315	2.412	CG13315

CG2611	2.412	CG2611
CG17956	2.409	Male-specific RNA 87F
CG4485	2.405	Cytochrome P450-9b1
CG13293	2.401	CG13293
CG6403	2.399	CG6403
CG4187	2.398	CG4187
CG14322	2.396	CG14322
CG10262	2.394	CG10262
CG18279	2.393	Immune induced molecule 10
CG6372	2.385	CG6372
CG17309	2.376	C-terminal Src kinase
CG3850	2.374	sugarbabe
CG31537	2.373	CG31537
CG17876	2.362	Amylase distal
CG8952	2.359	CG8952
CG16996	2.352	CG16996
CG10562	2.35	CG10562
CG14302	2.349	CG14302
CG15616	2.348	Acp53C14b
CG8749	2.348	small nuclear ribonucleoprotein 70K
CG18107	2.34	CG18107
CG10279	2.329	Rm62
CG8134	2.327	CG8134
CG3408	2.326	CG3408
CR33356	2.323	-
CG7697	2.321	Cleavage stimulation factor 64 kilodalton subunit
CG3219	2.32	Klp59C
CG14670	2.317	CG14670
CG2577	2.314	CG2577
CG11961	2.31	CG11961
CG32707	2.305	Anaphase Promoting Complex 4
CG30029	2.3	CG30029
CG7742	2.297	CG7742
CG12225	2.296	Spt6
CG11820	2.284	CG11820
CG5016	2.284	Male-specific RNA 57Db
CG8784	2.284	CG8784
CG17945	2.283	Male-specific RNA 84Dc
CG13614	2.282	CG13614
CG7518	2.273	CG7518
CG7197	2.254	CG7197

CG10505	2.245	CG10505
CG6503	2.234	CG6503
CG18106	2.229	Immune induced molecule 2
CG7896	2.222	CG7896
CG3184	2.22	CG3184
CG18594	2.219	CG18594
CG5004	2.214	CG5004
CG1775	2.209	Medea
CG10824	2.205	CG10824
CG7757	2.2	CG7757
CG7714	2.188	CG7714
CG11864	2.183	CG11864
CG12879	2.178	CG12879
CR32905	2.177	-
CG14346	2.175	CG14346
CG7874	2.167	CG7874
CG32118	2.164	CG32118
CG17191	2.161	CG17191
CR32901	2.16	-
CG8871	2.155	Jonah 25Biii
CG16978	2.15	CG16978
CG10348	2.149	CG10348
CG14330	2.148	CG14330
CG14795	2.129	CG14795
CG11295	2.128	lethal-(2)-denticleless
CG14916	2.124	Gustatory receptor 32a
CG4795	2.123	Calphotin
CG10347	2.113	CG10347
CG10587	2.11	CG10587
CG13561	2.091	CG13561
CG9496	2.084	Tetraspanin 29Fb
CG13722	2.083	CG13722
CG18130	2.082	CG18130
CG6355	2.074	CG6355
CG15829	2.073	CG15829
CG1462	2.068	Alkaline phosphatase 4
CG2559	2.061	-
CG3497	2.055	Suppressor of Hairless
CG4213	2.054	CG4213
CG3492	2.047	CG3492
CG8195	2.043	CG8195

CG13323	2.035	CG13323
CG4630	2.032	CG4630
CG10184	2.029	CG10184
CG13630	2.027	CG13630
CG13937	2.027	CG13937
CG4183	2.024	Heat shock protein 26
CG33115	2.022	CG33115
CG7546	2.02	CG7546
CG16749	2.018	CG16749
CG5279	2.016	Rhodopsin 5
CG7398	2.01	Transportin
CG18444	2.009	-
CG2047	2.008	fushi tarazu
CG13460	2.005	CG13460
CG32952	2.003	-
CG2171	1.991	Triose phosphate isomerase
CG3924	1.991	Chip
CG4463	1.985	Heat shock protein 23
CG9485	1.978	CG9485
CG1776	1.966	CG1776
CG10934	1.964	CG10934
CG7918	1.96	CG7918
CG12794	1.951	la costa
CG12865	1.948	CG12865
CG7702	1.945	CG7702
CR32910	1.942	-
CG11124	1.938	secretory Phospholipase A2
CG14965	1.937	CG14965
CG12452	1.936	CG12452
CR32730	1.936	-
CG13946	1.925	CG13946
CG16740	1.925	Rhodopsin 2
CG12787	1.922	hoepel1
CG3194	1.922	-
CG32192	1.92	CG32192
CG17027	1.904	CG17027
CG3298	1.899	Juvenile hormone-inducible protein 1
CG16908	1.896	CG16908
CG31145	1.896	CG31145
CG9738	1.895	MAP kinase kinase 4
CG4703	1.888	Arc42

CG33281	1.887	-
CG11624	1.883	Ubiquitin-63E
CG33041	1.883	CG33041
CG6841	1.877	CG6841
CG41123	1.863	-
CG4351	1.862	CG4351
CG8651	1.862	trithorax
CG9938	1.853	CG9938
CG1128	1.85	-
CG3868	1.838	CG3868
CG31893	1.837	Peritrophin-15b
CG5778	1.833	CG5778
CG1709	1.828	Vha100-1
CG3843	1.827	Ribosomal protein L10Aa
CG18103	1.825	fos-related gene at 28F
CG7710	1.825	-
CG5270	1.823	CG5270
CG13983	1.821	CG13983
CG18480	1.819	CG18480
CG17108	1.818	CG17108
CG3394	1.806	CG3394
CG13737	1.803	CG13737
CG2229	1.8	Jonah 99Fii
CG3458	1.797	-
CG30028	1.792	-
CG11099	1.79	CG11099
CG18648	1.788	-
CG3206	1.785	Odorant receptor 2a
CG5804	1.766	CG5804
CG12891	1.76	mitochondrial carnitine palmitoyltransferase I
CG8213	1.76	CG8213
CG8293	1.756	Inhibitor of apoptosis 2
CG41136	1.754	-
CG7556	1.751	CG7556
CG7803	1.75	zeste
CG11529	1.747	CG11529
CG5612	1.745	CG5612
CG7851	1.745	-
CG6966	1.738	CG6966
CG7719	1.733	greatwall
CG10265	1.732	CG10265

CG4879	1.731	homolog of RecQ
CG5682	1.73	CG5682
CG6467	1.729	Jonah 65Aiv
CG33096	1.728	CG33096
CG9271	1.728	Vitelline membrane 34Ca
CG32633	1.727	CG32633
CG7017	1.72	CG7017
CG15347	1.719	CG15347
CG9300	1.719	CG9300
CG7564	1.718	CG7564
CG14445	1.717	CG14445
CG8194	1.708	Ribonuclease X25
CG4221	1.7	CG4221
CG11089	1.699	CG11089
CG2260	1.699	CG2260
CG14218	1.696	CG14218
CG1112	1.693	-
CG3331	1.692	ebony
CG18160	1.688	-
CG14088	1.682	CG14088
CG10001	1.676	Allatostatin Receptor 2
CG1107	1.668	-
CG7758	1.666	pumpless
CG9525	1.663	CG9525
CG10297	1.654	Acp65Aa
CG15231	1.654	Immune induced molecule 4
CG13326	1.651	CG13326
CG1837	1.647	CG1837
CG7802	1.646	CG7802
CG4533	1.644	lethal (2) essential for life
CG7131	1.64	CG7131
CG32796	1.639	CG32796
CG17738	1.638	CG17738
CG11314	1.635	CG11314
CG14049	1.635	Ilp6
CG8253	1.635	tungus
CG9793	1.634	CG9793
CG12501	1.632	Odorant receptor 56a
CG14249	1.632	beat-VII
CG12057	1.628	CG12057
CG4525	1.626	CG4525

CG17083	1.622	CG17083
CG31839	1.622	CG31839
CG1324	1.619	CG1324
CG8256	1.619	lethal (2) k05713
CG17002	1.618	CG17002
CG10225	1.615	CG10225
CG2200	1.615	CG2200
CG9615	1.615	tex
CG10590	1.614	CG10590
CG1939	1.614	CG1939
CG14262	1.613	CG14262
CG3328	1.612	CG3328
CG5210	1.611	Chitinase-like
CG5793	1.607	CG5793
CG12952	1.606	salivary gland-expressed bHLH
CG1304	1.606	CG1304
CG6483	1.604	Jonah 65Aiii
CG6687	1.6	CG6687
CG17735	1.599	CG17735
CG12820	1.593	CG12820
CG3050	1.587	Cyp6d5
CG31611	1.586	His4:CG31611
CG10248	1.585	Cytochrome P450-6a8
CG12491	1.575	CG12491
CG4863	1.569	Ribosomal protein L3
CG4260	1.567	-
CR30024	1.566	-
CG17999	1.56	CG17999
CG10781	1.558	new glue 1
CG30501	1.558	CG30501
CG1453	1.557	Klp10A
CG4859	1.557	Matrix metalloproteinase 1
CG4617	1.552	CG4617
CG9506	1.551	slow as molasses
CG12350	1.548	-
CR9700	1.548	-
CG13617	1.545	CG13617
CG15422	1.544	CG15422
CG32717	1.542	stardust
CG13176	1.537	CG13176
CG4838	1.534	beaten path Ic

CG14217	1.533	Tao-1
CR32894	1.529	-
CG13693	1.528	CG13693
CG31049	1.526	-
CG4095	1.522	CG4095
CG13719	1.521	CG13719
CG13947	1.521	CG13947
CG17245	1.521	plexin B
CG18335	1.517	CG18335
CG3883	1.516	CG3883
CG14546	1.506	-
CG33134	1.504	death executioner Bcl-2 homologue
CG13422	1.502	CG13422

Table 8: List of down regulated genes upon ectopically activated metalloproteinase-1strain (Dm-mmp1)

Gene ID	Ratio of medians	Name
CG10250	-8.198	nautilus
CG31852	-6.844	Two A-associated protein of 42kDa
CG32091	-4.686	CG32091
CG40214	-4.618	-
CG33472	-4.565	-
CG3815	-4.403	CG3815
CG31619	-4.18	CG31619
CG15499	-4.123	CG15499
CG12042	-4.043	CG12042
CG13601	-3.899	CG13601
CG15355	-3.826	-
CG3125	-3.77	lethal (1) G0060
CG1801	-3.753	-
CG15380	-3.731	-
CG5913	-3.689	CG5913
CG4552	-3.586	CG4552
CG31178	-3.562	CG31178
CG6210	-3.561	Multidrug-Resistance like Protein 1
CG3983	-3.494	CG3983
CG14259	-3.486	CG14259
CG9632	-3.456	CG9632
CG17683	-3.437	-
CG5225	-3.328	CG5225
CG31247	-3.328	tincar
CG10391	-3.287	Cyp310a1

CG4020	-3.285	CG4020
CG5038	-3.259	CG5038
CG32986	-3.22	CG32986
CG2854	-3.198	-
CG13281	-3.172	CAS/CSE1 segregation protein
CG5830	-3.168	CG5830
CG14523	-3.16	CG14523
CG7400	-3.11	Fatty acid (long chain) transport protein
CG8233	-3.088	CG8233
CG15556	-3.062	CG15556
CG10017	-3.055	CG10017
CG9606	-3.025	Rrp45
CG12272	-3.008	CG12272
CG2254	-2.992	CG2254
CG30036	-2.974	CG30036
CG12653	-2.935	buttonhead
CG17290	-2.926	CG17290
CG1539	-2.926	tropomodulin
CG1279	-2.897	Rtnl2
CG9149	-2.89	CG9149
CG2160	-2.874	Suppressor of Cytokine Signaling at 44A
CG10563	-2.849	CG10563
CG13625	-2.819	CG13625
CG3006	-2.813	Flavin-containing monooxygenase 1
CG9820	-2.769	Odorant receptor 59a
CG32473	-2.754	CG32473
CG7421	-2.748	Nopp140
CG10207	-2.738	Na
CG31016	-2.732	-
CG5646	-2.723	CG5646
CG15418	-2.707	CG15418
CG5787	-2.696	CG5787
CG11873	-2.666	CG11873
CG6671	-2.649	Argonaute 1
CG7615	-2.646	fos intronic gene
CG5543	-2.636	CG5543
CG11210	-2.632	CG11210
CG1912	-2.63	-
CG30088	-2.621	CG30088
CG9362	-2.62	CG9362
CG5073	-2.575	CG5073

CG12161	-2.572	CG12161
CG32512	-2.566	CG32512
CG2062	-2.552	Cytochrome P450-4e1
CG10039	-2.551	CG10039
CG1499	-2.533	CG1499
CG7762	-2.524	Rpn1
CG4302	-2.522	CG4302
CG31519	-2.515	Odorant receptor 82a
CG1495	-2.511	Calcium/calmodulin-dependent protein kinase I
CG3739	-2.503	CG3739
CG13127	-2.499	CG13127
CG6870	-2.497	CG6870
CG9597	-2.486	CG9597
CG6394	-2.486	UDP-N-acetyl-
CG40449	-2.478	-
CG7058	-2.469	CG7058
CR32900	-2.462	-
CG1732	-2.453	CG1732
CG6476	-2.452	Suppressor of variegation 3-9
CG7290	-2.448	CG7290
CG10988	-2.446	lethal (1) discs degenerate 4
CG9209	-2.443	vacuolar peduncle
CG7535	-2.432	-
CG17764	-2.43	CG17764
CG14620	-2.42	touch insensitive larva B
CG17049	-2.417	CG17049
CG15233	-2.394	CG15233
CG13898	-2.394	CG13898
CG5237	-2.384	CG5237
CG5867	-2.378	CG5867
CG12158	-2.377	-
CG16801	-2.371	CG16801
CG15641	-2.371	CG15641
CG14017	-2.359	CG14017
CG13011	-2.358	CG13011
CG30017	-2.349	CG30017
CG1513	-2.339	CG1513
CG13270	-2.331	Ugt36Ba
CG6074	-2.327	CG6074
CG10660	-2.327	CG10660
CG31626	-2.32	CG31626

CG6120	-2.316	Tetraspanin 96F
CG9899	-2.308	CG9899
CG14501	-2.3	-
CG3191	-2.299	CG3191
CG6061	-2.284	Myb-interacting protein 120
CG11329	-2.282	CG11329
CG1630	-2.274	Inositol 1
CG15636	-2.272	CG15636
CG8664	-2.215	CG8664
CG16790	-2.206	CG16790
CG31742	-2.203	CG31742
CG32341	-2.2	CG32341
CG1651	-2.189	Ankyrin
CG10086	-2.189	CG10086
CG9723	-2.182	-
CG12818	-2.163	CG12818
CG14459	-2.16	CG14459
CG17760	-2.159	CG17760
CG13178	-2.154	CG13178
CG10174	-2.144	-
CG31336	-2.142	Gustatory receptor 93b
CG5494	-2.137	CG5494
CG11156	-2.136	mutagen-sensitive 101
CG31810	-2.132	CG31810
CG2145	-2.126	CG2145
CG10949	-2.119	CG10949
CG7771	-2.117	single-minded
CG32655	-2.116	CG32655
CG1407	-2.114	CG1407
CG3713	-2.102	CG3713
CG3203	-2.101	Ribosomal protein L17
CG32485	-2.098	CG32485
CG1231	-2.098	CG1231
CG13558	-2.097	CG13558
CG8590	-2.09	Kinesin-like protein at 3A
CG31090	-2.09	CG31090
CG12663	-2.09	CG12663
CG12278	-2.079	CG12278
CG15861	-2.076	CG15861
CG7080	-2.072	CG7080
CG12023	-2.071	GV1

CG11129	-2.069	Yolk protein 3
CG12530	-2.057	Cdc42
CG16959	-2.054	CG16959
CG12028	-2.051	disembodied
CG8118	-2.05	mastermind
CG13741	-2.049	CG13741
CG13363	-2.048	Suv4-20
CG12250	-2.043	CG12250
CG14247	-2.035	CG14247
CG7325	-2.031	Eig71Ek
CG1743	-2.023	Glutamine synthetase 2
CG13425	-2.023	bancal
CG3572	-2.02	visceral mesodermal armadillo-repeats
CG14211	-2.013	CG14211
CG12408	-2.007	-
CG11983	-2.004	CG11983
CG7370	-2.003	CG7370
CG13436	-2	CG13436
CG3171	-1.997	trapped in endoderm-1
CG11527	-1.997	Tiggrin
CG8442	-1.996	Glutamate receptor I
CG11422	-1.995	Olfactory-specific E
CG4439	-1.988	CG4439
CG7552	-1.982	-
CG8925	-1.981	CG8925
CG3790	-1.98	CG3790
CG14122	-1.979	CG14122
CG4558	-1.978	CG4558
CG7992	-1.977	CG7992
CG7861	-1.976	CG7861
CG31304	-1.974	CG31304
CG14495	-1.97	CG14495
CG17759	-1.969	-
CG10399	-1.969	CG10399
CG7881	-1.965	CG7881
CG3376	-1.96	CG3376
CG5352	-1.957	Small ribonucleoprotein particle protein B
CG12781	-1.956	nahoda
CG8782	-1.954	Ornithine aminotransferase precursor
CG5893	-1.952	Dichaete
CG5232	-1.95	Sialic acid phosphate synthase

CG18510	-1.942	-
CG5216	-1.94	Sir2
CG5079	-1.935	CG5079
CG4373	-1.933	Cyp6d2
CG3725	-1.933	Calcium ATPase at 60A
CG10695	-1.933	Pat1
CG32134	-1.929	breathless
CG1983	-1.919	CG1983
CG13951	-1.919	lethal (2) k10201
CG8234	-1.912	CG8234
CG3732	-1.912	CG3732
CG13392	-1.911	CG13392
CG40346	-1.907	-
CG9806	-1.898	CG9806
CG32239	-1.897	Guanine nucleotide exchange factor GEF64C
CG9471	-1.892	CG9471
CG5790	-1.89	CG5790
CG15028	-1.89	CG15028
CG15522	-1.889	CG15522
CG3757	-1.887	yellow
CG6192	-1.885	CG6192
CG31385	-1.884	-
CG15144	-1.884	CG15144
CG10701	-1.884	Moesin
CG33005	-1.881	-
CG32549	-1.877	CG32549
CG7384	-1.875	CG7384
CG14959	-1.875	CG14959
CG7149	-1.873	CG7149
CG11801	-1.873	CG11801
CG4676	-1.871	CG4676
CG32685	-1.87	CG32685
CG18783	-1.867	Kruppel homolog 1
CG5708	-1.866	CG5708
CG3835	-1.861	CG3835
CG7164	-1.857	CG7164
CG14972	-1.855	CG14972
CG8687	-1.854	Cyp6a14
CG7904	-1.85	punt
CG6761	-1.843	CG6761
CG6435	-1.843	CG6435

CG17118	-1.843	CG17118
CG1629	-1.839	yellow-h
CG14536	-1.839	CG14536
CG5036	-1.83	CG5036
CG5303	-1.829	meiotic from via Salaria 332
CG3612	-1.828	bellwether
CG14511	-1.828	CG14511
CG5025	-1.826	Selenophosphate synthetase 2
CG11412	-1.824	CG11412
CG10699	-1.824	Lim3
CG33341	-1.823	-
CG1411	-1.823	-
CG10778	-1.82	CG10778
CG30338	-1.819	CG30338
CG1072	-1.815	Arrowhead
CG3655	-1.808	CG3655
CG33302	-1.806	CG33302
CG32984	-1.806	CG32984
CG1394	-1.806	CG1394
CG4151	-1.805	-
CG10244	-1.805	Cad96Ca
CG10582	-1.804	Sex-lethal interactor
CG41042	-1.801	-
CG5889	-1.798	Mdh
CG12118	-1.798	CG12118
CG32599	-1.794	CG32599
CG17386	-1.793	CG17386
CG12035	-1.783	CG12035
CG6730	-1.782	Cyp4d21
CG3454	-1.782	Histidine decarboxylase
CG15166	-1.78	CG15166
CG15345	-1.779	CG15345
CG6967	-1.773	CG6967
CG2096	-1.771	flap wing
CG6717	-1.767	-
CG16963	-1.766	Crystallin
CG4563	-1.762	CG4563
CG15101	-1.762	Juvenile hormone epoxide hydrolase 1
CG6657	-1.761	vegetable
CG9875	-1.759	CG9875
CG3705	-1.759	astray

CG32365	-1.758	CG32365
CG9568	-1.757	CG9568
CG32428	-1.75	CG32428
CG14517	-1.746	-
CG17347	-1.741	CG17347
CG8311	-1.738	CG8311
CG5451	-1.732	CG5451
CG30396	-1.732	Gustatory receptor 58a
CG13563	-1.731	CG13563
CG32195	-1.729	CG32195
CG12677	-1.728	CG12677
CG3077	-1.727	CG3077
CG6562	-1.725	synaptojanin
CG30450	-1.721	Odorant-binding protein 56f
CG33455	-1.72	CG33455
CG15884	-1.72	CG15884
CG15710	-1.719	CG15710
CG11471	-1.717	Isoleucyl-tRNA synthetase
CG32088	-1.716	CG32088
CG15196	-1.715	CG15196
CG12617	-1.713	CG12617
CG8730	-1.712	drosha
CG4962	-1.71	CG4962
CG2004	-1.706	CG2004
CG9900	-1.703	-
CG2835	-1.702	-
CR32665	-1.701	-
CG9428	-1.701	Zinc/iron regulated transporter-related protein 1
CG11592	-1.698	CG11592
CG9815	-1.691	CG9815
CG7361	-1.69	-
CG16732	-1.69	CG16732
CG12835	-1.682	CG12835
CG5222	-1.681	CG5222
CG8580	-1.676	-
CG30419	-1.674	CG30419
CG18809	-1.674	CG18809
CG5644	-1.671	CG5644
CG17952	-1.671	-
CG8007	-1.667	CG8007
CG5998	-1.665	Adenosine deaminase-related growth factor B

CG5241	-1.664	CG5241
CG31084	-1.664	CG31084
CG14593	-1.66	CG14593
CG3502	-1.655	CG3502
CG7573	-1.651	-
CG32629	-1.648	CG32629
CG2706	-1.648	female sterile (1) Yb
CG3740	-1.645	CG3740
CG8885	-1.643	CG8885
CG1169	-1.643	Osiris 18
CG7820	-1.642	Carbonic anhydrase 1
CG15293	-1.64	CG15293
CG31694	-1.639	CG31694
CG13126	-1.638	CG13126
CG14551	-1.636	CG14551
CG6106	-1.635	CG6106
CG13538	-1.632	CG13538
CG11373	-1.631	CG11373
CG32486	-1.627	CG32486
CG10470	-1.627	CG10470
CG41107	-1.624	-
CG13541	-1.622	CG13541
CG16918	-1.62	CG16918
CG13643	-1.62	CG13643
CG8051	-1.609	CG8051
CG33493	-1.608	-
CG14512	-1.607	-
CG10005	-1.605	CG10005
CG10243	-1.601	Cyp6a19
CG6094	-1.599	CG6094
CG11847	-1.596	CG11847
CG10698	-1.593	GRHRII
CG30337	-1.591	CG30337
CG18467	-1.59	CG18467
CG11110	-1.589	CG11110
CG33136	-1.587	CG33136
CG40198	-1.586	-
CG9594	-1.584	Chd3
CG1066	-1.583	Shaker cognate b
CG6056	-1.58	-
CG31795	-1.574	ia2

CG4005	-1.572	CG4005
CG18669	-1.572	CG18669
CG12224	-1.568	CG12224
CG12576	-1.566	CG12576
CG31778	-1.564	CG31778
CR40474	-1.561	-
CG3599	-1.56	CG3599
CG12348	-1.557	Shaker
CG14756	-1.551	CG14756
CG14491	-1.551	CG14491
CG11922	-1.551	forkhead domain 96Cb
CG17838	-1.548	CG17838
CG32167	-1.545	CG32167
CG17023	-1.543	-
CG13318	-1.541	CG13318
CG11788	-1.541	CG11788
CG14958	-1.533	CG14958
CG7103	-1.531	PDGF- and VEGF-related factor 1
CG15916	-1.531	CG15916
CG10535	-1.529	CG10535
CG14089	-1.527	CG14089
CG7140	-1.526	CG7140
CG14618	-1.524	CG14618
CG10211	-1.522	CG10211
CR31940	-1.52	-
CG14396	-1.518	Ret oncogene
CG13111	-1.513	CG13111
CG7408	-1.51	CG7408
CG12560	-1.509	CG12560
CG1218	-1.509	CG1218
CG10164	-1.508	CG10164
CG15296	-1.506	CG15296
CG18773	-1.502	Lcp65Ab2
CG10117	-1.502	tout-velu
CG17390	-1.5	CG17390

Figure 38: Fly construction scheme

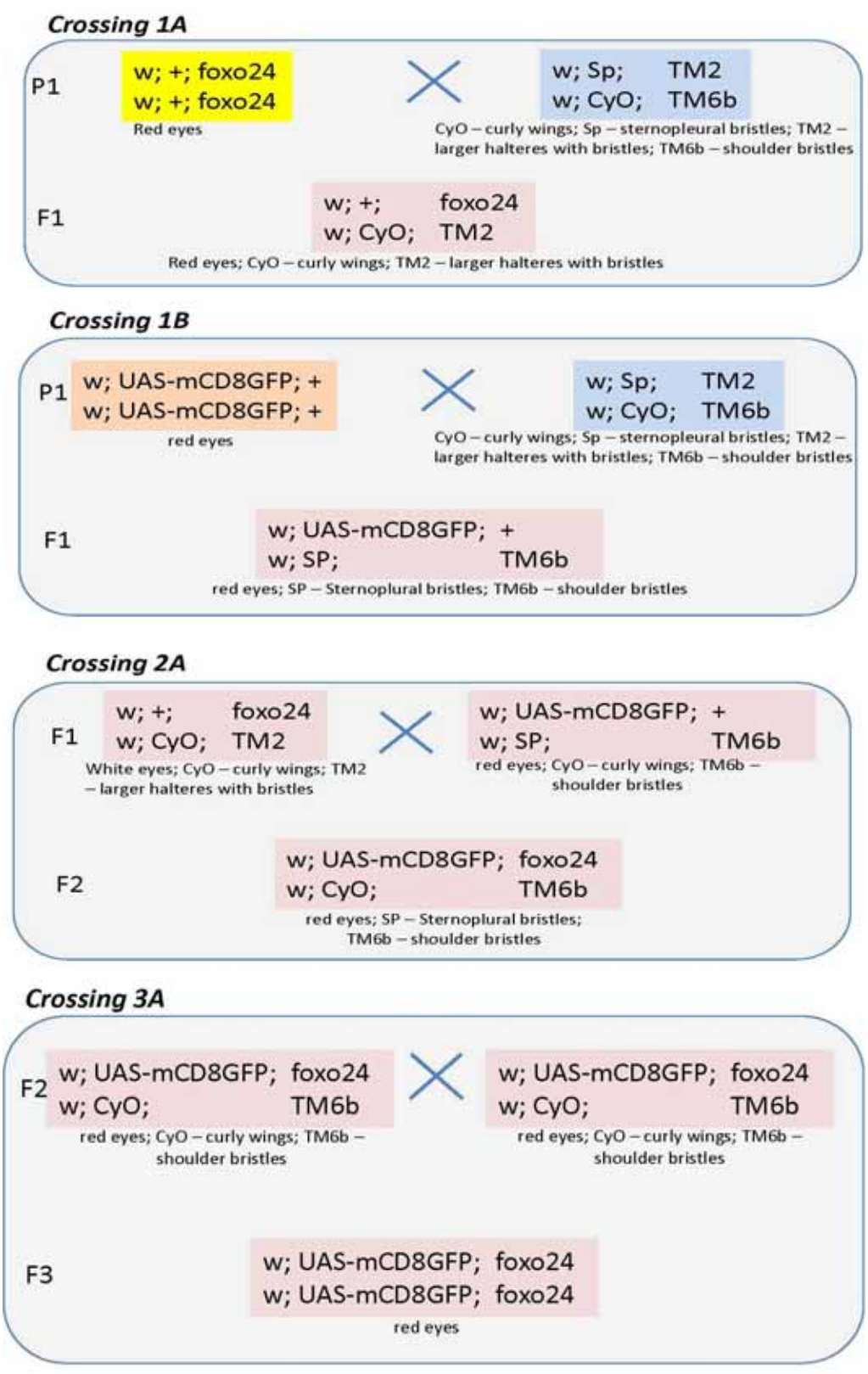

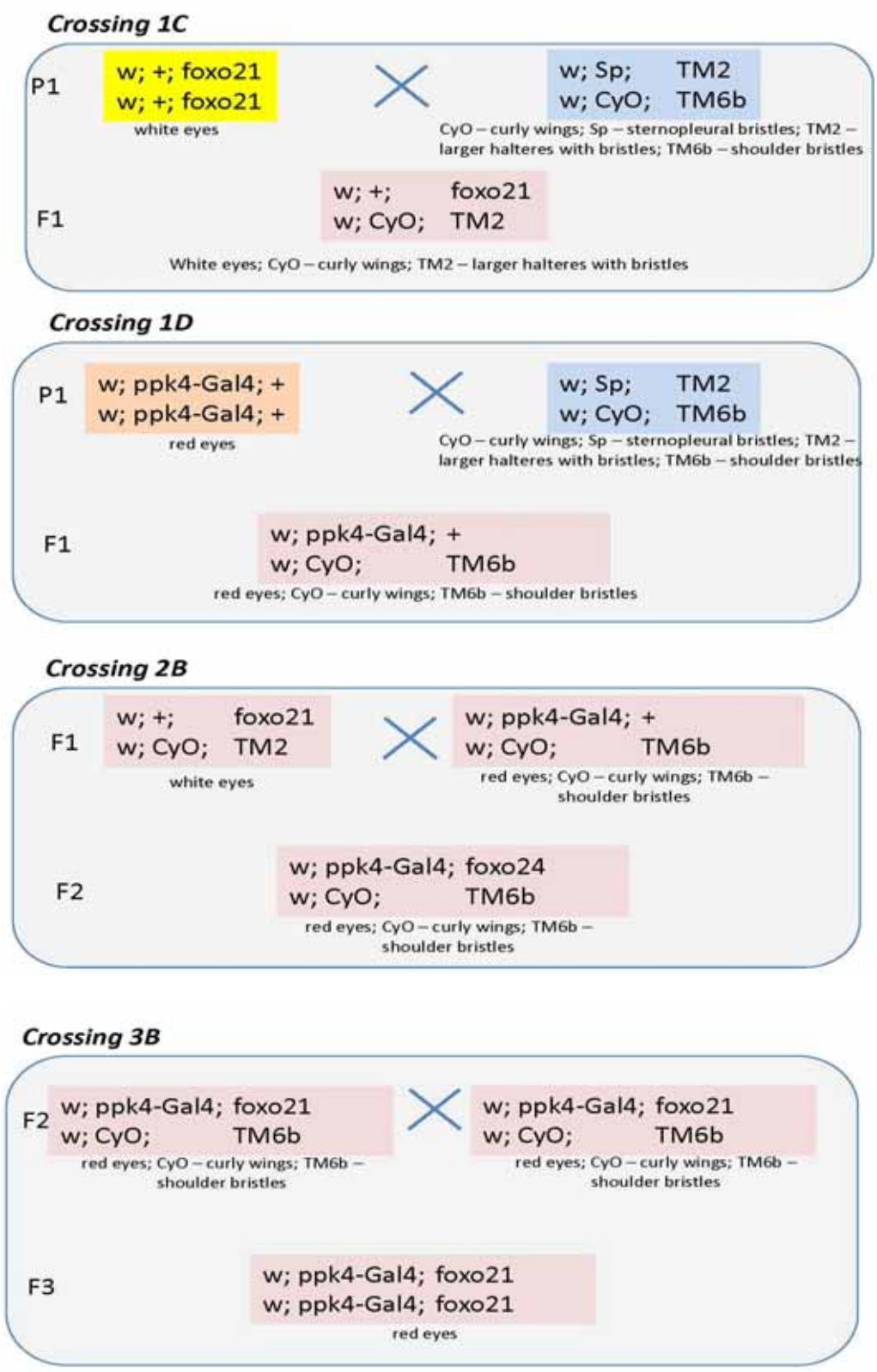
Crossing 1C
P1
w; +; foxo21
w; +; foxo21
white eyes
w; Sp; TM2
w; CyO; TM6b
CyO – curly wings; Sp – sternopleural bristles; TM2 – larger halteres with bristles; TM6b – shoulder bristles
F1
w; +; foxo21
w; CyO; TM2
White eyes; CyO – curly wings; TM2 – larger halteres with bristles
Crossing 1D
P1
w; ppk4-Gal4; +
w; ppk4-Gal4; +
red eyes
w; Sp; TM2
w; CyO; TM6b
CyO – curly wings; Sp – sternopleural bristles; TM2 – larger halteres with bristles; TM6b – shoulder bristles
F1
w; ppk4-Gal4; +
w; CyO; TM6b
red eyes; CyO – curly wings; TM6b – shoulder bristles
Crossing 2B
F1
w; +; foxo21
w; CyO; TM2
white eyes
w; ppk4-Gal4; +
w; CyO; TM6b
red eyes; CyO – curly wings; TM6b – shoulder bristles
F2
w; ppk4-Gal4; foxo24
w; CyO; TM6b
red eyes; CyO – curly wings; TM6b – shoulder bristles
Crossing 3B
F2
w; ppk4-Gal4; foxo21
w; CyO; TM6b
red eyes; CyO – curly wings; TM6b – shoulder bristles
w; ppk4-Gal4; foxo21
w; CyO; TM6b
red eyes; CyO – curly wings; TM6b – shoulder bristles
F3
w; ppk4-Gal4; foxo21
w; ppk4-Gal4; foxo21
red eyes

9. Acknowledgements

It is a great pleasure to thank the people who made this thesis come to fruition.

First, I thank my principal supervisor Prof. Dr. Thomas Roeder for giving me the great opportunity to study my Ph.D. at the honor Institute of Zoophysiology at the Christian- Albrechts University zu Kiel. His help, support and patience were invaluable. I appreciate all his contributions of time, ideas, and funding to make my Ph.D. experience productive and encourage.

I would like to acknowledge the Ministry of Higher Education, Egypt and Deutsche Forschungsgemeinschaft (DFG) for financial support. I am very grateful also to all kind members of the Zoophysiology Institute. Their compassionate help through the course of this work played a vital role in this thesis.

I am deeply grateful to my entire extended family: my parents, sisters and brother, who were supportive of providing an affectionate environment for me, despite missing me for a long time. I wish to express my deep and sincere thanks to my wife, who was overwhelmed with duties during my study.

Thanks to Yousouf and Zeaid, my sons, who are always giving me happiness and hope.

It is no doubt that I appreciate the deep thanks to all my professors, colleagues and friends at the Zoology department, Aswan University, Egypt.

10. Curriculum Vitae

Name:	Ahmed Abdelsadik Mohammed Khalil
Date of birth:	April, 01, 1981
Place of birth:	Aswan, Egypt
Gender:	Male

EDUCATION:

2008-2012	Ph.D. in Immunogenetics, Christian-Albrechts University of Kiel, Germany.
Dissertation:	Hypoxia induces processes related-inflammation and remodelling in the airways of the fruit fly *Drosophila melanogaster*.
2007-2008	M.Sc. in Molecular biology, Zoophysiology Dep., Christian-Albrechts University of Kiel, Germany
Dissertation:	Transcriptome of *Drosophila melanogaster* salivary glands.
2002	B.S. in Zoology, Faculty of Science, South Valley University, Egypt.

SCIENTIFIC CAREER:

1998- date	Assistant Professor; Faculty of Science, South Valley University, Egypt

SCHOLARSHIPS AND AWARDS

2007-2008	Master Scholarship: Awarded from the Egyptian higher Education ministry.
2008-2012	Full PhD Scholarship: Awarded from the Egyptian higher Education ministry.
2011	Award of European Academy of Allergy and Clinical Immunology (EAACI).

LIST OF PUBLICATIONS:

1. Abdelsadik, A. and T. Roeder (2010). "Chronic activation of the epithelial immune system of the fruit fly's salivary glands has a negative effect on organismal growth and induces a peculiar set of target genes." BMC Genomics **11**(1): 265-265.

2. Abdelsadik, A. and A. Trad (2011). "Toll-like receptors on the fork roads between innate and adaptive immunity." Hum Immunol **72**(12): 1188-1193.

11. Affirmation

I hereby affirm that I have completed my doctoral degree thesis entitled

"**Hypoxia induces processes related to inflammation and remodelling in the airways of the fruit fly *Drosophila melanogaster***" entirely on my own and unassisted, and that I have especially marked all of quotes I have used from other authors as well as those passage in my work that are extremely close to the thoughts presented by other authors, and listed the sources in accordance with the regulation I have been given.

Ahmed Abdelsadik

Kiel at, _____

Signature _____